Appendix K
Modeling Attainment Demonstration

San Joaquin Valley Air Pollution Control District
2018 PM2.5 SIP

Photochemical Modeling

Photochemical Modeling for the 2018 San Joaquin Valley Annual/24-Hour $PM_{2.5}$ State Implementation Plan

Prepared by

California Air Resources Board

San Joaquin Valley Air Pollution Control District

Prepared for

United States Environmental Protection Agency Region IX

June, 2018

TABLE OF CONTENTS

List of Figures

List of Tables

ACRONYMS

ARB – Air Resources Board

BCs – Boundary Conditions

CMAQ Model – Community Multi-scale Air Quality Model

CRPAQS – California Regional Particulate Air Quality Study

CSN – Chemical Speciation Network

DISCOVER-AQ – Deriving Information on Surface Conditions from Column and Vertically Resolved Observations Relevant to Air Quality

DV – Design Value

EC – Elemental Carbon

FEM – Federal Equivalent Method

FRM – Federal Reference Method

GEOS-5 – Goddard Earth Observing System Model, Version 5

GMAO – Global Modeling and Assimilation Office

ICs – Initial Conditions

MEGAN – Model of Emissions of Gases and Aerosols from Nature

MFB – Mean Fractional Bias

MFE – Mean Fractional Error

MOZART – Model for Ozone and Related chemical Tracers

NARR – North American Regional Reanalysis

NASA – National Aeronautics and Space Administration

NCR – National Center for Atmospheric Research

NMB – Normalized Mean Bias

NME – Normalized Mean Error

NO_x – Oxides of Nitrogen

OC – Organic Carbon

OM – Organic Matter

$PM_{2.5}$ – Particulate Matter of Aerodynamic Diameter less than 2.5 micrometers

RMSE – Root Mean Square Error

ROG – Reactive Organic Gases

RRF – Relative Response Factors

SANWICH – Sulfate, Adjusted Nitrate, Derived Water, Inferred Carbon Hybrid material balance

SAPRC – Statewide Air Pollution Research Center

SIP – State Implementation Plan

SJV – San Joaquin Valley

SOA – Secondary Organic Aerosol

SO_x – Sulfur oxides

U.S. EPA – United States Environmental Protection Agency

VOCs – Volatile Organic Compounds

WRF – Weather and Research Forecasting

1 INTRODUCTION

The purpose of this document is to demonstrate the attainment of multiple National Ambient Air Quality Standards (NAAQS) for $PM_{2.5}$ in the San Joaquin Valley nonattainment area (SJV or the Valley), which forms the scientific basis for the 2018 SJV $PM_{2.5}$ State Implementation Plan (SIP). Specifically, the plan addresses the following $PM_{2.5}$ standards.

1.) 1997 annual $PM_{2.5}$ standard (15 µg/m^3) and 24-hour $PM_{2.5}$ standard (65 µg/m^3) with an attainment deadline of 2020 for both standards.
2.) 2006 24-hour $PM_{2.5}$ standard (35 µg/m^3) with an attainment deadline of 2024.
3.) 2012 annual $PM_{2.5}$ standard (12 µg/m^3) with an attainment deadline of 2025.

Modeling for these standards shows that:

1.) In 2020, the highest projected annual $PM_{2.5}$ design value (DV) under a future baseline emissions scenario (i.e., no additional emission reductions beyond what will be achieved by the current regulatory program) is 14.6 µg/m^3 at the Bakersfield-Planz site, and the highest projected 24-hour $PM_{2.5}$ DV is 47.6 µg/m^3 at the Bakersfield-California Avenue site, which demonstrates that SJV will attain the 1997 annual and 24-hour $PM_{2.5}$ standards by 2020.
2.) In 2024, the highest projected 24-hour $PM_{2.5}$ DV under the future attainment emissions scenario (i.e., including additional emission reductions beyond the future baseline emissions) is 35.1 µg/m^3 at the Fresno-HW site, which demonstrates that SJV will attain the 2006 24-hour $PM_{2.5}$ standard by 2024 (based on the form of the standard, the DV can be as high as 35.4 µg/m^3 and still be in attainment).
3.) In 2025, the highest projected annual $PM_{2.5}$ DV under the future attainment emission scenario is 11.9 µg/m^3 at both the Madera and Bakersfield-Planz sites, which demonstrates that SJV will attain the 2012 annual $PM_{2.5}$ standard by 2025.

The remainder of this document is organized as follows: Section 2 describes the general approach for projecting design values (DVs) to future years (i.e., 2020, 2024, and 2025). Section 3 discusses the meteorological modeling and evaluation. Section 4 describes the emissions inventory. Section 5 shows $PM_{2.5}$ model performance, projected future year DVs (i.e., 2020, 2024, 2025), $PM_{2.5}$ precursor sensitivities for 2013, 2020, and 2024, and the un-monitored area analysis. A more detailed description of the modeling and development of the model-ready emissions inventory can be found in the Photochemical Modeling Protocol and Modeling Emission Inventory Appendices.

2 APPROACHES

This section briefly describes the Air Resources Board's (ARB's) procedures, based on U.S. EPA guidance (U.S. EPA, 2014), for projecting future year annual and 24-hour $PM_{2.5}$ Design Values (DVs) using model output and a Relative Response Factor (RRF) approach.

2.1 METHODOLOGY

The U.S. EPA modeling guidance (U.S. EPA, 2014) outlines the approach for using models to predict future year annual and 24-hour $PM_{2.5}$ DVs. The guidance recommends using model predictions in a "relative" rather than "absolute" sense. In this relative approach, the fractional change (or ratio) in $PM_{2.5}$ concentration between the model future year and model baseline year are calculated for all valid monitors. These ratios are called relative response factors (RRFs). Since $PM_{2.5}$ is comprised of different chemical species, which respond differently to changes in emissions of various pollutants, separate RRFs are calculated for the individual $PM_{2.5}$ species. Baseline DVs are then projected to the future on a species-by-species basis, where the DV is separated into individual $PM_{2.5}$ species and each species is multiplied by its corresponding RRF. The individual species are then summed to obtain the future year $PM_{2.5}$ DV.

A brief summary of the modeling procedures utilized in this attainment analysis, as prescribed by the U.S. EPA modeling guidance (U.S. EPA, 2014), is provided below. A more detailed description can be found in the Photochemical Modeling Protocol Appendix.

2.2 MODELING PERIOD

Based on analysis of recent years' ambient $PM_{2.5}$ levels and meteorological conditions leading to elevated $PM_{2.5}$ concentrations, the year 2013 was selected for baseline modeling calculations. The National Aeronautics and Space Administration (NASA) launched the DISCOVER-AQ (Deriving Information on Surface Conditions from Column and Vertically Resolved Observations Relevant to Air Quality) field campaign in the SJV from January 16th to Mid-February, 2013. This field study provided unprecedented observations of wintertime $PM_{2.5}$ and its precursors not available in the SJV since the CRPAQS (i.e., California Regional Particulate Air Quality Study) study more than 15 years ago. These observations aided in development of the modeling platform used in this SIP work.

2.3 BASELINE DESIGN VALUES

Specifying the baseline DV is a key consideration in the model attainment test, because this value is projected forward to the future and used to test for future attainment of the standard at each monitor. U.S. EPA guidance (2014) defines the annual $PM_{2.5}$ DV for a given year as the 3-year average (ending in that year) of the annual average $PM_{2.5}$ concentrations, where the annual average is calculated as the average of the quarterly averages for each calendar quarter (e.g., January-March, April-June, July-September, October-December). For example, the 2012 $PM_{2.5}$ DV is the average of the annual $PM_{2.5}$ concentrations from 2010, 2011, and 2012. Similarly, the 24-hour $PM_{2.5}$ DV for a given year is also defined as the 3-year average of the measured 98th percentile concentration from each of those 3 years. For example, the 2012 24-hour $PM_{2.5}$ DV is the average of the 98th percentile 24-hour $PM_{2.5}$ concentrations from years 2010, 2011, and 2012, respectively.

To minimize the influence of year-to-year variability in demonstrating attainment, the U.S. EPA (2014) optionally allows the averaging of three DVs, where one of the years is the baseline emissions inventory and modeling year. This average DV is referred to as the baseline DV. Since each DV represents an average over three years, observational data from 2010, 2011, 2012, 2013, and 2014 will influence the average DV, with each year receiving a different weighting. Table 1 illustrates the observational data from each year that goes into the baseline DV.

Table1. Illustrates the data from each year that are utilized in the baseline DV calculation.

DV Year	Years averaged for the DV				
2012	2010	2011	2012		
2013		2011	2012	2013	
2014			2012	2013	2014

Yearly weighting for the baseline DV calculation*

$$2012 - 2014\ Average = \frac{PM2.5_{2010} + 2 \times PM2.5_{2011} + 3 \times PM2.5_{2012} + 2 \times PM2.5_{2013} + PM2.5_{20}}{9}$$

*: For annual $PM_{2.5}$, $PM_{2.5}$ for a particular year is the annual average of that year. For 24-hour $PM_{2.5}$, $PM_{2.5}$ for a particular year is the 98th percentile 24-hour concentration from that year.

Table 2 shows the 2012-2014 average annual DVs (or annual baseline DVs) for each Federal Reference Method (FRM) /Federal Equivalent Method (FEM) site in the SJV, which had sufficient data to calculate a DV. For two sites with incomplete data, assumptions were made to calculate the baseline DVs and the assumptions were annotated following Table 2. The highest DV occurred at the Bakersfield – Planz site with a baseline DV of 17.2 µg/m^3.

Table 2. Average baseline DVs for each FRM monitoring site in the SJV, as well as the yearly annual DVs from 2012-2014 utilized in calculating the baseline DVs.**

AQS site ID	Monitoring Site Name	2012	2013	2014	2012-2014 Average Baseline
60290016	Bakersfield - Planz	15.3	16.9	19.3	17.2
60392010	Madera		18.1	15.8	16.9*
60311004	Hanford	15.8	17.0	16.8	16.5
61072002	Visalia	14.8	16.6	17.2	16.2
60195001	Clovis	16.0	16.4	16.0	16.1
60290014	Bakersfield – California Ave.	14.5	16.4	17.2	16.0
60190011	Fresno –Garland	14.2	15.4	15.3	15.0
60990006	Turlock	14.9	15.7	14.1	14.9
60195025	Fresno –Hamilton & Winery	13.9	14.7	14.1	14.2
60771002	Stockton	11.6	13.8	14.1	13.1
60470003	Merced – S Coffee	14.3	13.3	11.7	13.1
60990005	Modesto	12.9	13.6	12.5	13.0
60472510	Merced -Main Street	10.4	11.1	11.4	11.0
60772010	Manteca		10.2	9.9	10.1*
60192009	Tranquility	7.5	7.9	7.7	7.7

* Because of incomplete data at Madera and Manteca, DVs from 2013 and 2014 were averaged to determine the baseline DV for these two sites.
** Note that a design value for the Corcoran monitor cannot be calculated due to missing/incomplete data.

Table 3 shows the 2012-2014 average 24-hour DVs (or 24-hour baseline DVs) for each FRM/FEM site in the SJV, which had sufficient data to calculate a DV. For Manteca with incomplete data, assumption was made to calculate the baseline DVs and that assumption was annotated following Table 3. The highest DV occurred at the Bakersfield – California Avenue site with a baseline DV of 64.1 µg/m^3.

Table 3. Average baseline 24-hour DVs for each FRM/FEM monitoring site in the SJV, as well as the yearly 24-hour DVs from 2012-2014 utilized in calculating the baseline DVs.**

AQS site ID	Monitoring Site Name	2012	2013	2014	2012-2014 Average Baseline
60290014	Bakersfield – California Ave.	58.4	64.6	69.4	64.1
60311004	Hanford	53.8	60.2	65.9	60.0
60190011	Fresno –Garland	57.0	62.0	61.0	60.0
60195025	Fresno –Hamilton & Winery	53.0	63.5	61.6	59.3
60195001	Clovis	53.6	57.6	56.3	55.8
60290016	Bakersfield - Planz	43.7	55.8	67.0	55.5
61072002	Visalia	46.9	55.7	63.9	55.5
60392010	Madera	51.0	52.3	49.6	51.0
60990006	Turlock	48.8	52.7	50.7	50.7
60990005	Modesto	44.3	50.6	48.9	47.9
60472510	Merced -Main Street	39.8	49.2	51.7	46.9
60771002	Stockton	36.1	45.0	44.9	42.0
60470003	Merced – S Coffee	41.0	41.8	40.6	41.1
60772010	Manteca		36.7	37.0	36.9*
60192009	Tranquility	27.1	30.0	31.3	29.5

* Due to incomplete data, DVs for 2013 and 2014 are averaged to obtain baseline DV for Manteca.

** Note that a design value for the Corcoran monitor cannot be calculated due to missing/incomplete data.

2.4 BASE, REFERENCE, AND FUTURE YEARS

The modeling assessment consists of the following five primary model simulations, which all utilized the same model inputs for meteorology, chemical boundary conditions, and biogenic emissions. The only difference between the simulations was the year represented by the anthropogenic emissions (2013 versus 2020, 2024, and 2025) and certain day-specific emissions.

1. *Base Year (or Base Case) Simulation*
   The base year simulation for 2013 was used to assess model performance and includes as much day-specific detail as possible in the emissions inventory such as hourly adjustments to the motor vehicle and biogenic inventories based on observed local meteorological conditions, as well as known wildfire and agricultural burning events.

2. *Reference (or Baseline) Year Simulation*
   The reference year simulation was identical to the base year simulation, except that certain emissions events which are either random and/or cannot be projected to the future were removed from the emissions inventory. For the 2013 reference year modeling, the only category/emissions source that was excluded was wildfires, which are difficult to predict in the future and can significantly influence the model response to anthropogenic emissions reductions in regions with large fires.

3. *Future Year Simulations*
   The future year simulations are identical to the reference year simulation, except that projected future years' (2020, 2024, and 2025) anthropogenic emission levels were used rather than 2013 emission levels. All other model inputs (e.g., meteorology, chemical boundary conditions, biogenic emissions, and calendar for day-of-week specifications in the inventory) were the same as those used in the reference year simulation.

To summarize (Table 4), the base year 2013 simulation was used for evaluating model performance, while the reference (or baseline) 2013 and future years 2020, 2024, and 2025 simulations were used to project the average DVs to the future as described in the Photochemical Modeling Protocol Appendix and in subsequent sections of this document.

Table 4. Description of CMAQ model simulations used to evaluate model performance and project baseline design values to the future years.

Simulation	Anthropogenic Emissions	Biogenic Emissions	Meteorology	Chemical Boundary Conditions
Base year (2013)	2013 w/ wildfires	2013 MEGAN	2013 WRF	2013 MOZART
Reference year (2013)	2013 w/o wildfires	2013 MEGAN	2013 WRF	2013 MOZART
Future year (2020)	2020 w/o wildfires	2013 MEGAN	2013 WRF	2013 MOZART
Future year (2024)	2024 w/o wildfires	2013 MEGAN	2013 WRF	2013 MOZART
Future year (2025)	2025 w/o wildfires	2013 MEGAN	2013 WRF	2013 MOZART

2.5 $PM_{2.5}$ SPECIES CALCULATIONS

Since $PM_{2.5}$ consists of different chemical components, it is necessary to assess how each individual component will respond to emission reductions. As a first step in this process, the measured total $PM_{2.5}$ must be separated into its various components. In the SJV, the primary components on the filter based $PM_{2.5}$ measurements include sulfates, nitrates, ammonium, organic carbon (OC), elemental carbon (EC), particle-bound water, other primary inorganic particulate matter, and passively collected mass (blank mass). Species concentrations were obtained from the four chemical speciation network (CSN) sites in the SJV. These four CSN sites are located at: Bakersfield – California Avenue, Fresno – Garland, Visalia – North Church, and Modesto – 14th Street. Chemical species were measured once every three or six days at those sites. Since not all of the 16 FRM/FEM $PM_{2.5}$ sites in the Valley have collocated speciation monitors, it was necessary to utilize the speciated $PM_{2.5}$ measurements at one of the four CSN sites to represent the speciation profile at each of the FRM/FEM sites. The choice of which CSN site to represent the speciation profile at a given FRM monitor (Table 5) was determined based on geographic proximity, analysis of local emission sources, and measurements from previous field studies (e.g., CRPAQS), and is consistent with previous $PM_{2.5}$ SIPs in the Valley.

Table 5. $PM_{2.5}$ speciation data used for each $PM_{2.5}$ design site.

AQS Site ID	$PM_{2.5}$ Design Site (FRM/FEM Monitor)	$PM_{2.5}$ Speciation Site
60290016	Bakersfield – Planz	Bakersfield – California
60392010	Madera	Fresno – Garland
60311004	Hanford	Visalia – Church
61072002	Visalia	Visalia – Church
60195001	Clovis	Fresno – Garland
60290014	Bakersfield – California Ave.	Bakersfield – California
60190011	Fresno – Garland	Fresno – Garland
60990006	Turlock	Modesto – 14th
60195025	Fresno – Hamilton & Winery	Fresno – Garland
60771002	Stockton	Modesto – 14th
60470003	Merced – S Coffee	Modesto – 14th
60990005	Modesto	Modesto – 14th
60472510	Merced – Main Street	Modesto – 14th
60772010	Manteca	Modesto – 14th
60192009	Tranquility	Fresno – Garland

Since the FRM $PM_{2.5}$ monitors do not retain all of the $PM_{2.5}$ mass that is measured by the speciation samplers, the U.S. EPA (2014) recommends using the SANDWICH approach (Sulfate, Adjusted Nitrate, Derived Water, Inferred Carbon Hybrid material balance) described by Frank (2006) to apportion the FRM $PM_{2.5}$ mass to individual $PM_{2.5}$ species based on nearby CSN speciation data. A detailed description of the SANDWICH method can be found in the modeling protocol and in the U.S. EPA (2014) modeling guidance. In addition, based on completeness of the data, $PM_{2.5}$ speciation data from 2010 – 2013 were utilized. For the annual DV calculation, for each quarter, percent contributions from individual chemical species to FRM $PM_{2.5}$ mass were calculated as the average of the corresponding quarters from 2010-2013. For the 24-hour DV calculation, percent contributions were calculated for each quarter as the average of the top 10% measured $PM_{2.5}$ days from the corresponding quarter from 2010-2013. In general, the inter-annual variability of the species fractions is small compared to the variability in the species concentrations and so the use of average data from 2010 – 2013 is appropriate.

2.6 FUTURE YEAR DESIGN VALUES

The approach to projecting future year annual and 24-hour $PM_{2.5}$ DVs is described briefly below. See U.S. EPA (2014) and the Photochemical Modeling Protocol Appendix for additional details. Projecting baseline annual $PM_{2.5}$ DVs to the future involves the following steps.

Step 1: Compute observed quarterly weighted average concentrations (consistent with the weighted average DV calculation) at each monitor for the following species: ammonium, nitrate, sulfate, organic carbon, elemental carbon, and other primary PM. This is done by multiplying quarterly weighted average FRM $PM_{2.5}$ concentrations by the fractional composition of $PM_{2.5}$ species for each quarter.

Step 2: Compute the component-specific RRF for each quarter and each species at each monitor based on the reference and future year modeling. The RRF for a specific component *j* is calculated using the following expression:

$$RRF_j = \frac{[C]_{j,\ future}}{[C]_{j,\ reference}} \quad (1)$$

Where $[C]_{j,\ future}$ is the modeled quarterly mean concentration for component *j* predicted for the future year averaged over the 3x3 array of grid cells surrounding the monitor, and $[C]_{j,reference}$ is the same, but for the reference year simulation. An RRF was calculated for each species in Step 1 and at each monitor and for each quarter.

Step 3: Apply the component specific RRF from Step 2 to the observed quarterly weighted average concentrations from Step 1 to obtain projected quarterly species concentrations.

Step 4: Use the online E-AIM model (http://www.aim.env.uea.ac.uk/aim/aim.php) to calculate future year particle-bound water for each quarter at each monitor based on projected ammonium sulfate and ammonium nitrate concentrations.

Step 5: The projected concentration for each quarter is summed over all species, including particle bound water from Step 4, as well as a blank mass of 0.5 $\mu g/m^3$ to obtain the future quarterly average $PM_{2.5}$ concentration. Finally, the future annual $PM_{2.5}$ DVs are calculated as the average of the projected $PM_{2.5}$ concentrations from the four quarters. If the projected annual DV is ≤ NAAQS, then the attainment test is passed.

Similarly, projecting baseline 24-hour $PM_{2.5}$ DVs to the future involves the steps outlined below. See U.S. EPA (2014) and the Photochemical Modeling Protocol Appendix for additional details.

Step 1: Determine the top eight days with the highest observed 24-hour $PM_{2.5}$ concentrations in each quarter and year used in the design value calculation (a total of 32 days per year).

Step 2: Calculate quarterly ambient species fractions on “high” $PM_{2.5}$ days for each of the major $PM_{2.5}$ component species (i.e., sulfate, nitrate, ammonium, elemental carbon, organic carbon, other primary $PM_{2.5}$ material). The “high” days are represented by the top 10% of measured days in each quarter. Depending on the sampling frequency, the number of days captured in the top 10% would range from three to nine. The species fractions of $PM_{2.5}$ are calculated using the “SANDWICH” approach which was described previously. These quarter-specific fractions along with the FRM $PM_{2.5}$ concentrations are then used to calculate species concentrations for each of the 32 days per year determined in Step 1.

Step 3: quarterly RRFs are calculated based on the average for each component over the top 10% of modeled days (or the top nine days per quarter) with the highest total 24-hour average $PM_{2.5}$ concentration from the reference year. Peak $PM_{2.5}$ values are selected and averaged using the $PM_{2.5}$ concentration simulated at the single grid cell containing the monitoring site for calculating the 24-hour $PM_{2.5}$ RRF (as opposed to the 3x3 array average used in the annual $PM_{2.5}$ RRF calculation).

Step 4: Apply the component and quarter specific RRF to observed daily species concentrations from Step 2 to obtain future year concentrations of ammonium, sulfate, nitrate, elemental carbon, organic carbon and other primary $PM_{2.5}$.

Step 5: Calculate future year concentrations for particle bound water using the E-AIM model for each of the top days from each quarter. Then, sum the concentration of each of the species components plus a blank mass of 0.5 $\mu g/m^3$ to obtain the total $PM_{2.5}$ concentration for each of the 32 days per year and at each site. Sort the 32 days for each site and year, and calculate the 98^{th} percentile value corresponding to each year.

Step 6: Calculate the future design value at each site based on the 98^{th} percentile concentrations calculated in Step 5 following the standard protocol for calculating design values (see Table 3). Compare the future-year 24-hour design values to the

NAAQS. If the projected design value is ≤ the NAAQS, then the attainment test is passed.

3 METEOROLOGICAL MODELING

California's proximity to the ocean, complex terrain, and diverse climate represent a unique challenge for developing meteorological fields that adequately represent the synoptic and mesoscale features of the regional meteorology. In summertime, the majority of the storm tracks are far to the north of the state and a semi-permanent Pacific high typically sits off the California coast. Interactions between this eastern Pacific subtropical high pressure system and the thermal low pressure further inland over the Central Valley or South Coast lead to conditions conducive to pollution buildup (Fosberg and Schroeder, 1966; Bao et al., 2008). In wintertime, periods of high atmospheric pressure bring light winds and, sometimes, low solar insolation (Daly et al. 2009) to the Central Valley. Because of the topographical features surrounding San Joaquin Valley, under such conditions, a layer of cold and wet air can be overlaid by warm air aloft creating strong and long-lasting stagnation in the area (Whiteman et al. 2001). It is under such conditions that high surface particulate matter concentrations typically occur (Gilles et al. 2010; Baker et al. 2011).

In the past, the ARB has utilized both prognostic and diagnostic meteorological models, as well as hybrid approaches in an effort to develop meteorological fields for use in air quality modeling that most accurately represent the meteorological processes which are important to air quality (e.g., Jackson et al., 2006). In this work, the state-of-the-science Weather and Research Forecasting (WRF) prognostic model (Skamarock et al., 2005) version 3.6 was utilized to develop the meteorological fields used in the subsequent photochemical model simulations.

3.1 WRF MODEL SETUP

The WRF meteorological modeling domain consisted of three nested Lambert projection grids of 36-km (D01), 12-km (D02), and 4-km (D03) uniform horizontal grid spacing (Figure 1). WRF was run simultaneously for the three nested domains with two-way feedback between the parent and the nest grids. The D01 and D02 grids were used to resolve the larger scale synoptic weather systems, while the D03 grid resolved the finer details of the atmospheric conditions and was used to drive the air quality model simulations. All three domains utilized 30 vertical sigma layers (defined in Table 6), with the major physics options for each domain listed in Table 7.

Initial and boundary conditions (IC/BCs) for the WRF modeling were based on the 32-km horizontal resolution North American Regional Reanalysis (NARR) data that are archived at the National Center for Atmospheric Research (NCAR). Boundary conditions to WRF were updated at 6-hour intervals for the 36-km grid (D01). In addition, surface and upper air observations obtained from NCAR were used to further refine the analysis data that were used to generate the IC/BCs. Analysis nudging was employed in the outer 36-km grid (D01) to ensure that the simulated meteorological fields were adequately constrained and did not deviate from the observed meteorology. No nudging was used on the two inner domains to allow model physics to work fully without externally imposed forcing (Rogers et al., 2013).

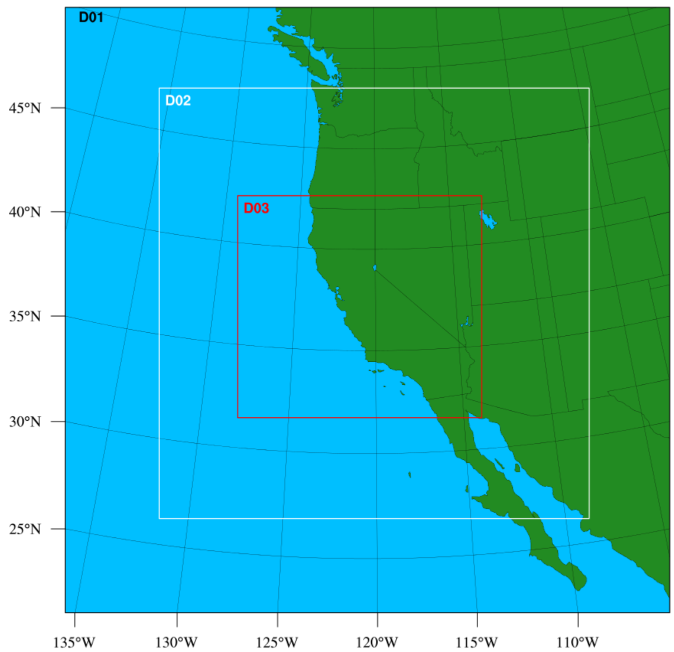

Figure 1. WRF modeling domains (D01 36km; D02 12km; and D03 4km).

Table 6. WRF vertical layer structure.

Layer Number	Height (m)	Layer Thickness (m)
30	16082	1192
29	14890	1134
28	13756	1081
27	12675	1032
26	11643	996
25	10647	970
24	9677	959
23	8719	961
22	7757	978
21	6779	993
20	5786	967
19	4819	815
18	4004	685
17	3319	575
16	2744	482
15	2262	403
14	1859	334
13	1525	279
12	1246	233
11	1013	194
10	819	162
9	657	135
8	522	113
7	409	94
6	315	79
5	236	66
4	170	55
3	115	46
2	69	38
1	31	31
0	0	0

Note: Shaded layers denote the subset of vertical layers used in the CMAQ photochemical model simulations.

Table 7. WRF Physics Options.

Physics Option	**Domain**		
	D01 (36 km)	**D02 (12 km)**	**D03 (4 km)**
Microphysics	WSM 6-class graupel scheme	WSM 6-class graupel scheme	WSM 6-class graupel scheme
Longwave radiation	RRTM	RRTM	RRTM
Shortwave radiation	Dudhia scheme	Dudhia scheme	Dudhia scheme
Surface layer	Revised MM5 Monin-Obukhov	Revised MM5 Monin-Obukhov	Revised MM5 Monin-Obukhov
Land surface	TD Scheme (Jan., Feb., Nov. and Dec.) Pleim-Xiu LSM (others)	TD Scheme (Jan., Feb., Nov. and Dec.) Pleim-Xiu LSM (others)	TD Scheme (Jan., Feb., Nov. and Dec.) Pleim-Xiu LSM (others)
Planetary Boundary Layer	YSU	YSU	YSU
Cumulus Parameterization	Kain-Fritsch scheme	Kain-Fritsch scheme	None

3.2 WRF MODEL RESULTS AND EVALUATION

Simulated surface wind speed, temperature, and relative humidity from the 4 km domain were validated against hourly observations at 77 surface stations in the SJV. Observational data for the surface stations were obtained from the ARB's archived meteorological database (http://www.arb.ca.gov/aqmis2/aqmis2.php). Table 8 lists the observational stations and the parameters measured at each station, including wind speed and direction (wind), temperature (T) and relative humidity (RH). The location of each of these sites is shown in Figure 2. Quarterly and annual quantitative performance metrics for 2013 were used to compare hourly surface observations and modeled estimates: mean bias (MB), mean error (ME) and index of agreement (IOA) based on recommendations from Simon et al. (2012). A summary of these statistics by performance region is shown in Tables 9 through 13. The performance regions cover roughly the Modesto, Fresno, Visalia, and Bakersfield regions, as well as one for the entire San Joaquin Valley (SJV), respectively. The region around Modesto includes sites 5737, 2833, and 2080. The region surrounding Fresno encompasses sites 5741, 2449, 2013, and 2844. The region around Visalia includes sites 2032, 5386, and 3250, while the region covering Bakersfield includes sites 5287 and 3146 (note that valid relative humidity observations in the Bakersfield area were only available at site 5287 for the months of January through May 2013). Model performance statistical metrics were calculated using all of the available data. All the sites in the valley are included in the SJV performance region (in addition to the sites mentioned above). The distribution of daily mean bias and mean error are shown in Figures 3 and 4. Figures 5 and 6 show observed vs. modeled scatter plots.

From a valley-wide perspective, the wind speed biases were positive in each quarter of 2013. At Bakersfield the biases turn slightly negative throughout the year, and are mostly less than 0.6 m/s. The annual temperature biases are less than 1 K in all performance regions, with the quarterly temperature biases reaching as high as -1.87 K in Bakersfield during the second quarter of 2013. Simulated temperature is generally in good agreement with the observations in all regions with the index of agreement (IOA) above 0.90 (1.0 represents perfect agreement). Relative humidity biases are positive except in the Modesto region. The annual bias values range from -1.53% to 12.47%, with the largest bias occurring in Visalia. These results are comparable to other recent WRF modeling efforts in California investigating ozone formation in Central California (e.g., Hu et al., 2012) and modeling analysis for the CalNex and CARES field studies (e.g., Fast et al., 2014; Baker et al., 2013; Kelly et al., 2014; Angevine et al., 2012). Detailed hourly time-series of surface temperature, relative humidity, wind speed, and wind direction for SJV can be found in the supplementary material, together with 2013 quarterly mean bias and mean error distributions of these parameters.

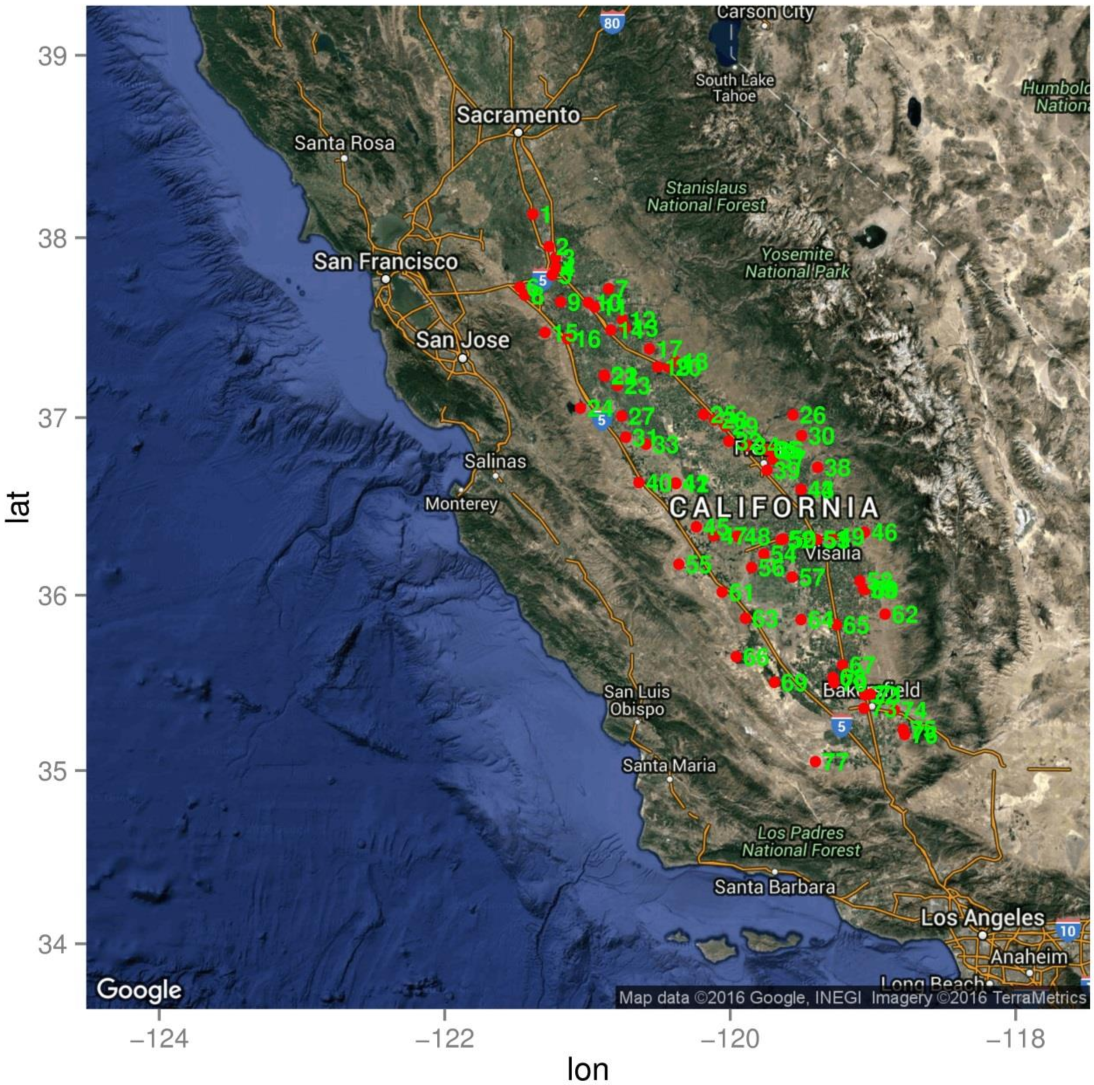

Figure 2. Meteorological observation sites in San Joaquin Valley. The numbers correspond to the sites listed in Table 8.

Table 8. Meteorological monitor location and parameter(s) measured.

Site	Site ID	Site Name	Parameter Measured	Site	Site ID	Site Name	Parameter Measured
1	5809	LodiWest	T, RH	40	3309	PanocheRd	Wind, T, RH
2	2094	Stockton-Haz	Wind, T, RH	41	3759	Tranquility	Wind, T
3	5362	StocktonArpt	Wind, T	42	5757	Westlands	T, RH
4	5736	Manteca	T, RH	43	5723	Parlier2	T, RH
5	3772	Manteca-Fish	Wind, T	44	2114	Parlier	Wind, T, RH
6	5810	Tracy	T, RH	45	5828	FivePointsSW	T, RH
7	5831	Oakdale2	T, RH	46	5746	Lindcove	T, RH
8	3696	Tracy_Air	Wind, T	47	5708	FivePoints2	T, RH
9	5737	Modesto3	T, RH	48	2544	Lemoore-Met	Wind, T
10	2833	Modesto-14th	Wind	49	2032	Visalia-NChu	Wind, T
11	2080	Modesto-Met	Wind, T	50	5308	HanfordMuni	Wind, T
12	7233	DenairII	T, RH	51	5386	VisaliaMuni	Wind, T
13	3303	RosePeak	Wind, T, RH	52	3129	Hanford-Irwn	Wind, T
14	2996	Turlock-SMin	Wind, T	53	3250	Visalia-Airp	Wind, T, RH
15	3449	Pulgas	Wind, T, RH	54	3712	StRosaRnchria	Wind, T
16	5805	Patterson2	T, RH	55	6028	CoalingaCIM	T, RH
17	2814	Merced-AFB	Wind, T	56	5715	Stratford2	T, RH
18	5793	Merced	T, RH	57	3194	Corcoran-Pat	Wind, T
19	5318	MercedMuni	Wind, T	58	5812	Portervl	T, RH
20	3022	Merced-SCofe	Wind, T	59	5351	PortervlMuni	Wind, T
21	6079	MERCED 23WSW	T	60	3763	Portrvlle-Ne	Wind, T
22	5752	Kesterson	T, RH	61	3330	KettlemanHls	Wind, T, RH
23	3647	SanLuisNWR	Wind, T, RH	62	3350	FountnSpr	Wind, T, RH
24	3307	LosBanos	Wind, T, RH	63	5717	Kettleman	T, RH
25	5790	Madera	T, RH	64	6813	Alpaugh	T, RH
26	3522	Hurley1	Wind, T, RH	65	5823	Delano2	T, RH
27	5730	LosBanos2	T, RH	66	5729	BlackwllCnr	T, RH
28	5317	MaderaMuni	Wind, T	67	5783	Famoso	T, RH
29	3771	Madera-Av14	Wind, T, RH	68	5709	ShafterUSDA	T, RH
30	3346	FancherCreek	Wind, T, RH	69	5791	Belridge	T, RH
31	5770	Panoche	T, RH	70	2981	Shafter-Wlkr	Wind, T, RH
32	3211	Madera-Rd29	Wind, T, RH	71	2772	Oildale-3311	Wind, T
33	5711	Firebgh-Tel	T, RH	72	5287	MeadowsFld	Wind, T
34	2844	Fresno-Sky#2	Wind, T	73	3146	Baker-5558Ca	Wind, T, RH
35	5741	FSU2	T, RH	74	2312	Edison	Wind, T
36	3026	Clovis	Wind, T, RH	75	3758	Arvin-DiG	Wind, T
37	2449	Fresno-FAT	Wind, T	76	5771	Arvin-Edison	T, RH
38	5787	OrangeCove	T, RH	77	2919	Maricopa-Stn	Wind, T
39	2013	Fresno-Drmnd	Wind, T				

Table 9. Hourly surface wind speed, temperature and relative humidity statistics in Modesto.

Quarter	Observed Mean	Modeled Mean	Mean Bias	Mean Error	IOA
		Wind Speed (m/s)			
Q1	2.08	2.62	0.54	1.16	0.74
Q2	3.04	3.51	0.46	1.43	0.73
Q3	2.64	2.94	0.30	1.18	0.65
Q4	1.66	2.35	0.69	1.23	0.68
Annual	2.41	2.89	0.49	1.26	0.73
		Temperature (K)			
Q1	282.62	282.93	0.31	2.16	0.94
Q2	293.18	292.86	-0.32	2.07	0.96
Q3	295.98	297.06	1.07	2.35	0.93
Q4	283.95	285.73	1.78	2.73	0.93
Annual	288.93	289.65	0.71	2.33	0.97
		Relative Humidity (%)			
Q1	73.52	74.38	0.86	9.14	0.89
Q2	57.03	53.28	-3.75	10.99	0.86
Q3	62.17	55.26	-6.91	13.98	0.72
Q4	67.75	71.40	3.66	11.48	0.85
Annual	65.10	63.57	-1.53	11.40	0.86

Table 10. Hourly surface wind speed, temperature and relative humidity statistics in Fresno.

Quarter	Observed Mean	Modeled Mean	Mean Bias	Mean Error	IOA
		Wind Speed (m/s)			
Q1	1.47	1.90	0.43	1.11	0.56
Q2	2.54	3.12	0.58	1.53	0.59
Q3	2.14	2.65	0.51	1.42	0.47
Q4	1.12	1.69	0.57	1.05	0.52
Annual	1.85	2.37	0.52	1.29	0.61
		Temperature (K)			
Q1	283.76	282.90	-0.86	1.79	0.96
Q2	295.23	294.04	-1.19	2.16	0.95
Q3	299.69	299.22	-0.47	2.22	0.94
Q4	285.65	286.01	0.36	1.93	0.96
Annual	291.18	290.65	-0.53	2.03	0.98
		Relative Humidity (%)			
Q1	71.46	76.39	4.93	10.71	0.86
Q2	48.01	53.07	5.06	11.88	0.83
Q3	45.12	51.45	6.33	14.95	0.65
Q4	64.03	70.79	6.77	13.49	0.83
Annual	57.09	62.87	5.78	12.77	0.86

Table 11. Hourly surface wind speed, temperature and relative humidity statistics in Visalia.

Quarter	Observed Mean	Modeled Mean	Mean Bias	Mean Error	IOA
		Wind Speed (m/s)			
Q1	1.48	1.64	0.16	0.82	0.55
Q2	2.07	2.53	0.45	1.04	0.65
Q3	1.91	2.22	0.31	0.86	0.59
Q4	1.62	1.58	-0.04	0.73	0.60
Annual	1.77	2.00	0.24	0.88	0.65
		Temperature (K)			
Q1	283.66	282.87	-0.79	1.85	0.95
Q2	294.38	293.09	-1.29	2.23	0.95
Q3	298.73	298.42	-0.31	2.56	0.91
Q4	285.19	286.03	0.84	2.11	0.95
Annual	290.03	289.55	-0.48	2.16	0.97
		Relative Humidity (%)			
Q1	73.28	80.72	7.44	11.11	0.82
Q2	47.80	59.94	12.13	17.23	0.73
Q3	47.08	63.07	15.99	21.49	0.49
Q4	61.22	75.43	14.21	16.36	0.77
Annual	57.37	69.84	12.47	16.56	0.76

Table 12. Hourly surface wind speed, temperature and relative humidity statistics in Bakersfield (valid RH data available from January through May only; statistics are based on the available data).

Quarter	Observed Mean	Modeled Mean	Mean Bias	Mean Error	IOA
		Wind Speed (m/s)			
Q1	1.84	1.80	-0.04	0.88	0.59
Q2	2.63	2.47	-0.15	1.03	0.74
Q3	2.12	2.10	-0.02	1.10	0.68
Q4	2.23	1.86	-0.37	0.98	0.61
Annual	2.21	2.09	-0.12	1.00	0.70
		Temperature (K)			
Q1	284.94	283.97	-0.97	1.91	0.95
Q2	295.66	293.78	-1.87	2.44	0.94
Q3	301.17	299.54	-1.63	2.63	0.90
Q4	286.85	286.97	0.12	1.73	0.97
Annual	291.33	290.17	-1.16	2.16	0.97
		Relative Humidity (%)			
Q1	62.65	72.70	10.04	15.15	0.81
Q2	36.94	51.46	14.52	16.82	0.74
Annual	52.27	64.12	11.85	15.83	0.83

Table 13. Hourly surface wind speed, temperature and relative humidity statistics in the San Joaquin Valley.

Quarter	Observed Mean	Modeled Mean	Mean Bias	Mean Error	IOA
		Wind Speed (m/s)			
Q1	2.08	2.62	0.54	1.16	0.74
Q2	3.04	3.51	0.46	1.43	0.73
Q3	2.64	2.94	0.30	1.18	0.65
Q4	1.66	2.35	0.69	1.23	0.68
Annual	2.41	2.89	0.49	1.26	0.73
		Temperature (K)			
Q1	283.31	283.30	-0.01	2.17	0.94
Q2	294.23	293.42	-0.81	2.46	0.94
Q3	298.22	298.21	-0.02	2.82	0.90
Q4	285.08	286.20	1.12	2.65	0.93
Annual	290.19	290.25	0.07	2.52	0.96
		Relative Humidity (%)			
Q1	69.36	71.65	2.29	12.87	0.81
Q2	47.95	52.53	4.57	13.73	0.79
Q3	46.35	54.48	8.12	17.33	0.59
Q4	58.62	68.35	9.72	16.00	0.75
Annual	55.70	61.84	6.14	14.96	0.79

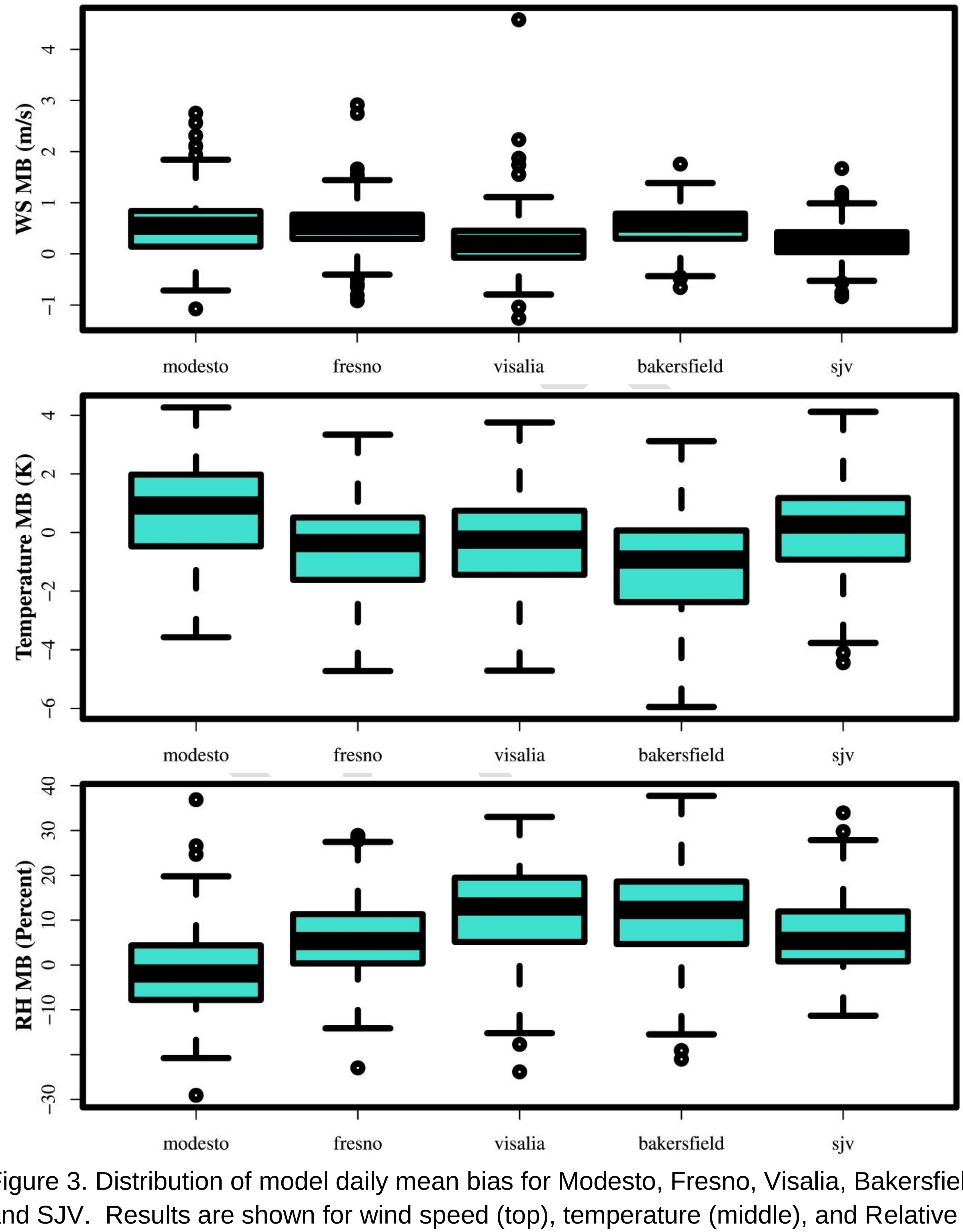

Figure 3. Distribution of model daily mean bias for Modesto, Fresno, Visalia, Bakersfield and SJV. Results are shown for wind speed (top), temperature (middle), and Relative Humidity (bottom).

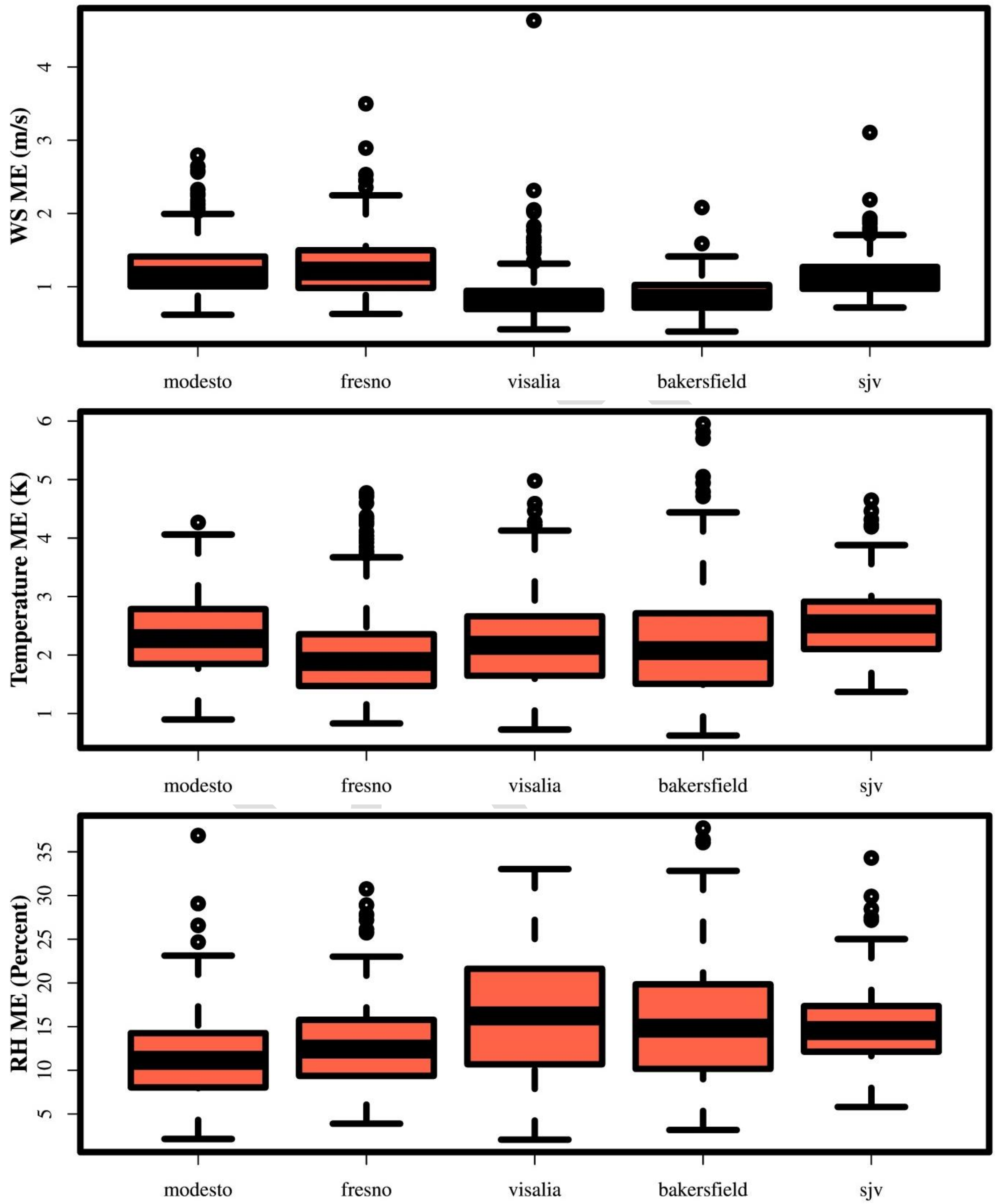

Figure 4. Distribution of model daily mean error for Modesto, Fresno, Visalia, Bakersfield and SJV. Results are shown for wind speed (top), temperature (middle), and Relative Humidity (bottom).

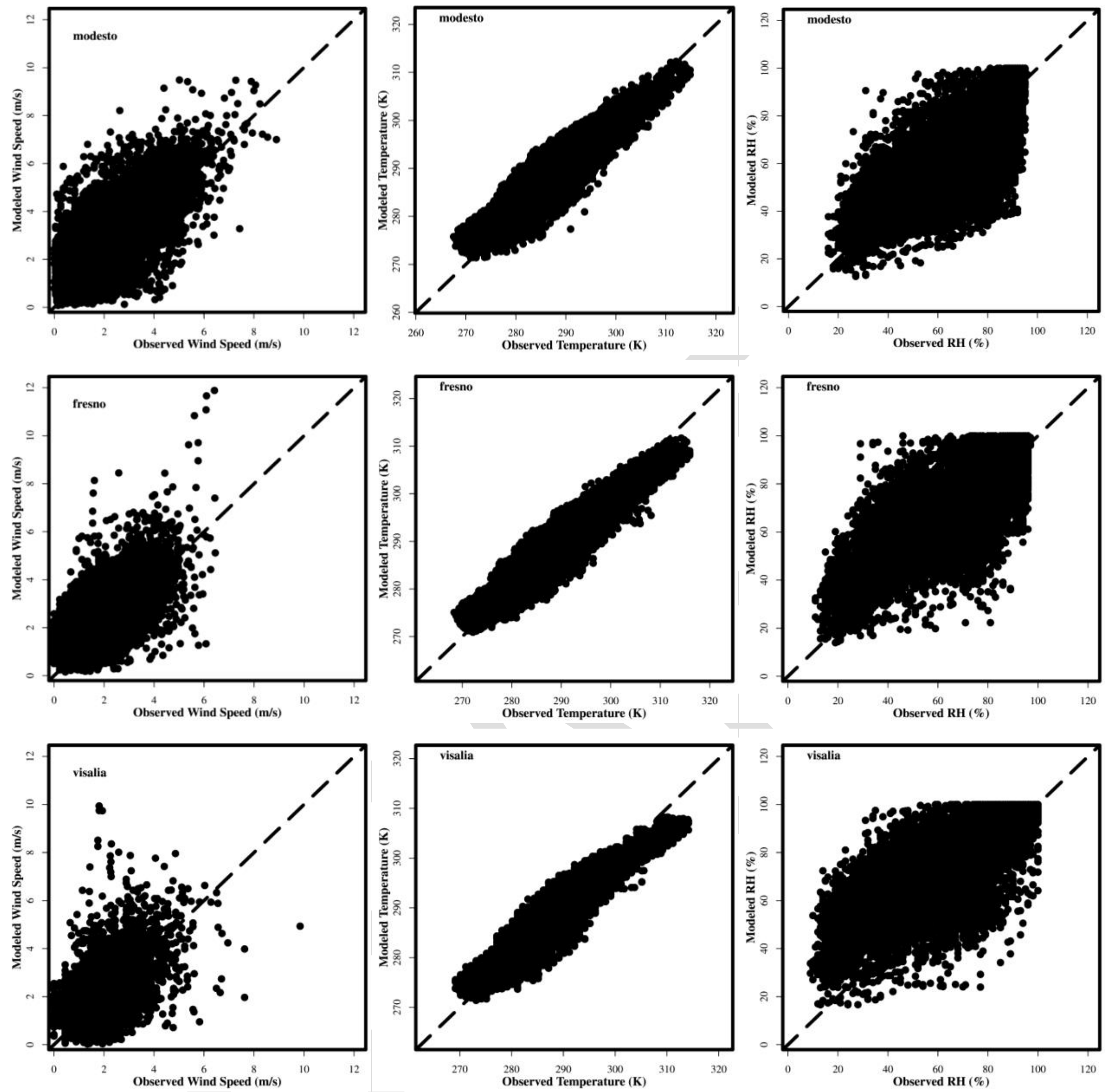

Figure 5. Comparison of modeled and observed hourly wind speed (left column), 2-meter temperature (middle column), and relative humidity (right column). Results for Modesto are shown in the top row, Fresno in the middle row, and Visalia in the bottom row.

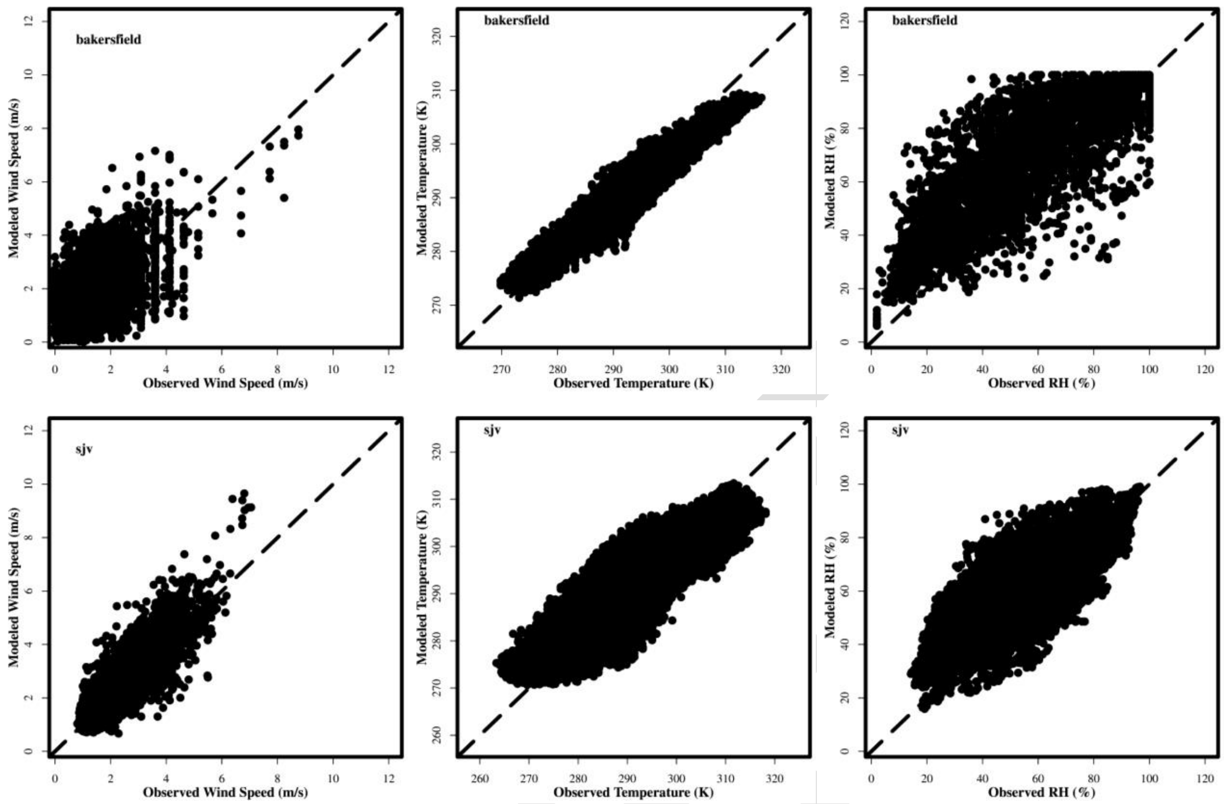

Figure 6. Comparison of modeled and observed hourly wind speed (left column), 2-meter temperature (middle column), and relative humidity (right column). Results for Bakersfield are shown in the top row and SJV in the bottom row.

3.2.1 PHENOMENOLOGICAL EVALUATION

Conducting a detailed phenomenological evaluation for all modeled days can be resource intensive given that the entire year was modeled. However, some insight and confidence that the model is able to reproduce the meteorological conditions leading to elevated particulate matter can be gained by investigating the meteorological conditions during a period of peak PM within the Valley in more detail. The highest $PM_{2.5}$-conducive meteorological conditions in the Valley occurred around January 20, 2013. Surface weather analysis shows that on January 20, the western US was under a typical Great Basin high pressure system. In the 500 hPa map (not shown), a strong high pressure ridge extends from Northern California along the west Pacific coast all the way to Alaska. As shown in Figures 7, 8, and 9, the winds, though weak, are mainly offshore along the northern California coast. Under this type of weather system, conditions in SJV are driven by diurnal cycles of the local winds. Figure 7 shows that at 13:00 PST, January 20, the upslope flows along the eastern side of the Coastal Ranges and the western side of the Sierras, lead to a weak northwesterly flow on the floor of the valley. The downslope winds form at nighttime and in the early morning (Figure 8 and Figure 9). They converge towards the valley and the winds in the center of the valley floor turn southeasterly. At the southern end of the valley, an eddy-like pattern occurs due to the interaction of the katabatic flows. The surface wind distributions of the modeled and observed winds indicate the model was able to capture many of the important features of the meteorological fields in the SJV.

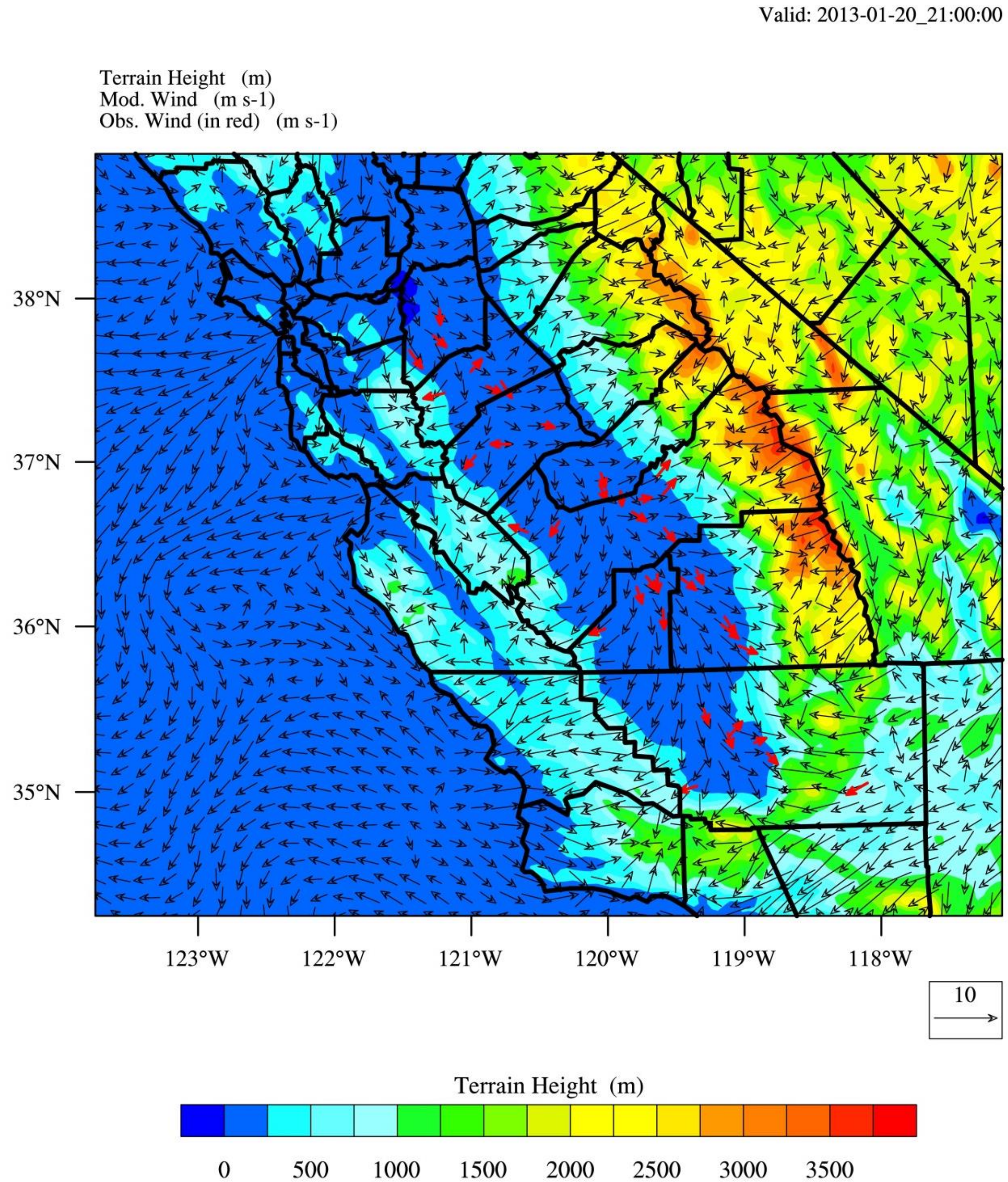

Figure 7. Surface wind field at 13:00 PST January 20, 2013.

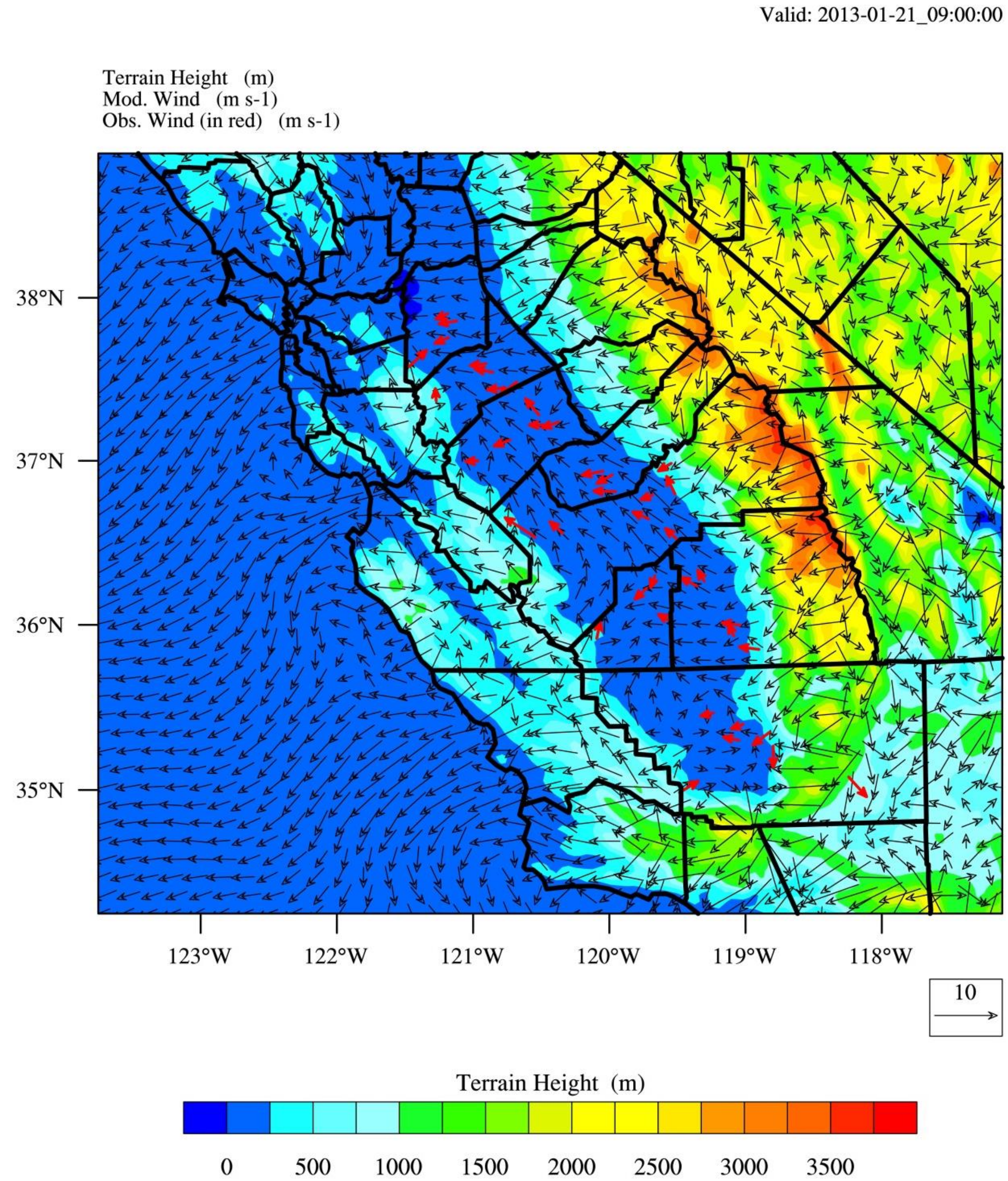

Figure 8. Surface wind field at 01:00 PST January 21, 2013.

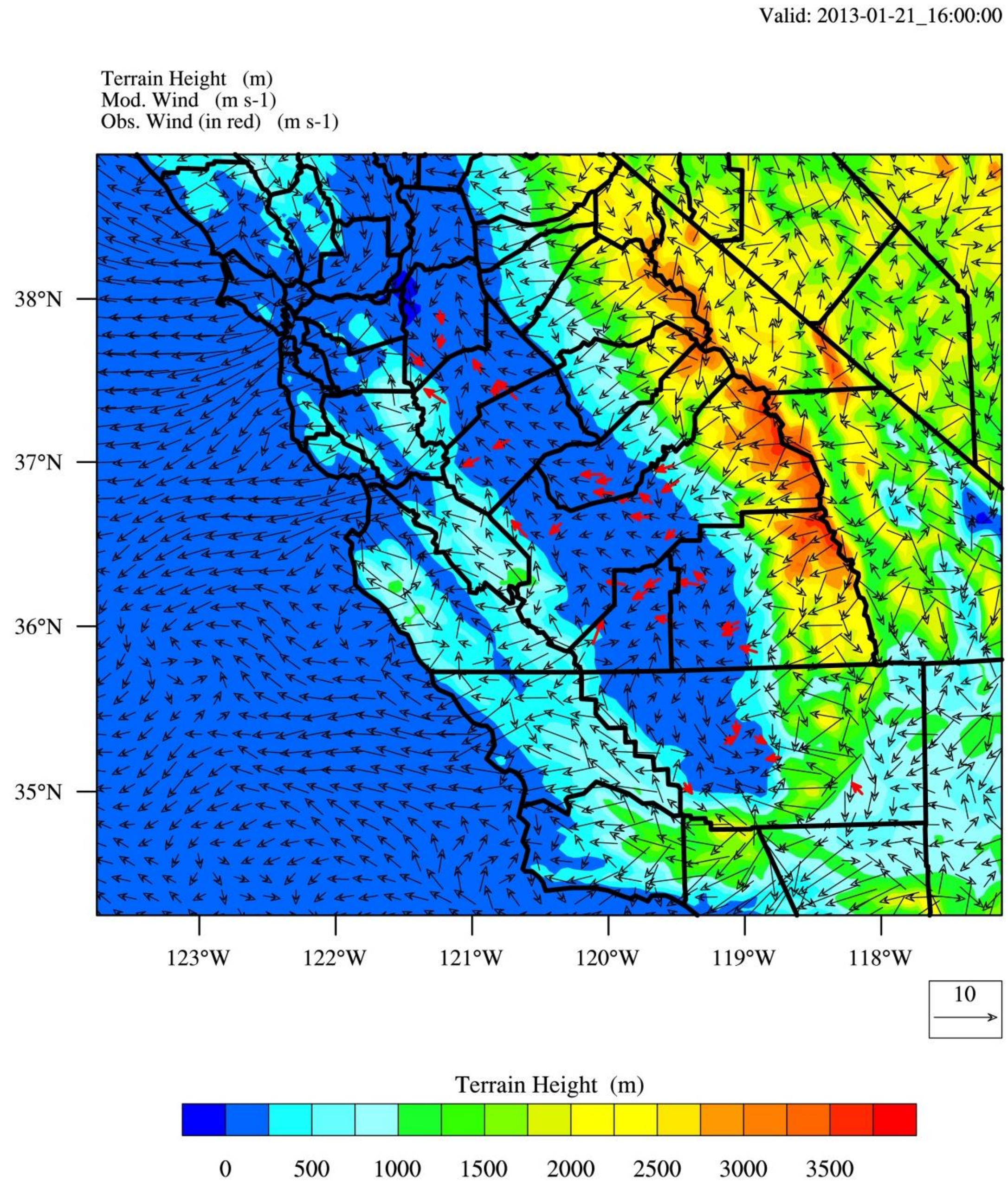

Figure 9. Surface wind field at 08:00 PST January 21, 2013.

4 EMISSIONS

The emissions inventory used in this modeling was based on the most recent inventory submitted to the U.S. EPA, with base year 2012 and projected to 2013 under growth and control conditions (http://www.arb.ca.gov/planning/sip/2012iv/2012iv.htm). For a detailed description of the emissions inventory, updates to the inventory, and how it was processed from the planning totals to a gridded inventory for modeling, see the Modeling Emissions Inventory Appendix.

4.1 EMISSIONS SUMMARIES

Table 14 summarizes 2013, 2020, 2024, and 2025 SJV annual anthropogenic emissions for the five $PM_{2.5}$ precursors. These emission totals are based on the model-ready emission inventory and are inherently different from the planning emission inventory because the model-ready inventory considers additional factors such as weekday/weekend differences in on-road mobile emissions, day-to-day changes in residential wood burning activity, and the effects of meteorology on ammonia emissions. From 2013 to 2020, anthropogenic emissions in the SJV will drop approximately 35%, 8%, 6%, 8%, and 1% for NO_x, ROG, primary $PM_{2.5}$, SO_x, and NH_3, respectively. Among these five precursors, anthropogenic NO_x emissions show the largest relative reduction, dropping from 288 tons/day in 2013 to 187 tons/day in 2020. Anthropogenic $PM_{2.5}$ emissions will drop from 61 tons/day to 57 tons/day, reflecting a 6% reduction from 2013 to 2020. From 2020 to 2024, NO_x and $PM_{2.5}$ emissions will further drop by 42% and 7%, respectively, while emissions of other pollutants will stay nearly flat. From 2024 to 2025, NO_x emissions will drop a further 3%, while emissions of other pollutants remain relatively constant.

Note that the emission totals presented in Table 14 were calculated from the modeling inventory based on CEPAM version 1.0.5. Since the modeling inventory includes day-specific adjustments not included in the planning inventory, the planning and modeling inventories are expected to be comparable, but not identical. In addition, the 2024 and 2025 emission totals in Table 14 are from the attainment inventory, and so include additional emission reductions beyond the future baseline inventory for the respective year. These additional emission reductions for 2024 and 2025 are summarized in Tables 15-16 for NO_x and $PM_{2.5}$, respectively. A description of these emission control measures can be found in the SIP under the chapter describing the control strategy. Here, only the control factors for under-fired charbroil and residential wood combustion (RWC) are described in more detail.

Table 14. SJV annual modeling emissions for 2013, 2020 (baseline), 2024 (attainment), and 2025 (attainment)*.

Category	NO_x	ROG	$PM_{2.5}$	SO_x	NH_3
2013 (tons/day)					
Stationary	38.5	90.8	8.5	7.2	13.9
Area	8.1	153.3	40.2	0.3	310.0
On-road Mobile	154.6	45.1	5.7	0.6	4.4
Other Mobile	87.1	35.8	6.2	0.3	6.0
Total	288.2	325.0	60.5	8.4	334.3
2020 (tons/day)					
Stationary	28.5	95.1	8.4	6.5	15.2
Area	7.8	151.8	40.0	0.3	306.9
On-road Mobile	81.0	22.4	3.2	0.6	3.6
Other Mobile	69.8	28.7	5.4	0.3	6.0
Total	187.1	298.0	57.0	7.7	331.7
2024 (tons/day)					
Stationary	26.1	99.2	8.5	6.7	16.2
Area	6.9	152.5	37.8	0.3	304.7
On-road Mobile	32.1	17.5	3.1	0.6	3.4
Other Mobile	42.5	25.9	3.8	0.3	6.0
Total	107.6	295.1	53.2	7.9	330.2
2025 (tons/day)					
Stationary	26.0	100.3	8.6	6.8	16.4
Area	6.8	152.9	38.5	0.3	304.1
On-road Mobile	30.5	16.9	3.1	0.6	3.4
Other Mobile	41.2	25.3	3.6	0.3	6.0
Total	104.6	295.4	53.7	7.9	330.0

*: Note: emissions here are based on the model-ready inventory, which considers additional factors such as weekday/weekend difference in on-road mobile emissions. Therefore, emission values here are different from planning inventory presented in other documents.

Table 15: Additional NO_x emission reductions (tons/day) implemented in the 2024 and 2025 attainment inventories.

Emission Reduction	2024	2025
Electrification of agricultural combustion engines (50% reduction)	0.79	0.77
Stationary source fuel combustion	1.04	1.04
Agricultural equipment	11.50	10.00
Off-road equipment	2.10	1.70
Locomotives	1.40	1.30
Heavy duty diesel trucks	18.20	18.90
Flaring operations (20% reduction)	0.05	0.05

Table 16: Additional $PM_{2.5}$ emission reductions (tons/day) implemented in the 2024 and 2025 attainment inventories.

Emission Reduction	2024	2025
Residential wood combustion	0.47	0.47
Under-fired charbroils	0.56	0.57
Electrification of agricultural combustion engines (50% reduction)	0.025	0.024
Agricultural equipment	0.80	0.80
Enhanced conservation management practices (tillage)	0.46	0.46
Enhanced conservation management practices (fallow land)	0.19	0.19
Woodchips at Bakersfield (75% reduction)	0.00012	0.00012

In an effort to achieve the emission reductions needed to attain the $PM_{2.5}$ standards, a control strategy has been developed to reduce $PM_{2.5}$ emissions from under-fired charbroilers by approximately 30%. The strategy includes $PM_{2.5}$ emission reductions from large new restaurants and existing restaurants with charbroilers within urban boundaries in what are classified as hot spot areas. The percent reduction in direct $PM_{2.5}$ emissions from under-fired charbroilers for each county fully or partially classified as a hot spot area is given in Table 17. In addition, Figure 10 shows the hot spot areas in which the under-fired charbroiling $PM_{2.5}$ reductions will be applied.

Table 17. $PM_{2.5}$ percent reductions from under-fired charbroiling controls in 2024 (the same reductions were applied to 2025).

County / City	Reduction from existing restaurants	Reduction from large new restaurants	Total reductions
Fresno County	22.8%	7.8%	30.6%
Kern County	22.5%	7.8%	30.3%
City of Corcoran	22.9%	7.8%	30.7%
City of Madera	22.5%	7.8%	30.3%
City of Visalia	22.5%	7.8%	30.3%

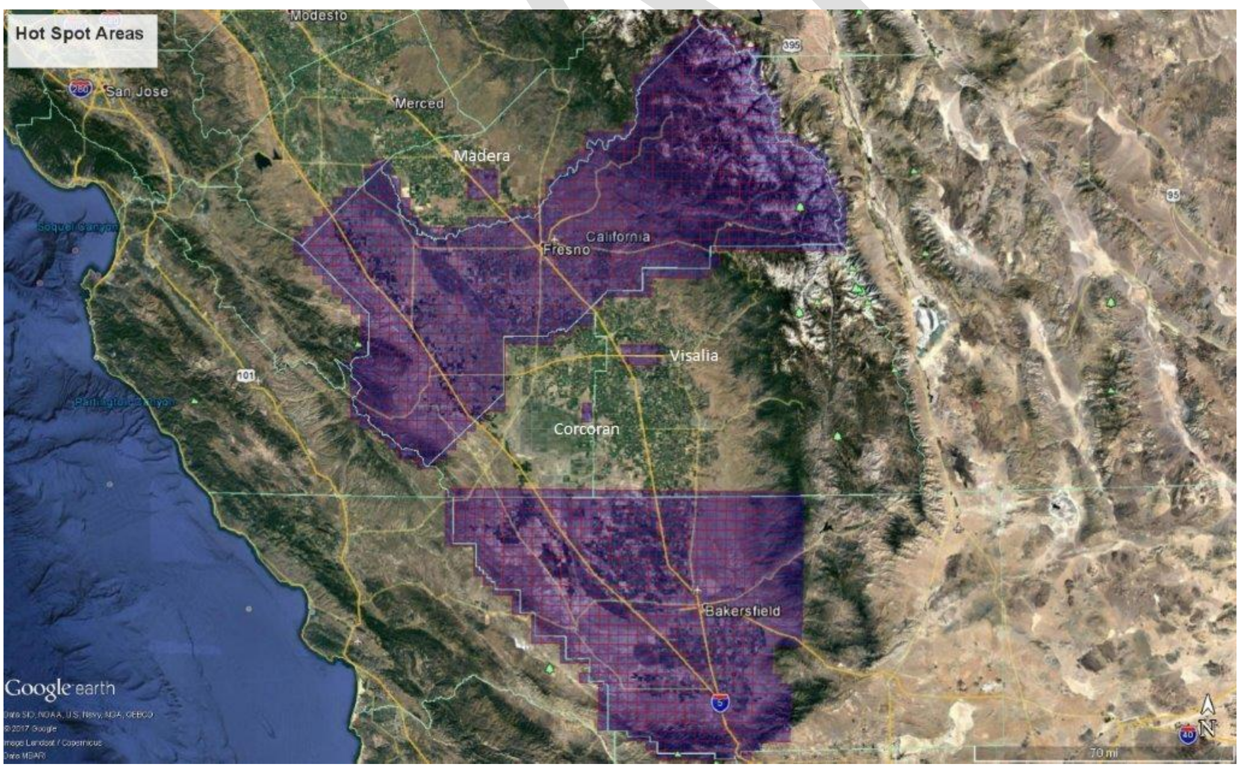

Figure 10. Hot spot areas for application of under-fired charbroiling/residential wood combustion $PM_{2.5}$ reductions

In 2024 and 2025, RWC emissions are subject to more stringent control. First, RWC emissions are reduced through the enhanced Burn Cleaner program, which focuses on changing out old high emitting wood stoves with cleaner burning stoves (a description of the Burn Cleaner program can be found in the chapter describing the control strategy). Table 18 shows the county-specific Burn Cleaner reductions (expressed as retention factors) for each county, which was provided by the San Joaquin Valley Air Pollution Control District. The RWC hot spot zones are defined to be the same as those for the charbroiling control, so no hot spot area is specified for the counties of Merced, San Joaquin, and Stanislaus.

Table 18: County-specific burn cleaner retention factors for 2024 (the same retention factors were applied for 2025).

County	Hot spot area retention factor	Non-hot spot area retention factor
Fresno	0.564	1.000
Kern	0.635	1.000
Kings	0.800	0.900
Madera	0.800	0.900
Merced	N/A	0.922
San Joaquin	N/A	0.812
Stanislaus	N/A	0.872
Tulare	0.800	0.900

In addition to the Burn Cleaner program, the current RWC curtailment program implemented in the SJV will be strengthened. Currently, the SJV has the following RWC curtailment program:

1.) Level 0 – burning allowed if forecasted $PM_{2.5}$ concentration is less than 20 µg/m^3
2.) Level 1 – burning permitted by registered, clean-burning devices if forecasted $PM_{2.5}$ concentration is between 20 µg/m^3 and 65 µg/m^3
3.) Level 2 – no burning is allowed if forecasted $PM_{2.5}$ concentration is higher than 65 µg/m^3

The curtailment program is applied on a county-specific basis (i.e., curtailment only applies to that county where forecasted $PM_{2.5}$ is above the threshold) and only applies to areas with access to natural gas service. In 2024/2025, in hot spot areas (shown in Figure 10, for Fresno/Kern counties, curtailment hot spot is limited to areas with access to natural gas service), the Level 1 threshold of the Burn Cleaner program is strengthened and will be triggered when forecasted $PM_{2.5}$ is greater than 12 µg/m^3, while Level 2 is triggered when forecasted $PM_{2.5}$ is greater than 35 µg/m^3. For non-hotspot areas, the current triggering thresholds are maintained. A compliance rate of 97% is assumed in 2024/2025 when curtailment is triggered. Finally, RWC emission reductions are assumed to be the same for 2024 and 2025 given the lack of growth in RWC emissions and the application of the same curtailment program.

Monthly biogenic ROG totals for 2013 in the SJV are shown in Figure 11 (note that the 2013 biogenic emissions were used for all model runs). Biogenic ROG emissions are highest in the summer at nearly 1800 tons/day in July when temperature, insolation, and leaf area are generally at their peak, and drop to near zero during winter months.

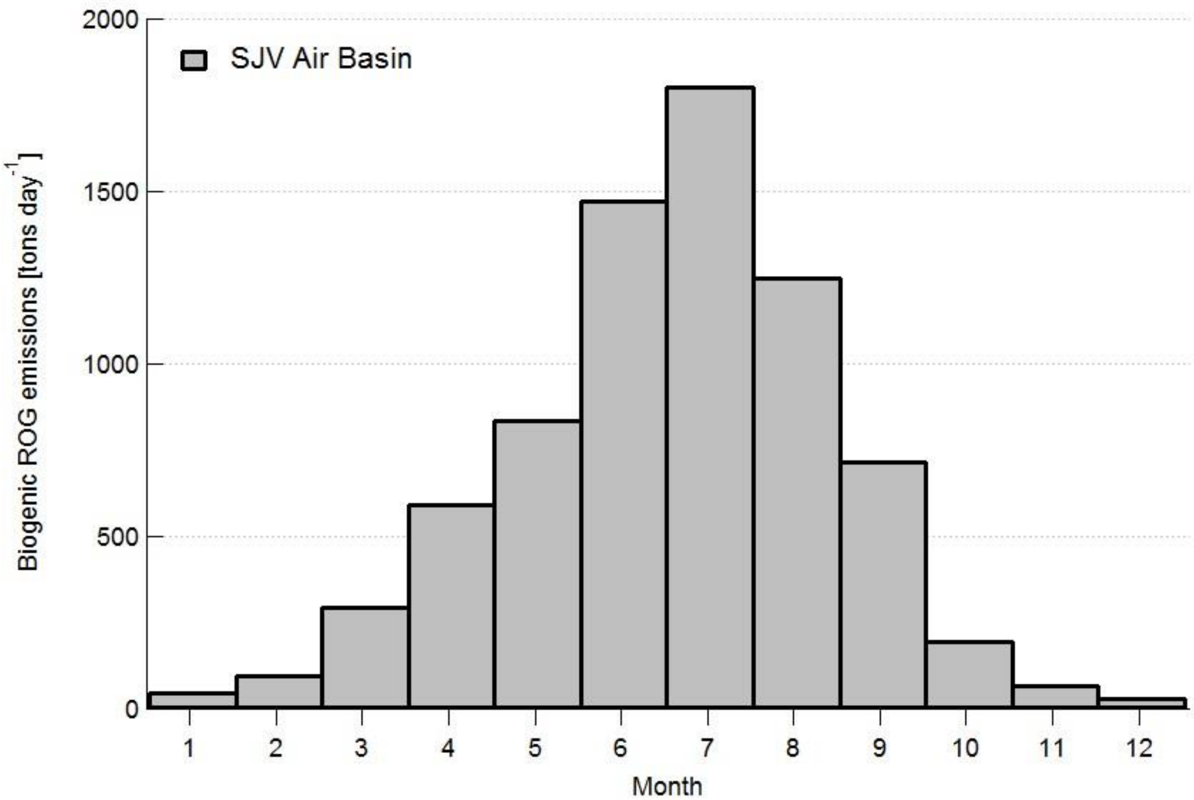

Figure 11. Monthly average biogenic ROG emissions for 2013.

5 $PM_{2.5}$ MODELING

5.1 CMAQ MODEL SETUP

Figure 12 shows the CMAQ modeling domains used in this work. The larger domain covering all of California has a horizontal grid resolution of 12 km with 107 x 97 lateral grid cells for each vertical layer and extends from the Pacific Ocean in the west to Eastern Nevada in the east and runs from the U.S.-Mexico border in the south to the California-Oregon border in the north. The smaller nested domain covering the SJV region has a finer scale 4 km grid resolution and includes 87 x 103 lateral grid cells. While the nested domain is smaller than that used for ozone modeling in the Valley (see the Photochemical Modeling Protocol), as long as the larger statewide 12 km domain is utilized to provide dynamic boundary condition inputs to the smaller 4 km domain, there is no appreciable difference in simulated $PM_{2.5}$ predictions between the smaller domain utilized for $PM_{2.5}$ modeling and the larger domain used for ozone modeling. Both the 12 km and 4 km domains are based on a Lambert Conformal Conic projection with reference longitude at – 120.5ºN and 60ºN, which is consistent with WRF domain settings. The 30 vertical layers from WRF were mapped onto 18 vertical layers for CMAQ, extending from the surface to 100 mb such that a majority of the vertical layers fall within the planetary boundary layer (see the Photochemical Modeling Protocol for details).

The CMAQ model version 5.0.2 (http://www.airqualitymodeling.org/cmaqwiki/index.php?title=CMAQ_version_5.0.2_%28April_2014_release%29_Technical_Documentation) released by the U.S. EPA in May 2014 was used for all air quality model simulations, consistent with the 2016 SJV $PM_{2.5}$ SIP (CARB, 2016). The SAPRC07 chemical mechanism and aerosol module aero6 were selected as the gas-phase and aerosol modules, respectively. Further details of the CMAQ configuration can be found in Table 19 and in the Photochemical Modeling Protocol. The same configuration was used for all simulations.

Annual simulations were conducted on a simultaneous month-by-month basis, rather than one single continuous simulation. For each month, the CMAQ simulations included a seven day spin-up period (i.e., the last seven days of the previous month) for the outer 12 km domain, where initial conditions were set to the default CMAQ initial conditions. These outer domain simulations were used to provide initial and lateral boundary conditions for the inner 4 km simulation, which utilized a three day spin-up period.

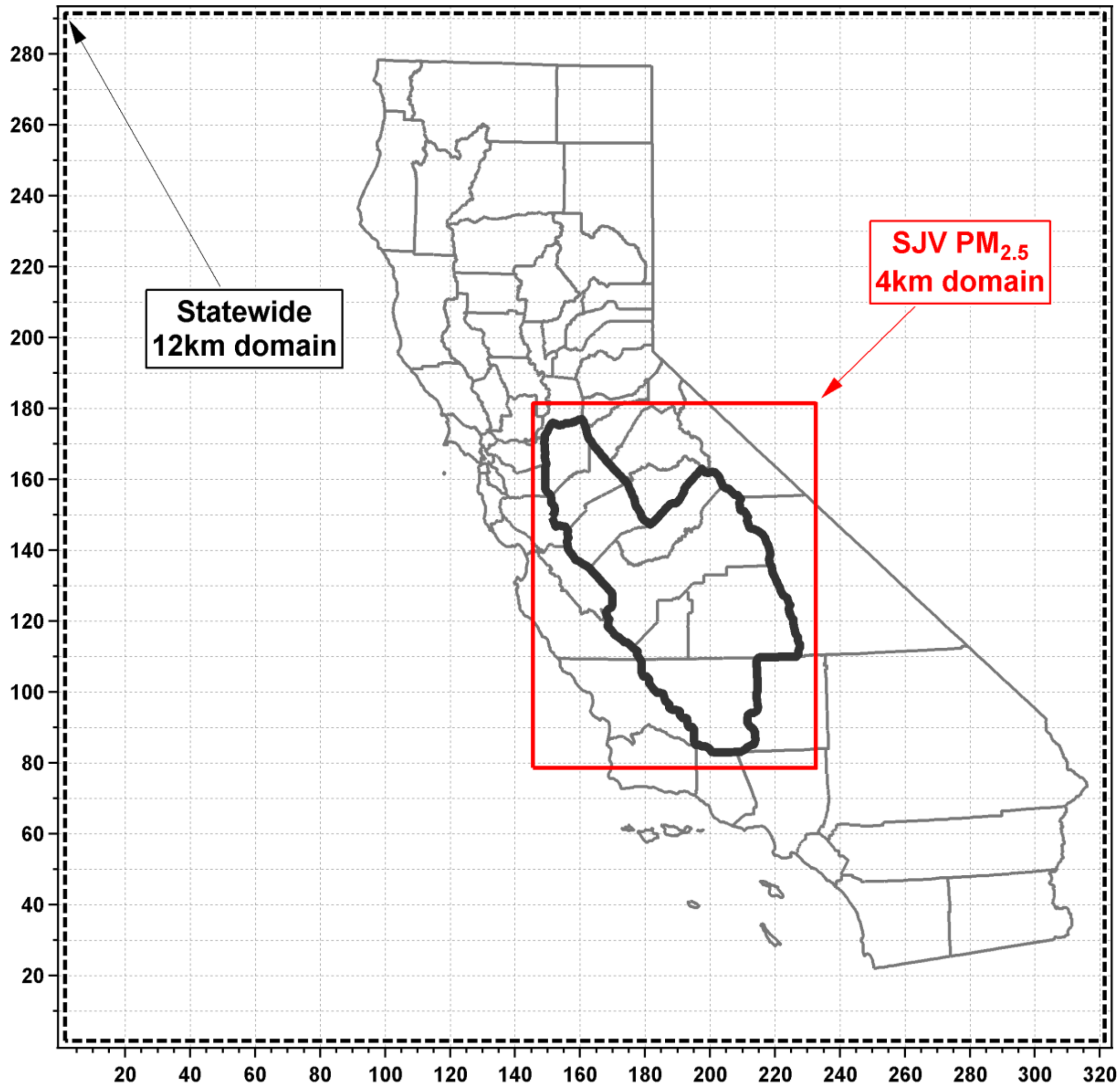

Figure 12. CMAQ modeling domains utilized in the modeling assessment.

Chemical boundary conditions for the outer 12 km domain were extracted from the global chemical transport Model for Ozone and Related chemical Tracers, version 4 (MOZART-4; Emmons et al., 2014). The MOZART-4 model output for 2013 was obtained from the National Center for Atmospheric Research (NCAR; https://www2.acom.ucar.edu/gcm/mozart) using the simulations driven by meteorological fields from the NASA GMAO GEOS-5 model. The same MOZART derived BCs for the 12 km outer domain were used in all simulations.

Table 19. CMAQ configuration and settings.

Process	Scheme
Horizontal advection	Yamo (Yamartino scheme for mass-conserving advection)
Vertical advection	WRF-based scheme for mass-conserving advection
Horizontal diffusion	Multi-scale
Vertical diffusion	ACM2 (Asymmetric Convective Model version 2)
Gas-phase chemical mechanism	SAPRC-07 gas-phase mechanism version "B"
Chemical solver	EBI (Euler Backward Iterative solver)
Aerosol module	Aero6 (the sixth-generation CMAQ aerosol mechanism with extensions for sea salt emissions and thermodynamics; includes a new formulation for secondary organic aerosol yields)
Cloud module	ACM_AE6 (ACM cloud processor that uses the ACM methodology to compute convective mixing with heterogeneous chemistry for AERO6)
Photolysis rate	phot_inline (calculate photolysis rates in-line using simulated aerosols and ozone concentrations)

5.2 CMAQ MODEL EVALUATION

CMAQ model performance was evaluated for $PM_{2.5}$ mass, individual $PM_{2.5}$ chemical species, as well as a number of gas-phase species based on observations from an extensive network of monitors in the SJV.

Time series of observed and modeled $PM_{2.5}$ chemical species based on CSN measurements are shown in the supplemental material (Figures S37-S40 of the supplemental materials for Bakersfield, Fresno, Modesto, and Visalia, respectively). $PM_{2.5}$ species are measured every 3 or 6 days at these sites. Observed $PM_{2.5}$ concentrations are higher in winter months and are much lower in summer months.

During winter months, $PM_{2.5}$ in the SJV is dominated by ammonium nitrate and directly emitted OC. The CMAQ model was able to reasonably reproduce these key characteristics of $PM_{2.5}$ pollution in the SJV, including successfully capturing many elevated wintertime nitrate events, which is key for accurately simulating both peak wintertime $PM_{2.5}$ as well as annual average $PM_{2.5}$ in the SJV.

Tables 20-23 summarize the key model performance metrics for major $PM_{2.5}$ chemical species at the four CSN sites. Model performance was evaluated on a quarterly basis for each species at each monitor. Average observations, average modeled values, mean bias, mean error, mean fractional bias (MFB), and mean fractional error (MFE) are given for individual $PM_{2.5}$ species at these four sites. Detailed definitions for these metrics can be found in the Photochemical Modeling Protocol Appendix. In general, model performance was similar at different monitors. Modeling somewhat over predicted $PM_{2.5}$ concentrations for quarter one, but in general under predicted $PM_{2.5}$ concentrations for other quarters. Boylan and Russell (2006) proposed two criteria for model performance evaluation: Model performance goals are considered as the level of accuracy that is close to the best a model can be expected to achieve. Model performance criteria are considered as the level of accuracy that is acceptable for modeling applications. For more abundant species (e.g., concentrations $\geqslant$ 3 $\mu g/m^3$), model performance criteria are met when MFE $\leqslant$ 75% and MFB $\leqslant$ ±60%; model performance goals are met when MFE $\leqslant$ 50% and MFB $\leqslant$ ± 30%. For less abundant species, the performance criteria and goals are less stringent. A graphical representation of the quarterly MFB and MFE values in Tables 20-23 is shown in Figure 13 for each CSN site, along with suggested model performance goals and criteria (green and red lines, respectively) from Boylan and Russell (2006). Based on these metrics, the current CMAQ modelling system met the model performance criteria and in many instances exceeded model performance goals.

Table 20. Quarterly $PM_{2.5}$ model performance based on CSN measurement at Fresno – Garland.

Quarter	Species	# of Obs.	Avg. Obs. (µg/m³)	Avg. Mod. (µg/m³)	Mean bias (µg/m³)	Mean error (µg/m³)	MFB	MFE
1	$PM_{2.5}$	30	21.1	23.6	2.5	7.2	0.24	0.40
1	Ammonium	30	1.7	2.3	0.6	1.0	0.36	0.62
1	Nitrate	30	5.8	7.7	1.9	3.1	0.25	0.55
1	Sulfate	30	0.8	0.9	0.1	0.3	0.18	0.41
1	OC	28	4.9	5.4	0.4	1.9	0.22	0.41
1	EC	28	1.2	1.9	0.7	0.8	0.58	0.62
2	$PM_{2.5}$	30	7.8	6.0	-1.8	2.5	-0.29	0.39
2	Ammonium	30	0.4	0.2	-0.3	0.3	-0.81	0.87
2	Nitrate	30	0.9	0.4	-0.5	0.5	-0.94	0.97
2	Sulfate	30	1.1	0.6	-0.5	0.5	-0.50	0.56
2	OC	29	1.8	1.7	0.0	0.4	-0.06	0.26
2	EC	29	0.3	0.6	0.3	0.3	0.65	0.65
3	$PM_{2.5}$	30	9.4	6.3	-3.1	3.7	-0.36	0.44
3	Ammonium	30	0.4	0.1	-0.2	0.3	-0.83	0.94
3	Nitrate	30	0.7	0.2	-0.6	0.6	-1.41	1.45
3	Sulfate	30	0.9	0.7	-0.2	0.3	-0.19	0.36
3	OC	30	2.4	1.7	-0.8	0.9	-0.31	0.39
3	EC	30	0.5	0.6	0.1	0.2	0.25	0.34
4	$PM_{2.5}$	29	25.8	22.9	-2.9	8.9	-0.03	0.36
4	Ammonium	29	2.9	2.0	-0.9	1.6	-0.23	0.64
4	Nitrate	28	9.0	7.2	-1.8	4.3	-0.27	0.55
4	Sulfate	28	1.0	0.8	-0.2	0.3	-0.19	0.32
4	OC	29	6.0	4.7	-1.3	1.9	-0.16	0.36
4	EC	29	1.6	1.8	0.2	0.6	0.22	0.40

Table 21. Quarterly $PM_{2.5}$ model performance based on CSN measurement at Visalia.

Quarter	Species	# of Obs.	Avg. Obs. (μg/m³)	Avg. Mod. (μg/m³)	Mean bias (μg/m³)	Mean error (μg/m³)	MFB	MFE
1	$PM_{2.5}$	15	20.5	21.7	1.2	5.6	0.14	0.32
1	Ammonium	15	2.0	2.7	0.8	1.1	0.36	0.59
1	Nitrate	15	6.7	9.2	2.6	3.3	0.32	0.50
1	Sulfate	15	1.0	0.7	-0.4	0.4	-0.33	0.46
1	OC	15	4.6	3.7	-0.9	1.6	-0.12	0.34
1	EC	15	0.9	1.3	0.4	0.5	0.49	0.52
2	$PM_{2.5}$	15	9.8	7.0	-2.8	2.8	-0.41	0.41
2	Ammonium	15	0.7	0.3	-0.3	0.3	-0.66	0.73
2	Nitrate	10	2.2	1.3	-0.9	0.9	-0.65	0.66
2	Sulfate	15	1.6	0.6	-1.0	1.0	-0.88	0.88
2	OC	17	2.6	1.6	-1.0	1.0	-0.54	0.54
2	EC	17	0.4	0.5	0.2	0.2	0.37	0.38
3	$PM_{2.5}$	17	10.5	6.7	-3.8	4.1	-0.38	0.45
3	Ammonium	17	0.6	0.2	-0.4	0.4	-0.77	0.81
3	Nitrate	17	1.6	0.3	-1.3	1.3	-1.32	1.32
3	Sulfate	17	1.4	0.8	-0.6	0.6	-0.50	0.51
3	OC	17	2.9	1.7	-1.2	1.4	-0.57	0.60
3	EC	17	0.5	0.6	0.2	0.2	0.28	0.31
4	$PM_{2.5}$	16	33.1	28.2	-4.9	12.5	-0.04	0.35
4	Ammonium	16	4.3	3.1	-1.2	2.1	-0.12	0.46
4	Nitrate	16	14.3	11.1	-3.2	6.6	-0.08	0.44
4	Sulfate	16	1.4	0.8	-0.6	0.7	-0.44	0.51
4	OC	16	5.8	3.6	-2.2	2.3	-0.45	0.49
4	EC	16	1.3	1.4	0.2	0.5	0.09	0.31

Table 22. Quarterly $PM_{2.5}$ model performance based on CSN measurement at Bakersfield.

Quarter	Species	# of Obs.	Avg. Obs. (μg/m^3)	Avg. Mod. (μg/m^3)	Mean bias (μg/m^3)	Mean error (μg/m^3)	MFB	MFE
1	$PM_{2.5}$	21	20.5	23.2	2.7	9.6	0.37	0.54
1	Ammonium	21	2.2	2.4	0.2	1.4	0.41	0.69
1	Nitrate	19	7.9	7.8	0.0	3.6	0.10	0.45
1	Sulfate	21	0.9	0.8	-0.1	0.4	0.11	0.52
1	OC	22	3.9	5.6	1.7	2.2	0.43	0.49
1	EC	22	1.1	1.9	0.8	0.8	0.59	0.59
2	$PM_{2.5}$	25	11.0	7.4	-3.6	4.1	-0.40	0.46
2	Ammonium	25	0.6	0.3	-0.3	0.3	-0.67	0.71
2	Nitrate	25	1.1	0.8	-0.3	0.6	-0.61	0.80
2	Sulfate	25	1.4	0.7	-0.7	0.7	-0.63	0.64
2	OC	22	2.2	2.3	0.1	0.5	0.03	0.23
2	EC	22	0.4	0.7	0.4	0.4	0.77	0.77
3	$PM_{2.5}$	19	15.5	8.0	-7.5	8.0	-0.56	0.60
3	Ammonium	19	0.5	0.2	-0.3	0.3	-0.81	0.86
3	Nitrate	19	0.8	0.4	-0.4	0.5	-0.93	1.04
3	Sulfate	19	1.3	0.8	-0.6	0.6	-0.51	0.51
3	OC	17	2.6	2.4	-0.2	0.9	-0.11	0.34
3	EC	17	0.5	0.9	0.4	0.4	0.60	0.60
4	$PM_{2.5}$	0	NA	NA	NA	NA	NA	NA
4	Ammonium	0	NA	NA	NA	NA	NA	NA
4	Nitrate	0	NA	NA	NA	NA	NA	NA
4	Sulfate	0	NA	NA	NA	NA	NA	NA
4	OC	0	NA	NA	NA	NA	NA	NA
4	EC	0	NA	NA	NA	NA	NA	NA

Table 23. Quarterly $PM_{2.5}$ model performance based on CSN measurement at Modesto.

Quarter	Species	# of Obs.	Avg. Obs. (μg/m^3)	Avg. Mod. (μg/m^3)	Mean bias (μg/m^3)	Mean error (μg/m^3)	MFB	MFE
1	$PM_{2.5}$	15	17.3	20.0	2.7	5.6	0.31	0.41
1	Ammonium	15	1.0	2.0	1.0	1.0	0.60	0.70
1	Nitrate	15	5.0	6.2	1.2	1.6	0.15	0.39
1	Sulfate	15	0.8	1.0	0.2	0.4	0.24	0.39
1	OC	14	5.5	5.5	0.0	2.2	0.23	0.44
1	EC	14	1.2	1.8	0.6	0.7	0.57	0.61
2	$PM_{2.5}$	15	6.5	5.0	-1.5	2.5	-0.24	0.40
2	Ammonium	15	0.3	0.3	0.0	0.1	0.10	0.44
2	Nitrate	13	0.7	0.5	-0.2	0.4	-0.68	0.81
2	Sulfate	15	1.0	0.8	-0.2	0.3	-0.18	0.36
2	OC	15	1.6	1.2	-0.4	0.6	-0.27	0.36
2	EC	15	0.3	0.4	0.1	0.1	0.40	0.40
3	$PM_{2.5}$	14	7.9	6.0	-1.9	3.1	-0.13	0.35
3	Ammonium	15	0.3	0.2	0.0	0.1	0.17	0.48
3	Nitrate	15	0.7	0.2	-0.5	0.5	-1.10	1.10
3	Sulfate	15	1.1	0.9	-0.2	0.3	-0.11	0.28
3	OC	15	2.6	1.5	-1.1	1.2	-0.37	0.40
3	EC	15	0.4	0.5	0.1	0.2	0.20	0.35
4	$PM_{2.5}$	17	25.6	27.1	1.5	4.1	0.11	0.21
4	Ammonium	17	2.4	2.6	0.2	0.6	0.27	0.38
4	Nitrate	17	8.2	9.0	0.8	2.2	0.19	0.32
4	Sulfate	17	1.1	1.1	-0.1	0.3	-0.02	0.25
4	OC	17	6.2	4.3	-1.9	1.9	-0.33	0.33
4	EC	17	1.6	1.5	-0.1	0.3	-0.01	0.22

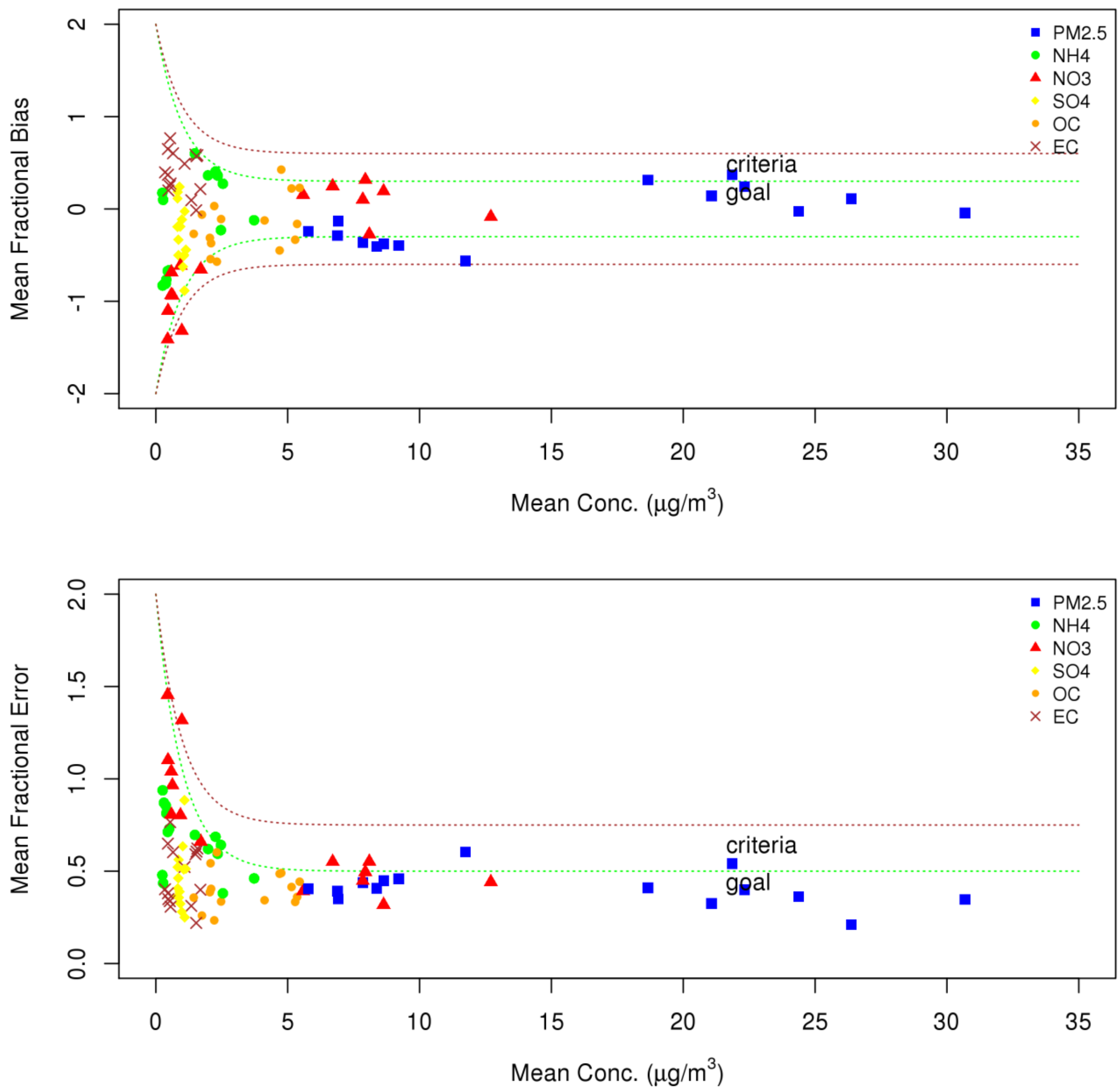

Figure 13. Bugle plot of quarterly $PM_{2.5}$ model performance in terms of MFB and MFE at the four CSN sites in the SJV (i.e., Bakersfield, Fresno, Modesto, and Visalia).

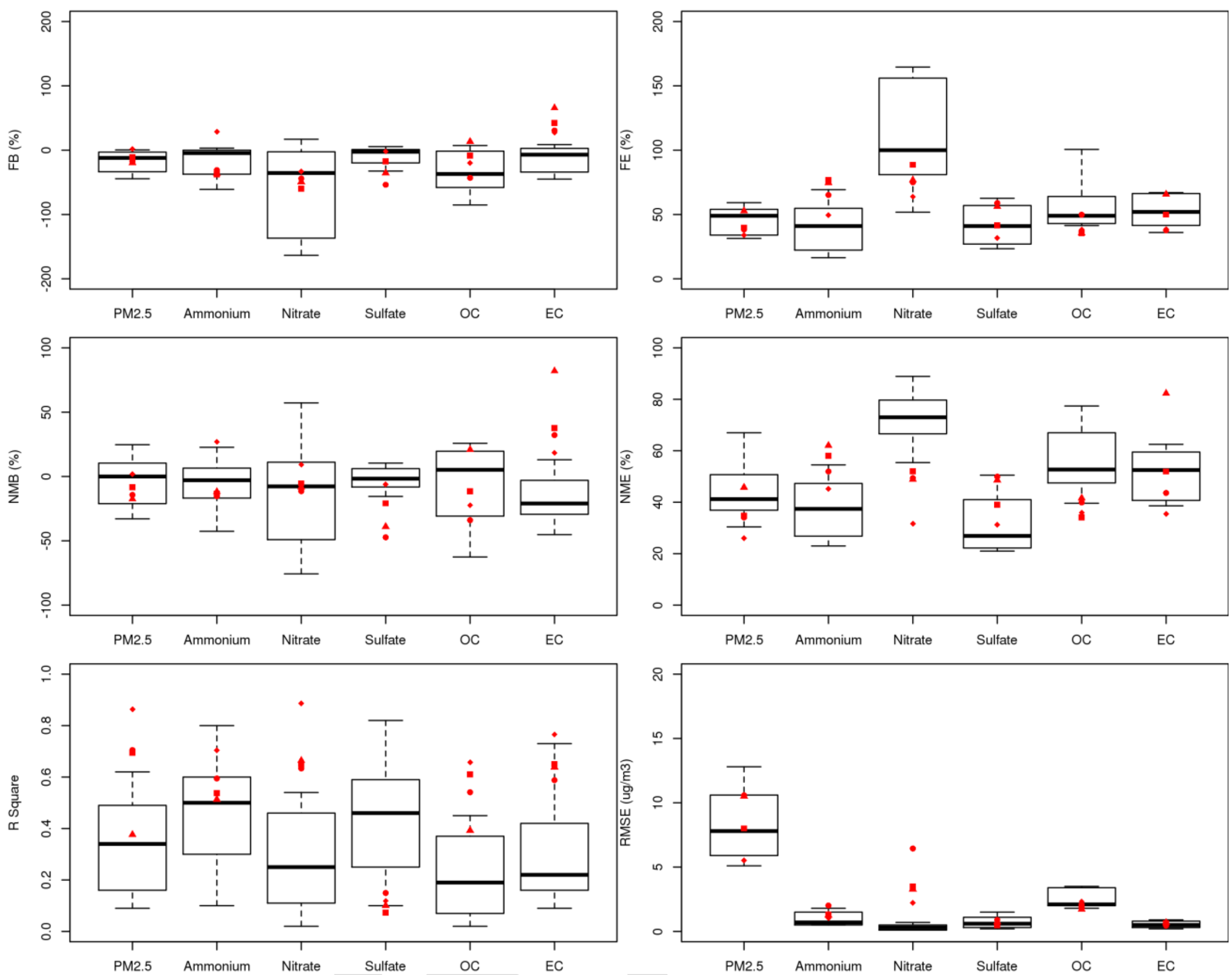

Figure 14. Comparison of annual $PM_{2.5}$ model performance to other modeling studies in Simon et al. (2012). Red symbols represent performance at the four CSN sites in the SJV.

In addition to evaluating the standard statistical performance metrics, it is also informative to put these performance statistics in the context of other studies published in the scientific literature. Figure 14 compares key performance statistics from the modeling platform presented in this document to the range of published performance statistics from 2006 to 2012 and summarized in Simon et al. (2012). In Figure 14, the black centerline shows the median value (i.e., median model performance) from those studies, the boxes outline the 25th and 75th percentile values, and the whiskers show the 10th and 90th percentile values. The model performance for each of the four CSN sites in the SJV is shown in red. Performance metrics including MFB, MFE, normalized mean bias (NMB), normalized mean error (NME), R squared, and root mean square error (RMSE) are compared. Definitions for these statistics can be found in the

Photochemical Modeling Protocol or Simon et al. (2012). Model performance metrics in the SJV are typically equal to or better than the corresponding statistics from other studies. One exception is the higher RMSE for nitrate in the SJV, which is simply a reflection of the higher nitrate concentrations in the SJV compared to other regions. In fact, MFB, MFE, NME, and R squared for nitrate in the SJV is consistently better than the majority of the model studies summarized in Simon et al. (2012). Finally, the model performance is also comparable to that of the 2012 SJV $PM_{2.5}$ SIP (Chen et al., 2014).

Since CSN monitors do not measure $PM_{2.5}$ on a daily basis, it is also advantageous to compare modeled 24-hour average $PM_{2.5}$ concentrations to observations from continuous $PM_{2.5}$ samplers, which typically report 24-hour average $PM_{2.5}$ concentrations on a daily basis. Figures S-41 – S-52 show the time series of modeled and observed 24-hour average $PM_{2.5}$ concentrations at these sites located throughout the SJV. Distinct seasonal variations in $PM_{2.5}$ concentrations are observed throughout the Valley, and are also reasonably captured by the model. Of particular importance, the modeling system was able to capture the elevated $PM_{2.5}$ events during the winter months and the lower $PM_{2.5}$ which is common in the summer months. In addition, Table 24 summarizes the corresponding model performance statistics at these sites. All the sites met or exceeded the $PM_{2.5}$ model performance criteria defined in Boyland and Russell (2006).

In addition to the $PM_{2.5}$ performance evaluation, gas phase model performance was also evaluated for nitrogen dioxide (NO_2) and ozone, which are key products of the photochemical processes in the atmosphere. Scatter plots of observed and modeled one-hour NO_2 mixing ratios at 16 sites are shown in Figures S-53 to S-68 in the supplemental materials. On average, there is good agreement between observed and modeled NO_2 mixing ratios. The slope of the regression line between the observed and modeled hourly NO_2 mixing ratios is within ±30% of the 1:1 correlation line at most of the sites. Scatter plots of observed and modeled hourly O_3 mixing ratios at 25 sites are shown in Figures S-69 to S-93 in the supplemental materials. Modeled O_3 mixing ratios show excellent agreement with observed mixing ratios and the slopes of the regression lines between observed and modeled O_3 are all within ±15% of the 1:1 correlation line.

Table 24. Model performance for 24-hour $PM_{2.5}$ concentrations measured from continuous $PM_{2.5}$ monitors.

Sites	# of Obs.	Avg. Obs. (µg/m³)	Avg. Mod. (µg/m³)	Mean bias (µg/m³)	Mean error (µg/m³)	MFB	MFE
Fresno-Drummond Street	246	14.8	13.0	-1.8	4.9	-0.20	0.40
Clovis	300	16.4	13.6	-2.7	6.1	-0.26	0.46
Bakersfield-California Avenue	267	20.2	15.7	-4.4	7.7	-0.31	0.47
Tranquility	301	8.5	8.6	0.1	4.1	-0.19	0.51
Fresno-Garland	312	19.3	15.0	-4.3	6.7	-0.36	0.47
Stockton	302	18.0	13.2	-4.8	7.5	-0.54	0.63
Merced	326	13.2	12.7	-0.6	5.3	-0.19	0.46
Hanford	329	18.0	14.6	-3.4	6.3	-0.33	0.49
Madera	323	18.0	12.0	-6.0	8.1	-0.57	0.67
Manteca	325	11.7	13.1	1.4	6.0	-0.13	0.56
Visalia	309	18.6	17.0	-1.7	6.6	-0.19	0.43
Modesto	315	14.4	14.3	-0.1	5.1	-0.06	0.43
Turlock	316	14.8	14.2	-0.6	4.5	-0.08	0.43

5.3 FUTURE YEAR 2020 DESIGN VALUES

Projected future year 2020 annual $PM_{2.5}$ and 24-hour $PM_{2.5}$ DVs for each site are given in Tables 25 and 26, respectively. For the annual standard, the Bakersfield-Planz site has the highest projected DV at 14.6 µg/m^3, which is below the 15 µg/m^3 annual $PM_{2.5}$ standard established by the U.S. EPA in 1997. For the 24-hour standard, the Bakersfield-California Avenue site has the highest projected DV at 47.6 µg/m^3, which is also below the 65 µg/m^3 24-hour $PM_{2.5}$ standard established by the U.S. EPA in 1997.

The Corresponding Relative Response Factors (RRFs) for both the annual $PM_{2.5}$ and 24-hour $PM_{2.5}$ are given in Tables 27-28, respectively (Note, RRF is calculated on a quarterly basis in the actual DV calculation, so the annual RRF is shown for illustrative purposes only). From 2013 to 2020, there are modest reductions projected for ammonium nitrate, EC, and organic matter (OM), a slight decrease in sulfate, but a slight increase in crustal material (i.e., other primary $PM_{2.5}$ such as fugitive dust emissions). The reduction in ammonium nitrate is a direct result of NO_x emission reductions in 2020 compared to 2013, while EC and OM reductions are primarily tied to the reduction in primary $PM_{2.5}$ emissions. Because future year projection is performed for each individual $PM_{2.5}$ specie, the base year annual and 24-hour based $PM_{2.5}$ compositions are given in Tables 29-30, respectively. In addition, the projected 2020 annual and 24-hour $PM_{2.5}$ compositions are shown in Tables 31-32, respectively. In 2020, for the annual $PM_{2.5}$ standard, OM is the dominant $PM_{2.5}$ component followed by ammonium nitrate, while for the 24-hour $PM_{2.5}$ standard, ammonium nitrate and OM are roughly equivalent in terms of their contribution to total $PM_{2.5}$.

Table 25. Projected future year 2020 annual $PM_{2.5}$ DVs at each monitor.

Site AQS ID	Name	Base DV (µg/m^3)	2020 Annual DV (µg/m^3)
60290016	Bakersfield - Planz	17.2	14.6
60392010	Madera	16.9	14.2
60311004	Hanford	16.5	13.3
61072002	Visalia	16.2	13.5
60195001	Clovis	16.1	13.4
60290014	Bakersfield - California	16.0	13.5
60190011	Fresno - Garland	15.0	12.4
60990006	Turlock	14.9	12.5
60195025	Fresno - Hamilton & Winery	14.2	11.9
60771002	Stockton	13.1	11.4
60470003	Merced - S Coffee	13.1	10.9
60990005	Modesto	13.0	11.0
60472510	Merced - Main Street	11.0	9.3
60772010	Manteca	10.1	8.7
60192009	Tranquility	7.7	6.4

Table 26. Projected future year 2020 24-hour $PM_{2.5}$ DVs at each monitor.

Site AQS ID	Name	Base DV (µg/m^3)	2020 24-hour DV (µg/m^3)
60290014	Bakersfield – California	64.1	47.6
60190011	Fresno – Garland	60.0	44.3
60311004	Hanford	60.0	43.7
60195025	Fresno – Hamilton & Winery	59.3	45.6
60195001	Clovis	55.8	41.1
61072002	Visalia	55.5	42.8
60290016	Bakersfield – Planz	55.5	41.2
60392010	Madera	51.0	38.9
60990006	Turlock	50.7	37.8
60990005	Modesto	47.9	35.8
60472510	Merced – Main Street	46.9	32.9
60771002	Stockton	42.0	33.5
60470003	Merced – S Coffee	41.1	30.0
60772010	Manteca	36.9	30.1
60192009	Tranquility	29.5	21.5

Table 27. 2020 Annual RRFs for $PM_{2.5}$ components.

Site	RRF for $PM_{2.5}$	RRF for NH_4	RRF for NO_3	RRF for SO_4	RRF for OM	RRF for EC	RRF for Crustal
Bakersfield - Planz	0.85	0.67	0.69	0.98	0.88	0.52	1.05
Madera	0.84	0.74	0.70	0.99	0.89	0.67	1.05
Hanford	0.80	0.71	0.67	1.02	0.91	0.70	1.00
Visalia	0.83	0.68	0.70	1.00	0.86	0.62	1.04
Clovis	0.83	0.71	0.71	1.00	0.84	0.61	1.08
Bakersfield - California	0.84	0.66	0.67	0.98	0.88	0.52	1.06
Fresno - Garland	0.83	0.73	0.72	0.99	0.84	0.57	1.07
Turlock	0.84	0.75	0.73	0.98	0.89	0.65	1.06
Fresno - H&W	0.83	0.75	0.75	1.00	0.84	0.55	1.06
Stockton	0.87	0.80	0.75	1.01	0.92	0.69	1.08
Merced - S Coffee	0.83	0.73	0.70	0.99	0.89	0.66	1.05
Modesto	0.84	0.75	0.73	0.98	0.90	0.65	1.06
Merced - Main St	0.85	0.72	0.70	0.99	0.88	0.66	1.06
Manteca	0.86	0.79	0.76	0.98	0.90	0.68	1.06
Tranquility	0.83	0.71	0.63	1.00	0.93	0.73	1.03

Table 28. 2020 24-hour RRFs for $PM_{2.5}$ components.

Site	RRF for $PM_{2.5}$	RRF for NH_4	RRF for NO_3	RRF for SO_4	RRF for OM	RRF for EC	RRF for Crustal
Bakersfield - California	0.74	0.70	0.70	0.98	0.77	0.45	1.07
Fresno – Garland	0.74	0.75	0.75	0.99	0.71	0.50	1.07
Hanford	0.73	0.67	0.68	1.04	0.84	0.65	1.02
Fresno - H&W	0.78	0.78	0.79	0.99	0.75	0.51	1.07
Clovis	0.73	0.72	0.73	1.00	0.72	0.54	1.08
Visalia	0.77	0.77	0.77	1.01	0.73	0.53	1.05
Bakersfield – Planz	0.73	0.73	0.73	0.97	0.66	0.42	1.05
Madera	0.76	0.75	0.75	0.99	0.76	0.60	1.07
Turlock	0.74	0.71	0.72	0.97	0.77	0.58	1.06
Modesto	0.75	0.73	0.72	0.98	0.75	0.58	1.07
Merced – Main St	0.70	0.71	0.71	0.97	0.65	0.53	1.06
Stockton	0.80	0.74	0.74	1.00	0.88	0.67	1.07
Merced – S Coffee	0.72	0.72	0.72	0.97	0.67	0.54	1.06
Manteca	0.82	0.80	0.80	0.97	0.82	0.68	1.07
Tranquility	0.72	0.61	0.61	1.05	0.85	0.72	1.08

Table 29. Base year Annual $PM_{2.5}$ compositions.*

Name	Base $PM_{2.5}$ (µg/m³)	Base NH_4 (µg/m³)	Base NO_3 (µg/m³)	Base SO_4 (µg/m³)	Base OM (µg/m³)	Base EC (µg/m³)	Base Crustal (µg/m³)
Bakersfield - Planz	17.2	1.38	2.61	1.66	6.65	0.99	2.53
Madera	16.9	1.74	4.07	1.49	6.06	0.91	1.22
Hanford	16.5	2.15	5.47	1.50	3.84	0.70	1.21
Visalia	16.2	1.41	2.99	1.45	7.13	0.68	1.15
Clovis	16.1	1.11	2.14	1.30	8.43	0.88	1.06
Bakersfield – Cali.	16.0	1.31	2.60	1.48	6.19	0.92	2.22
Fresno – Garland	15.0	1.04	2.15	1.11	7.80	0.82	0.90
Turlock	14.9	1.60	3.94	1.22	5.11	0.77	0.87
Fresno - H&W	14.2	0.99	2.05	1.05	7.39	0.78	0.85
Stockton	13.1	1.38	3.29	1.13	4.61	0.66	0.82
Merced - S Coffee	13.1	1.38	3.31	1.13	4.56	0.66	0.81
Modesto	13.0	1.39	3.41	1.08	4.46	0.67	0.77
Merced - M Street	11.0	0.82	1.70	0.88	5.40	0.56	0.62
Manteca	10.1	1.06	2.59	0.83	3.42	0.51	0.59
Tranquility	7.7	0.77	1.85	0.61	2.67	0.40	0.50

*: $PM_{2.5}$ compositions were based on CSN speciation measurement adjusted by the EPA SANDWICH method. Particle-bound water and blank mass are not shown. The same applies to the base year 24-hour DV compositions.

Table 30. Base year 24-hour $PM_{2.5}$ standard DV compositions.

Name	Base $PM_{2.5}$ (µg/m³)	Base NH_4 (µg/m³)	Base NO_3 (µg/m³)	Base SO_4 (µg/m³)	Base OM (µg/m³)	Base EC (µg/m³)	Base Crustal (µg/m³)
Bakersfield – Cali.	64.1	7.6	21.9	3.2	18.9	2.7	4.7
Fresno – Garland	60.0	6.7	20.8	1.7	22.9	2.5	0.9
Hanford	60.0	9.1	28.6	2.2	11.2	1.7	1.1
Fresno – H&W	59.3	6.4	20.3	1.4	23.2	2.7	0.9
Clovis	55.8	6.1	19.1	1.3	21.8	2.5	0.8
Visalia	55.5	7.6	23.5	2.1	14.7	1.6	1.0
Bakersfield - Planz	55.5	6.5	18.1	3.4	17.9	2.5	2.8
Madera	51.0	6.1	19.3	1.2	17.1	2.3	0.8
Turlock	50.7	6.5	20.0	1.9	14.6	2.4	1.0
Modesto	47.9	6.1	18.9	1.8	13.8	2.3	0.9
Merced - M Street	46.9	5.3	16.1	1.7	17.1	2.2	0.9
Stockton	42.0	5.4	15.9	2.1	11.8	2.2	1.0
Merced - S Coffee	41.1	5.4	16.1	1.8	11.6	1.8	0.8
Manteca	36.8	4.7	14.5	1.4	10.5	1.7	0.7
Tranquility	29.5	3.5	10.8	0.9	10.0	1.4	0.4

Table 31. Projected 2020 Annual $PM_{2.5}$ compositions.

Name	Future $PM_{2.5}$ (µg/m³)	Future NH_4 (µg/m³)	Future NO_3 (µg/m³)	Future SO_4 (µg/m³)	Future OM (µg/m³)	Future EC (µg/m³)	Future Crustal (µg/m³)	Future Water (µg/m³)	Blank (µg/m³)
Bakersfield – Planz	14.6	0.92	1.81	1.62	5.84	0.51	2.66	0.72	0.5
Madera	14.2	1.30	2.85	1.47	5.40	0.61	1.28	0.75	0.5
Hanford	13.3	1.53	3.68	1.53	3.50	0.49	1.21	0.86	0.5
Visalia	13.5	0.96	2.09	1.45	6.16	0.42	1.20	0.72	0.5
Clovis	13.4	0.78	1.52	1.29	7.06	0.54	1.15	0.60	0.5
Bakersfield - California	13.5	0.86	1.75	1.44	5.45	0.48	2.34	0.65	0.5
Fresno – Garland	12.4	0.76	1.55	1.10	6.54	0.47	0.96	0.54	0.5
Turlock	12.5	1.20	2.90	1.20	4.56	0.50	0.92	0.69	0.5
Fresno – H &W	11.9	0.74	1.53	1.05	6.20	0.43	0.90	0.52	0.5
Stockton	11.4	1.10	2.48	1.14	4.27	0.46	0.88	0.61	0.5
Merced - S Coffee	10.9	1.00	2.30	1.12	4.07	0.44	0.85	0.58	0.5
Modesto	11.0	1.05	2.49	1.05	4.03	0.44	0.82	0.60	0.5
Merced –Main St	9.3	0.59	1.19	0.88	4.77	0.37	0.65	0.40	0.5
Manteca	8.7	0.84	1.98	0.81	3.09	0.35	0.63	0.47	0.5
Tranquility	6.4	0.54	1.16	0.61	2.47	0.29	0.51	0.30	0.5

Table 32. Projected 2020 24-hour $PM_{2.5}$ compositions

Name	Future $PM_{2.5}$ (µg/m³)	Future NH_4 (µg/m³)	Future NO_3 (µg/m³)	Future SO_4 (µg/m³)	Future OM (µg/m³)	Future EC (µg/m³)	Future Crustal (µg/m³)	Future Water (µg/m³)	Blank (µg/m³)
Bakersfield – California	47.6	5.8	17.8	2.3	12.6	1.2	4.1	3.5	0.5
Fresno - Garland	44.3	4.9	15.4	1.4	16.7	1.4	1.0	3.0	0.5
Hanford	43.7	6.1	19.3	2.3	9.5	1.2	1.1	3.8	0.5
Fresno – H&W	45.6	4.9	15.0	1.9	17.5	1.3	1.5	3.1	0.5
Clovis	41.1	3.8	12.0	1.4	18.4	1.6	1.0	2.3	0.5
Visalia	42.8	5.9	18.2	2.1	10.7	0.9	1.0	3.5	0.5
Bakersfield – Planz	41.2	5.3	14.9	3.5	10.8	1.0	2.3	3.0	0.5
Madera	38.9	4.5	14.5	1.2	13.1	1.4	0.8	2.8	0.5
Turlock	37.8	4.6	14.4	1.8	11.2	1.4	1.1	2.8	0.5
Modesto	35.8	4.5	13.3	2.1	10.0	1.4	1.3	2.6	0.5
Merced-Main St	32.9	3.8	11.5	1.6	11.2	1.2	1.0	2.2	0.5
Stockton	33.5	3.8	11.3	1.8	11.4	1.3	1.1	2.2	0.5
Merced – S Coffee	30.0	3.9	11.6	2.0	7.9	1.0	0.8	2.3	0.5
Manteca	30.1	3.8	11.7	1.3	8.7	1.2	0.8	2.3	0.5
Tranquility	21.5	2.1	6.6	0.9	8.6	1.0	0.5	1.3	0.5

5.4 FUTURE YEAR 2024 DESIGN VALUES

Projected future year 2024 annual $PM_{2.5}$ DVs and 24-hour $PM_{2.5}$ DVs for each site are given in Tables 33 and 34, respectively. For the 24-hour standard, the Fresno – Hamilton & Winery site has the highest projected DV at 35.1 $\mu g/m^3$, which meets the 35 $\mu g/m^3$ 24-hour $PM_{2.5}$ standard established by the U.S. EPA in 2006 (technically, the form of the 24-hour $PM_{2.5}$ standard means that a DV needs to be less than 35.5 $\mu g/m^3$ to demonstrate attainment). Although attainment of the annual $PM_{2.5}$ standard is due in 2025 and not 2024, all monitors meet the annual $PM_{2.5}$ standard in 2024. The Bakersfield-Planz and Madera monitors have the highest projected 2024 annual DV of 12.0 $\mu g/m^3$, which is below the 12 $\mu g/m^3$ annual $PM_{2.5}$ standard established by the U.S. EPA in 2012 (technically, the annual DV needs to be less than 12.05 $\mu g/m^3$ to show attainment).

Correspondingly, RRFs for both the annual $PM_{2.5}$ and 24-hour $PM_{2.5}$ are provided in Tables 35-36, respectively (note that the RRF is calculated on a quarterly basis in the actual DV calculation, so the annual RRFs are given for illustrative purposes only). From 2013 to 2024, there are significant reductions projected for ammonium nitrate and EC, modest reductions in OM, almost no change in sulfate, and a slight increase in crustal material (i.e., other primary $PM_{2.5}$ such as fugitive dust emissions). Again, because of the significant reduction in NO_x emissions from 2013 to 2024, there is a significant reduction projected for ammonium nitrate. The larger reductions in EC and modest reductions in OM are primarily due to emission reductions associated with primary $PM_{2.5}$ emission sources such as residential wood combustion and commercial cooking. Since future year projections are performed for each individual $PM_{2.5}$ species and then summed to obtain total $PM_{2.5}$, the projected 2024 annual and 24-hour $PM_{2.5}$ composition is shown in Tables 37-38, respectively. In 2024, for the 24-hour standard, OM and ammonium nitrate remain the two largest components. In contrast, for the annual standard, OM is the dominant component.

Table 33. Projected future year 2024 annual $PM_{2.5}$ DVs at each monitor

Site AQS ID	Name	Base DV (µg/m³)	2024 Annual DV (µg/m³)
60290016	Bakersfield - Planz	17.2	12.0
60392010	Madera	16.9	12.0
60311004	Hanford	16.5	10.5
61072002	Visalia	16.2	11.1
60195001	Clovis	16.1	11.4
60290014	Bakersfield - California	16.0	11.0
60190011	Fresno-Garland	15.0	10.4
60990006	Turlock	14.9	11.1
60195025	Fresno - Hamilton & Winery	14.2	10.0
60771002	Stockton	13.1	10.7
60470003	Merced - S Coffee	13.1	9.7
60990005	Modesto	13.0	10.0
60472510	Merced - Main Street	11.0	8.6
60772010	Manteca	10.1	8.0
60192009	Tranquility	7.7	5.5

Table 34. Projected future year 2024 24-hour $PM_{2.5}$ DVs at each monitor

Site AQS ID	Name	Base DV (µg/m³)	2024 24-hour DV (µg/m³)
60290014	Bakersfield – California	64.1	33.3
60190011	Fresno – Garland	60.0	32.8
60311004	Hanford	60.0	30.1
60195025	Fresno – Hamilton & Winery	59.3	35.1
60195001	Clovis	55.8	30.7
61072002	Visalia	55.5	30.2
60290016	Bakersfield – Planz	55.5	30.0
60392010	Madera	51.0	30.2
60990006	Turlock	50.7	30.2
60990005	Modesto	47.9	29.1
60472510	Merced – Main Street	46.9	27.4
60771002	Stockton	42.0	28.6
60470003	Merced – S Coffee	41.1	24.2
60772010	Manteca	36.9	25.8
60192009	Tranquility	29.5	16.2

Table 35. 2024 Annual RRFs for $PM_{2.5}$ components

Site	RRF for $PM_{2.5}$	RRF for NH_4	RRF for NO_3	RRF for SO_4	RRF for OM	RRF for EC	RRF for Crustal
Bakersfield - Planz	0.70	0.36	0.35	0.96	0.74	0.38	1.06
Madera	0.71	0.55	0.44	0.99	0.81	0.53	1.03
Hanford	0.64	0.48	0.38	1.01	0.85	0.55	0.92
Visalia	0.68	0.39	0.38	1.00	0.75	0.45	1.04
Clovis	0.71	0.46	0.43	0.99	0.72	0.49	1.11
Bakersfield - California	0.69	0.36	0.34	0.96	0.73	0.38	1.06
Fresno - Garland	0.70	0.48	0.45	0.98	0.72	0.44	1.09
Turlock	0.75	0.57	0.53	0.99	0.88	0.55	1.07
Fresno - H&W	0.70	0.50	0.47	0.99	0.72	0.43	1.08
Stockton	0.81	0.68	0.60	1.02	0.92	0.62	1.09
Merced - S Coffee	0.74	0.54	0.47	1.00	0.88	0.57	1.06
Modesto	0.77	0.60	0.54	0.99	0.90	0.57	1.08
Merced - Main St	0.78	0.52	0.47	1.00	0.87	0.58	1.07
Manteca	0.79	0.66	0.60	1.00	0.89	0.60	1.06
Tranquility	0.72	0.51	0.37	1.00	0.88	0.60	1.02

Table 36. 2024 24-hour RRF for $PM_{2.5}$ components

Site	RRF for $PM_{2.5}$	RRF for NH_4	RRF for NO_3	RRF for SO_4	RRF for OM	RRF for EC	RRF for Crustal
Bakersfield - California	0.52	0.35	0.36	0.96	0.70	0.37	1.04
Fresno – Garland	0.54	0.46	0.47	0.96	0.61	0.39	1.08
Hanford	0.50	0.37	0.38	1.03	0.80	0.53	0.89
Fresno - H&W	0.59	0.50	0.50	0.99	0.66	0.42	1.09
Clovis	0.60	0.43	0.44	0.99	0.70	0.46	1.10
Visalia	0.54	0.44	0.45	1.03	0.66	0.42	1.05
Bakersfield – Planz	0.58	0.37	0.39	0.96	0.68	0.35	1.04
Madera	0.59	0.47	0.48	0.99	0.72	0.53	1.05
Turlock	0.60	0.46	0.47	0.96	0.77	0.52	1.07
Modesto	0.62	0.50	0.49	0.98	0.76	0.53	1.09
Merced – Main St	0.59	0.48	0.48	0.97	0.66	0.49	1.07
Stockton	0.69	0.53	0.53	1.00	0.88	0.62	1.08
Merced – S Coffee	0.58	0.48	0.49	0.97	0.68	0.49	1.05
Manteca	0.69	0.59	0.60	0.99	0.82	0.61	1.06
Tranquility	0.54	0.31	0.31	1.05	0.82	0.61	1.10

Table 37. Projected 2024 Annual $PM_{2.5}$ compositions

Name	Future $PM_{2.5}$ (µg/m³)	Future NH_4 (µg/m³)	Future NO_3 (µg/m³)	Future SO_4 (µg/m³)	Future OM (µg/m³)	Future EC (µg/m³)	Future Crustal (µg/m³)	Future Water (µg/m³)	Blank (µg/m³)
Bakersfield – Planz	12.0	0.50	0.93	1.59	4.90	0.37	2.67	0.57	0.5
Madera	12.0	0.96	1.81	1.47	4.90	0.48	1.25	0.61	0.5
Hanford	10.5	1.03	2.10	1.52	3.26	0.39	1.11	0.62	0.5
Visalia	11.1	0.55	1.15	1.45	5.38	0.31	1.20	0.56	0.5
Clovis	11.4	0.51	0.91	1.28	6.07	0.43	1.17	0.50	0.5
Bakersfield - California	11.0	0.47	0.88	1.41	4.54	0.35	2.36	0.51	0.5
Fresno – Garland	10.4	0.50	0.96	1.09	5.59	0.36	0.98	0.44	0.5
Turlock	11.1	0.91	2.10	1.21	4.51	0.42	0.94	0.56	0.5
Fresno – H &W	10.0	0.50	0.96	1.04	5.35	0.33	0.91	0.42	0.5
Stockton	10.7	0.94	1.97	1.15	4.27	0.42	0.89	0.53	0.5
Merced - S Coffee	9.7	0.74	1.57	1.12	4.01	0.38	0.86	0.47	0.5
Modesto	10.0	0.83	1.85	1.06	4.02	0.38	0.83	0.49	0.5
Merced - Main St	8.6	0.43	0.80	0.88	4.68	0.32	0.66	0.34	0.5
Manteca	8.0	0.70	1.55	0.83	3.06	0.30	0.63	0.40	0.5
Tranquility	5.5	0.39	0.69	0.61	2.35	0.24	0.51	0.23	0.5

Table 38. Projected 2024 24-hour $PM_{2.5}$ compositions

Name	Future $PM_{2.5}$ (µg/m³)	Future NH_4 (µg/m³)	Future NO_3 (µg/m³)	Future SO_4 (µg/m³)	Future OM (µg/m³)	Future EC (µg/m³)	Future Crustal (µg/m³)	Future Water (µg/m³)	Blank (µg/m³)
Bakersfield – California	33.3	2.7	8.6	2.4	12.8	1.1	3.4	1.8	0.5
Fresno - Garland	32.8	3.0	9.7	1.3	14.4	1.0	1.0	1.9	0.5
Hanford	30.1	3.3	10.8	2.3	9.0	1.0	0.9	2.2	0.5
Fresno – H&W	35.1	3.2	10.3	1.4	15.5	1.1	1.0	2.0	0.5
Clovis	30.7	2.2	6.7	1.9	15.1	1.0	1.7	1.6	0.5
Visalia	30.2	3.4	10.6	2.1	9.7	0.7	1.0	2.1	0.5
Bakersfield – Planz	30.0	2.3	6.1	4.3	11.6	0.7	2.6	1.9	0.5
Madera	30.2	2.9	9.3	1.2	12.4	1.2	0.8	1.8	0.5
Turlock	30.2	3.0	9.4	2.1	11.0	1.2	1.1	1.9	0.5
Modesto	29.1	3.0	9.0	2.1	10.0	1.3	1.3	1.8	0.5
Merced – Main Street	27.4	2.5	7.8	1.6	11.3	1.1	1.0	1.6	0.5
Stockton	28.6	2.7	8.1	1.8	11.5	1.2	1.1	1.7	0.5
Merced – S Coffee	24.2	2.6	8.0	1.7	8.2	1.0	0.8	1.6	0.5
Manteca	25.8	2.8	8.8	1.4	8.7	1.1	0.8	1.7	0.5
Tranquility	16.2	1.1	3.4	0.9	8.3	0.9	0.5	0.7	0.5

5.5 FUTURE YEAR 2025 DESIGN VALUES

Projected future year 2025 annual $PM_{2.5}$ and 24-hour $PM_{2.5}$ DVs for each site are given in Tables 39 and 40, respectively. For the annual standard, the Bakersfield-Planz site has the highest projected DV at 12.0 µg/m^3, which meets the 12 µg/m^3 annual $PM_{2.5}$ standard established by the U.S. EPA in 2012 ((technically, the form of the annual $PM_{2.5}$ standard means that a DV needs to be less than 12.04 µg/m^3 to demonstrate attainment). For reference and to illustrate the effect of emission reductions on 24-hour $PM_{2.5}$ from 2024 to 2025, the Fresno – Hamilton & Winery monitor had the highest 24-hour $PM_{2.5}$ levels in 2025 and showed a reduction in DV from 35.1 µg/m^3 in 2024 to 34.7 µg/m^3 in 2025, with all of the reduction coming from lower ammonium nitrate levels resulting from NO_x reductions.

RRFs corresponding to the future DVs for both annual and 24-hour $PM_{2.5}$ are provided in Tables 41-42, respectively (as noted above, the RRF is actually calculated on a quarterly basis and the annual RRF is shown for illustrative purposes only). From 2013 to 2025, there were significant reductions projected for ammonium nitrate and EC, modest reductions in OM, almost no change in sulfate, and a slight increase in crustal material (i.e., other primary $PM_{2.5}$ such as fugitive dust emissions). As discussed previously, reductions in ammonium nitrate are a direct result of dramatic NO_x emission reductions from 2013 to 2025. Reductions in EC and OM are primarily due to emission reductions from primary $PM_{2.5}$ sources, such as residential wood combustion, commercial cooking and mobile sources. Because the future year projection is performed for each individual $PM_{2.5}$ species, the projected 2025 annual and 24-hour $PM_{2.5}$ composition is given in Tables 43 and 44, respectively. In 2025, OM will be the dominant component for the annual standard, and for the 24-hour standard, OM and ammonium nitrate remain the two largest components.

Table 39. Projected future year 2025 annual $PM_{2.5}$ DVs at each monitor.

Site AQS ID	Name	Base DV ($\mu g/m^3$)	2025 Annual DV ($\mu g/m^3$)
60290016	Bakersfield - Planz	17.2	12.0
60392010	Madera	16.9	11.9
60311004	Hanford	16.5	10.4
61072002	Visalia	16.2	11.1
60195001	Clovis	16.1	11.4
60290014	Bakersfield - California	16.0	11.0
60190011	Fresno-Garland	15.0	10.4
60990006	Turlock	14.9	11.1
60195025	Fresno - Hamilton & Winery	14.2	10.0
60771002	Stockton	13.1	10.6
60470003	Merced - S Coffee	13.1	9.6
60990005	Modesto	13.0	9.9
60472510	Merced - Main Street	11.0	8.6
60772010	Manteca	10.1	7.9
60192009	Tranquility	7.7	5.5

Table 40. Projected future year 2025 24-hour $PM_{2.5}$ DVs at each monitor.

Site AQS ID	Name	Base DV ($\mu g/m^3$)	2025 24-hour DV ($\mu g/m^3$)
60290014	Bakersfield – California	64.1	32.7
60190011	Fresno – Garland	60.0	32.3
60311004	Hanford	60.0	29.4
60195025	Fresno – Hamilton & Winery	59.3	34.7
60195001	Clovis	55.8	30.5
61072002	Visalia	55.5	29.7
60290016	Bakersfield – Planz	55.5	29.7
60392010	Madera	51.0	29.7
60990006	Turlock	50.7	29.6
60990005	Modesto	47.9	28.6
60472510	Merced – Main Street	46.9	27.0
60771002	Stockton	42.0	28.1
60470003	Merced – S Coffee	41.1	23.8
60772010	Manteca	36.9	25.4
60192009	Tranquility	29.5	16.0

Table 41. 2025 Annual RRFs for $PM_{2.5}$ components.

Site	RRF for $PM_{2.5}$	RRF for NH_4	RRF for NO_3	RRF for SO_4	RRF for OM	RRF for EC	RRF for Crustal
Bakersfield – Planz	0.70	0.35	0.34	0.96	0.74	0.37	1.06
Madera	0.70	0.54	0.43	0.99	0.81	0.52	1.03
Hanford	0.63	0.47	0.37	1.01	0.85	0.54	0.92
Visalia	0.68	0.38	0.37	1.00	0.76	0.44	1.05
Clovis	0.71	0.45	0.42	1.00	0.72	0.49	1.12
Bakersfield – California	0.69	0.35	0.33	0.96	0.74	0.37	1.07
Fresno - Garland	0.69	0.47	0.43	0.99	0.72	0.44	1.09
Turlock	0.74	0.56	0.52	0.99	0.89	0.54	1.08
Fresno - H&W	0.70	0.49	0.45	0.99	0.73	0.42	1.08
Stockton	0.81	0.67	0.58	1.02	0.93	0.62	1.10
Merced - S Coffee	0.73	0.53	0.46	1.00	0.88	0.56	1.07
Modesto	0.76	0.59	0.53	0.99	0.90	0.57	1.08
Merced - Main St	0.78	0.51	0.46	1.00	0.87	0.57	1.07
Manteca	0.79	0.65	0.58	1.00	0.90	0.59	1.07
Tranquility	0.71	0.51	0.36	1.00	0.88	0.59	1.02

Table 42. 2025 24-hour RRFs for $PM_{2.5}$ components.

Site	RRF for $PM_{2.5}$	RRF for NH_4	RRF for NO_3	RRF for SO_4	RRF for OM	RRF for EC	RRF for Crustal
Bakersfield - California	0.52	0.33	0.35	0.96	0.70	0.36	1.04
Fresno – Garland	0.54	0.44	0.45	0.96	0.61	0.38	1.08
Hanford	0.51	0.36	0.36	1.03	0.82	0.52	0.90
Fresno - H&W	0.58	0.48	0.49	0.99	0.66	0.41	1.10
Clovis	0.54	0.41	0.43	1.01	0.65	0.45	1.13
Visalia	0.53	0.43	0.44	1.04	0.66	0.41	1.06
Bakersfield – Planz	0.57	0.36	0.37	0.96	0.68	0.35	1.05
Madera	0.58	0.46	0.47	1.00	0.72	0.52	1.06
Turlock	0.59	0.44	0.45	0.97	0.77	0.52	1.08
Modesto	0.59	0.46	0.47	0.98	0.77	0.51	1.07
Merced – Main St	0.58	0.46	0.47	0.98	0.67	0.49	1.07
Stockton	0.66	0.51	0.51	1.01	0.87	0.62	1.08
Merced – S Coffee	0.57	0.46	0.48	0.98	0.68	0.49	1.05
Manteca	0.68	0.57	0.58	1.00	0.82	0.61	1.07
Tranquility	0.54	0.30	0.30	1.06	0.82	0.61	1.10

Table 43. Projected 2025 Annual $PM_{2.5}$ composition.

Name	Future $PM_{2.5}$ (µg/m³)	Future NH_4 (µg/m³)	Future NO_3 (µg/m³)	Future SO_4 (µg/m³)	Future OM (µg/m³)	Future EC (µg/m³)	Future Crustal (µg/m³)	Future Water (µg/m³)	Blank (µg/m³)
Bakersfield – Planz	12.0	0.49	0.89	1.59	4.93	0.36	2.68	0.57	0.5
Madera	11.9	0.94	1.76	1.48	4.91	0.48	1.26	0.60	0.5
Hanford	10.4	1.00	2.03	1.53	3.26	0.38	1.11	0.61	0.5
Visalia	11.1	0.53	1.11	1.45	5.39	0.30	1.21	0.55	0.5
Clovis	11.4	0.49	0.89	1.29	6.11	0.43	1.19	0.50	0.5
Bakersfield - California	11.0	0.46	0.85	1.41	4.56	0.34	2.36	0.50	0.5
Fresno – Garland	10.4	0.49	0.93	1.10	5.61	0.36	0.98	0.43	0.5
Turlock	11.1	0.89	2.04	1.21	4.52	0.42	0.94	0.55	0.5
Fresno – H &W	10.0	0.49	0.93	1.04	5.37	0.33	0.92	0.42	0.5
Stockton	10.6	0.93	1.92	1.16	4.28	0.41	0.90	0.52	0.5
Merced - S Coffee	9.6	0.73	1.53	1.12	4.02	0.37	0.86	0.46	0.5
Modesto	9.9	0.82	1.80	1.07	4.03	0.38	0.83	0.49	0.5
Merced - Main St	8.6	0.42	0.77	0.89	4.69	0.32	0.66	0.34	0.5
Manteca	7.9	0.69	1.51	0.83	3.07	0.30	0.64	0.40	0.5
Tranquility	5.5	0.39	0.67	0.61	2.36	0.24	0.51	0.23	0.5

Table 44. Projected 2025 24-hour $PM_{2.5}$ composition.

Name	Future $PM_{2.5}$ (µg/m³)	Future NH_4 (µg/m³)	Future NO_3 (µg/m³)	Future SO_4 (µg/m³)	Future OM (µg/m³)	Future EC (µg/m³)	Future Crustal (µg/m³)	Future Water (µg/m³)	Blank (µg/m³)
Bakersfield – California	32.7	2.6	8.2	2.4	12.9	1.0	3.4	1.7	0.5
Fresno - Garland	32.3	2.9	9.3	1.4	14.4	1.0	1.0	1.8	0.5
Hanford	29.4	3.0	9.4	2.4	9.8	1.0	1.4	2.0	0.5
Fresno – H&W	34.7	3.1	10.0	1.4	15.5	1.1	1.0	2.0	0.5
Clovis	30.5	2.6	8.3	1.6	13.8	1.1	0.9	1.7	0.5
Visalia	29.7	3.2	10.3	2.2	9.7	0.7	1.0	2.1	0.5
Bakersfield - Planz	29.7	2.2	5.9	4.3	11.7	0.7	2.6	1.9	0.5
Madera	29.7	2.8	9.0	1.2	12.4	1.2	0.8	1.8	0.5
Turlock	29.6	2.9	9.0	2.1	11.1	1.2	1.1	1.8	0.5
Modesto	28.6	2.9	8.8	1.7	10.7	1.2	1.0	1.8	0.5
Merced – Main Street	27.0	2.4	7.5	1.6	11.4	1.1	1.0	1.5	0.5
Stockton	28.1	2.8	8.4	2.0	10.7	1.2	0.8	1.7	0.5
Merced – S Coffee	23.8	2.5	7.7	1.7	8.2	1.0	0.8	1.6	0.5
Manteca	25.4	2.8	8.5	1.4	8.8	1.1	0.8	1.7	0.5
Tranquility	16.0	1.0	3.2	0.9	8.3	0.8	0.5	0.7	0.5

5.6 $PM_{2.5}$ PRECURSOR SENSITIVITY ANALYSIS

To evaluate the impact of reducing emissions of different $PM_{2.5}$ precursors on $PM_{2.5}$ DVs, a series of model sensitivity simulations were performed, for which anthropogenic emissions of the precursor species were reduced by a certain percentage from the baseline emissions. The U.S. EPA (USEPA, 2016) recommends a range of 30-70% reduction in precursor emissions in the nonattainment area, and that recommendation is followed here.

Comparing the difference in $PM_{2.5}$ DVs from the precursor reduction simulations and the baseline modeling shows the sensitivity of the $PM_{2.5}$ DVs to changes in baseline precursor emissions. Given the nature of $PM_{2.5}$ formation, the effect of reductions in the following $PM_{2.5}$ precursors were investigated: direct $PM_{2.5}$ (or primary $PM_{2.5}$), nitrogen oxides (NO_x), sulfur oxides (SO_x), ammonia (NH_3), and volatile organic compounds (VOCs). For each precursor sensitivity, only anthropogenic emissions in the San Joaquin Valley were reduced. Natural emissions and emissions outside of SJV were kept constant. Since it is known that NO_x and direct $PM_{2.5}$ contribute significantly to $PM_{2.5}$ formation in the SJV (Pusede et al., 2016) and the current control program already relies heavily on NO_x and direct $PM_{2.5}$ emission reductions, for NO_x and direct $PM_{2.5}$ only sensitivity runs for a 30% emission reduction were performed. Given the lower contribution of other precursor species to total $PM_{2.5}$ (i.e., ammonia, VOCs, and SO_x), both 30% and 70% emission reductions were performed for those species.

The precursor sensitivity modeling was performed for the 2013 base year, as well as future years 2020 and 2024. Given the small change in emissions between 2024 and 2025, precursor reduction simulations were not performed for 2025 because $PM_{2.5}$ sensitivity to precursor reductions is expected to be very similar between 2024 and 2025.

Tables 45 and 46 show the impact from precursor reductions on annual and 24-hour $PM_{2.5}$ DVs for 2013, respectively. 30% PM and 30% NO_x reductions clearly show significant impact on $PM_{2.5}$ DVs. Direct PM reduction is more effective than NO_x for the annual standard, while their impacts are roughly comparable for the 24-hour standard. Although both NO_x and ammonia contribute to ammonium nitrate formation, the impact on $PM_{2.5}$ DVs from ammonia reduction is less than that from NO_x reductions, because ammonium nitrate formation in the SJV is limited by the availability of nitric acid instead of by ammonia (Lurmann et al., 2006; Markovic, 2014; Parworth, et al., 2017; Prabhakar et al., 2017), and so ammonia reduction is less effective than NO_x reductions in reducing ammonium nitrate concentrations. This is consistent with previous modeling studies (Chen et al., 2014; Kleeman et al., 2005; Pun et al., 2009). Reducing SO_x emissions has a very small impact on annual DVs, and may have dis-benefit for 24-hour

DVs at many sites. The negative impact on 24-hour DVs from SO_x emission reductions is due to the non-linearity in inorganic thermodynamics that governs the partitioning of ammonium and nitrate onto particles (e.g., West et al., 2011). Reducing VOC emissions has a small positive impact on both annual and 24-hour DVs. In 2013, reducing VOC emissions reduced secondary organic aerosol (SOA) formation as well as slightly lowering ammonium nitrate formation, as demonstrated in Kleeman et al. (2005) and Pun et al. (2009).

Tables 47 and 48 show the impact on annual and 24-hour DVs from precursor reductions in 2020, respectively. Similar to 2013, 30% PM and 30% NO_x reductions lead to substantial reductions in both annual and 24-hour $PM_{2.5}$ DVs in 2020. While ammonia reduction also leads to reductions in both annual and 24-hour $PM_{2.5}$ DVs, an equivalent percentage of ammonia reduction is typically less effective than NO_x reductions, due to the excess of ammonia in the SJV (Parworth et al., 2017; Prabhaker et al., 2017). While NO_x emissions in 2020 exhibit substantial reductions from 2013 levels, ammonia emission tends are relatively flat, meaning ammonia is even more in excess in 2020 (i.e., NH_3 reductions will be even less effective at reducing $PM_{2.5}$ in 2020). Reducing SO_x emissions leads to a slight increase in annual DVs but a slight decrease in 24-hour DVs at most sites, which is consistent with the 2013 results. Reducing VOC emissions has a very small impact on annual DVs but do result in a small reduction in the 24-hour DVs.

Tables 49 and 50 show the impact on annual and 24-hour DVs from precursor reductions in 2024, respectively. For both PM and NO_x emissions, a 30% reduction leads to significant reductions in both annual and 24-hour DVs, similar to years 2013 and 2020. Ammonia reduction is less effective than the same percent reduction in NO_x emissions. As previously stated, in the SJV ammonia is in excess and as NO_x emissions decrease further into the future, ammonia becomes even more in excess. This means that ammonium nitrate formation is even more limited by the availability of nitric acid than by ammonia in 2024 compared to 2013. Similar to 2013 and 2020, reducing SO_x emissions also has a slightly negative impact on 24-hour DVs at several sites due to the non-linearity of inorganic aerosol thermodynamics (e.g., West et al., 2011). The impact of SO_x emission reductions on the annual DVs is fairly small, primarily because of the limited amount of SO_x emissions in the SJV. Reducing VOC emissions has essentially no effect on the annual DVs, and a slightly negative impact on 24-hour DVs. Reducing VOC emissions can reduce SOA formation. However, under 2024 emission levels, reducing VOC emissions can slightly increase ammonium nitrate formation in the wintertime. This is different from the reference year 2013, because modeled ammonium nitrate concentration is much smaller in 2024 than in 2013, such that the response in ammonium nitrate formation to VOC emission reductions is reversed. A previous modeling study by CARB (2016) utilizing the Integrated Reaction Rate (IRR) technique in the CMAQ model shows that reduced VOC emissions can lead to less peroxyacetyle nitrate (PAN) formation (Meng et al., 1997), increased availability of nitrogen dioxide and more nighttime nitric acid formation. However, since lower VOC levels also reduce daytime hydroxyl radical concentrations and result in less daytime nitric acid formation, these processes compete with each other and lead to a different net impact on ammonium nitrate formation depending on the NOx and VOC emission levels.

Table 45. Difference in Annual $PM_{2.5}$ DVs between the 2013 baseline run and precursor emission reduction runs.

Sites	Baseline DV	30% PM*	30% NO_x	30% NH_3	70% NH_3	30%ROG	70%ROG	30% SO_x	70% SO_x
Bakersfield - Planz	17.2	2.7	0.9	0.4	1.5	0.1	0.3	0.0	0.1
Madera	16.9	1.7	0.9	0.6	2.1	0.1	0.2	0.0	0.0
Hanford	16.5	1.4	1.7	0.7	2.3	0.1	0.2	0.0	0.0
Visalia	16.2	2.1	0.9	0.4	1.4	0.2	0.4	0.1	0.1
Clovis	16.1	2.5	0.6	0.3	1.2	0.1	0.3	0.0	0.0
Bakersfield - California	16.0	2.5	0.9	0.4	1.6	0.1	0.3	0.0	0.1
Fresno - Garland	15.0	2.3	0.5	0.3	1.1	0.1	0.3	0.0	0.1
Turlock	14.9	1.4	0.6	0.4	1.4	0.1	0.2	0.1	0.1
Fresno - H&W	14.2	2.2	0.4	0.3	1.1	0.1	0.3	0.0	0.1
Stockton	13.1	0.9	0.3	0.3	1.0	0.1	0.1	0.1	0.2
Merced - S Coffee	13.1	1.2	0.7	0.4	1.5	0.1	0.1	0.0	0.0
Modesto	13.0	1.2	0.5	0.4	1.3	0.1	0.1	0.1	0.1
Merced - M Street	11.0	1.2	0.4	0.2	0.7	0.1	0.1	0.0	0.0
Manteca	10.1	0.6	0.2	0.2	0.8	0.1	0.1	0.1	0.1
Tranquility	7.7	0.5	0.6	0.4	1.3	0.0	0.0	0.0	0.0

*: 30% PM means that anthropogenic PM emissions within SJV are reduced by 30% from the baseline emissions inventory. Same meaning applies to other precursor reduction runs.

Table 46. Difference in 24-hour $PM_{2.5}$ DVs between the 2013 baseline run and precursor emission reduction runs.

Sites	Baseline DV	30% PM*	30% NO_x	30% NH_3	70% NH_3	30%ROG	70%ROG	30% SO_x	70% SO_x
Bakersfield – California	64.1	8.1	6.8	3.3	12.4	1.4	3.6	-0.4	-1.1
Fresno – Garland	60.0	7.6	3.5	2.0	7.5	0.9	2.2	-0.1	-0.6
Hanford	60.0	4.5	7.8	2.1	9.4	1.1	3.0	-0.4	-1.4
Fresno – H&W	59.3	7.2	2.5	1.9	9.6	1.1	2.7	-0.1	-0.5
Clovis	55.8	7.6	3.8	1.9	8.8	0.9	2.2	-0.2	-0.6
Visalia	55.5	5.4	3.5	2.0	9.7	1.9	4.8	-0.3	-0.8
Bakersfield – Planz	55.5	7.6	4.2	2.2	9.0	1.2	3.0	-0.4	-1.0
Madera	51.0	5.2	3.0	1.7	7.6	0.9	2.1	-0.3	-1.2
Turlock	50.7	3.8	3.6	1.5	6.3	0.7	1.6	-0.1	-0.4
Modesto	47.9	3.6	3.1	1.5	6.4	0.6	1.3	0.1	-0.1
Merced – M Street	46.9	5.0	2.7	1.0	5.0	0.4	1.0	-0.1	-0.3
Stockton	42.0	2.6	2.0	1.0	4.1	0.5	1.3	0.2	0.2
Merced – S Coffee	41.1	3.3	2.9	1.1	4.5	0.4	1.0	-0.1	-0.3
Manteca	36.9	1.9	1.1	0.9	3.5	0.5	1.2	0.2	0.5
Tranquility	29.5	2.1	3.9	2.2	8.8	0.1	0.2	0.0	-0.2

*: 30% PM means that anthropogenic PM emissions within SJV are reduced by 30% from the baseline emissions inventory. Same meaning applies to other precursor reduction runs.

Table 47. Difference in Annual $PM_{2.5}$ DVs between the 2020 baseline run and precursor emission reduction runs.

Sites	Baseline DV	30% PM*	30% NO_x	30% NH_3	70% NH_3	30%ROG	70%ROG	30% SO_x	70% SO_x
Bakersfield - Planz	14.6	2.3	0.8	0.2	0.8	0.0	0.1	0.0	0.1
Madera	14.2	1.4	0.9	0.4	1.2	0.0	0.1	0.0	0.0
Hanford	13.3	1.2	1.4	0.4	1.3	0.0	-0.1	0.0	0.0
Visalia	13.5	1.8	0.9	0.2	0.8	0.0	0.1	0.1	0.1
Clovis	13.4	2.0	0.6	0.2	0.6	0.1	0.2	0.0	0.0
Bakersfield - California	13.5	2.2	0.8	0.2	0.8	0.0	0.0	0.0	0.1
Fresno - Garland	12.4	1.9	0.5	0.2	0.6	0.1	0.1	0.0	0.1
Turlock	12.5	1.1	0.7	0.3	0.9	0.0	0.0	0.1	0.1
Fresno - H&W	11.9	1.7	0.5	0.2	0.6	0.1	0.1	0.0	0.1
Stockton	11.4	0.8	0.4	0.2	0.7	0.0	0.0	0.1	0.2
Merced - S Coffee	10.9	1.0	0.6	0.3	0.8	0.0	0.0	0.0	0.0
Modesto	11.0	1.0	0.5	0.2	0.8	0.0	0.0	0.1	0.1
Merced - M Street	9.3	1.0	0.3	0.1	0.4	0.0	0.0	0.0	0.1
Manteca	8.7	0.5	0.3	0.2	0.5	0.0	0.0	0.1	0.1
Tranquility	6.4	0.4	0.4	0.2	0.6	0.0	0.0	0.0	0.0

*: 30% PM means that anthropogenic PM emissions within SJV are reduced by 30% from the baseline emissions inventory. Same meaning applies to other precursor reduction runs.

Table 48. Difference in 24-hour $PM_{2.5}$ DVs between the 2020 baseline run and precursor emission reduction runs.

Sites	Baseline DV	30% PM*	30% NO_x	30% NH_3	70% NH_3	30%ROG	70%ROG	30% SO_x	70% SO_x
Bakersfield – California	47.6	5.8	7.4	1.9	6.4	0.1	0.5	-0.2	-0.9
Fresno – Garland	44.3	5.0	4.8	1.1	4.6	0.3	0.8	-0.1	-0.5
Hanford	43.7	3.2	7.3	1.4	4.6	0.0	0.2	-0.5	-1.3
Fresno – H&W	45.6	4.9	4.3	1.1	5.8	0.4	1.0	-0.1	-0.2
Clovis	41.1	4.9	4.5	0.9	4.7	0.3	0.7	-0.1	-0.4
Visalia	42.8	3.7	6.5	1.3	5.8	0.6	1.5	-0.2	-0.5
Bakersfield – Planz	41.2	5.2	6.0	1.4	5.4	0.3	1.0	-0.1	-0.3
Madera	38.9	3.3	4.1	1.0	3.6	0.2	0.6	-0.3	-0.9
Turlock	37.8	2.4	4.2	1.0	3.2	0.1	0.2	0.0	-0.2
Modesto	35.8	2.2	3.6	0.9	3.3	0.1	0.2	0.2	0.0
Merced – M Street	32.9	2.7	2.9	0.6	2.3	0.0	0.1	-0.1	-0.2
Stockton	33.5	2.0	2.5	0.7	2.1	0.1	0.3	0.2	0.4
Merced – S Coffee	30.0	2.1	2.9	0.5	2.2	0.0	0.1	-0.1	-0.2
Manteca	30.1	1.1	1.9	0.5	1.6	0.1	0.3	0.2	0.5
Tranquility	21.5	1.4	3.0	1.2	4.0	-0.1	-0.2	0.0	0.0

*: 30% PM means that anthropogenic PM emissions within SJV are reduced by 30% from the baseline emissions inventory. Same meaning applies to other precursor reduction runs.

Table 49. Difference in Annual $PM_{2.5}$ DVs between the 2024 baseline run and precursor emission reduction runs

Sites	Baseline DV	30% PM*	30% NO_x	30% NH_3	70% NH_3	30%ROG	70%ROG	30% SO_x	70% SO_x
Bakersfield - Planz	12.0	1.9	0.5	0.1	0.4	0.0	0.0	0.1	0.1
Madera	12.0	1.2	0.6	0.2	0.7	0.0	0.0	0.0	0.1
Hanford	10.5	1.0	0.8	0.3	0.8	-0.1	-0.2	0.0	0.1
Visalia	11.1	1.5	0.6	0.1	0.4	0.0	0.0	0.1	0.2
Clovis	11.4	1.6	0.4	0.1	0.3	0.0	0.1	0.0	0.1
Bakersfield - California	11.0	1.8	0.5	0.1	0.4	0.0	0.0	0.1	0.1
Fresno - Garland	10.4	1.5	0.4	0.1	0.3	0.0	0.1	0.0	0.1
Turlock	11.1	1.1	0.5	0.2	0.6	0.0	0.0	0.1	0.1
Fresno - H&W	10.0	1.4	0.4	0.1	0.3	0.0	0.1	0.1	0.1
Stockton	10.7	0.8	0.3	0.2	0.5	0.0	0.0	0.1	0.2
Merced - S Coffee	9.7	0.9	0.4	0.2	0.5	0.0	0.0	0.0	0.1
Modesto	10.0	1.0	0.4	0.2	0.6	0.0	0.0	0.1	0.2
Merced - M Street	8.6	0.9	0.2	0.1	0.3	0.0	0.0	0.0	0.1
Manteca	8.0	0.4	0.3	0.1	0.4	0.0	0.0	0.1	0.1
Tranquility	5.5	0.3	0.2	0.1	0.4	0.0	0.0	0.0	0.0

*: 30% PM means that anthropogenic PM emissions within SJV are reduced by 30% from the baseline emissions inventory. Same meaning applies to other precursor reduction runs.

Table 50. Difference in 24-hour $PM_{2.5}$ DVs between the 2024 baseline run and precursor emission reduction runs

Sites	Baseline DV	30% PM*	30% NO_x	30% NH_3	70% NH_3	30%ROG	70%ROG	30% SO_x	70% SO_x
Bakersfield – California	33.3	5.1	4.0	1.0	2.8	-0.4	-0.9	-0.3	-0.7
Fresno – Garland	32.8	3.8	3.3	0.7	1.9	-0.1	-0.2	-0.1	-0.3
Hanford	30.1	2.6	4.5	1.0	3.0	-0.4	-1.0	-0.3	-1.1
Fresno – H&W	35.1	4.0	4.0	0.8	2.9	0.0	-0.1	0.0	-0.1
Clovis	30.7	4.2	3.4	0.7	2.3	0.0	0.0	0.0	0.0
Visalia	30.2	3.0	5.1	0.8	2.5	-0.3	-0.5	-0.1	-0.2
Bakersfield – Planz	30.0	4.0	3.6	0.7	2.2	-0.2	-0.5	0.1	0.2
Madera	30.2	2.9	2.6	0.7	1.6	-0.1	-0.3	-0.1	-0.6
Turlock	30.2	2.3	2.6	0.7	2.1	-0.1	-0.3	0.1	0.0
Modesto	29.1	2.3	2.6	0.6	2.2	-0.1	-0.2	0.2	0.2
Merced – M Street	27.4	2.6	2.1	0.5	1.4	-0.1	-0.3	0.0	-0.1
Stockton	28.6	2.1	2.1	0.5	1.5	-0.1	-0.1	0.3	0.6
Merced – S Coffee	24.2	2.1	1.9	0.4	1.2	-0.1	-0.3	-0.1	-0.1
Manteca	25.8	1.1	1.8	0.4	1.4	0.0	-0.1	0.3	0.6
Tranquility	16.2	1.2	1.5	0.6	1.8	-0.1	-0.4	0.0	0.1

*: 30% PM means that anthropogenic PM emissions within SJV are reduced by 30% from the baseline emissions inventory. Same meaning applies to other precursor reduction runs.

5.7 UNMONITORED AREA ANALYSIS

The unmonitored area analysis is performed to ensure that there are no regions outside of the existing monitoring network that could exceed the NAAQS if a monitor was present at that location (U.S. EPA, 2014). The U.S. EPA recommends combining spatially interpolated design value fields with modeled gradients for the pollutant of interest and grid-specific RRFs in order to generate gridded future year gradient adjusted design values. The spatial Interpolation of the observed design values is done only within the geographic region constrained by the monitoring network, since extrapolating to outside of the monitoring network is inherently uncertain. This analysis can be done using the Model Attainment Test Software (MATS) (Abt, 2014). However, this software is not open source and comes as a precompiled software package. To maintain transparency and flexibility in the analysis, in-house R codes (https://www.r-project.org/) developed at ARB are utilized in this analysis.

For annual $PM_{2.5}$ standards, the unmonitored area analysis involves the following steps:

Step 1: At each grid cell, the annual average $PM_{2.5}$ (total and by species) is calculated as the average of the 3x3 surrounding grid cells (i.e., consistent with the way that annual RRF is calculated) from the future year simulation, and a gradient in the annual averages between each grid cell and grid cells which contain a monitor is calculated.

Step 2: The annual future year speciated $PM_{2.5}$ design values are obtained for each design site from the attainment test. For each grid cell, the monitors within its Voronoi Region are identified, and the speciated $PM_{2.5}$ values are then interpolated using normalized inverse distance squared weightings for all monitors within a grid cell's Voronoi Region. The interpolated speciated $PM_{2.5}$ fields are further adjusted based on the appropriate gradients from Step 1.

Step 3: The concentration of each of the component $PM_{2.5}$ species are summed to calculate the total $PM_{2.5}$ concentration (or DV) for each grid cell.

Step 4: The future year gridded annual average $PM_{2.5}$ estimates are then compared to the annual $PM_{2.5}$ NAAQS to determine compliance.

The unmonitored area analysis for the 24-hour $PM_{2.5}$ standard include the following steps:

Step 1: At each grid cell, the quarterly average of the top 10% of the modeled days for 24-hour $PM_{2.5}$ (total and by species for the same top 10% of days) is calculated from the future year simulation, and a gradient in these quarterly speciated averages between each grid cell and grid cells which contain a monitor is calculated.

Step 2: The 24-hour future year speciated $PM_{2.5}$ design values are obtained for each design site from the attainment test. For each grid cell, the monitors within its Voronoi Region are identified, and the speciated $PM_{2.5}$ values are then interpolated using normalized inverse distance squared weightings for all monitors within a grid cell's Voronoi Region. The interpolated speciated $PM_{2.5}$ fields are further adjusted based on the appropriate gradients from Step 1.

Step 3: The concentration of each of the component $PM_{2.5}$ species are summed to calculate the total $PM_{2.5}$ concentration (or DV) for each grid cell.

Step 4: The future year gridded 24-hour average $PM_{2.5}$ estimates are then compared to the 24-hour $PM_{2.5}$ NAAQS to determine compliance.

For the year 2020, an unmonitored area analysis was performed for the USEPA 1997 annual and 24-hour $PM_{2.5}$ standards. For the year 2024, an unmonitored area analysis was performed for the USEPA 2006 24-hour $PM_{2.5}$ standard only, and for the year 2025, an unmonitored area analysis was performed for the USEPA 2012 annual $PM_{2.5}$ standard only.

Figure 15 shows the spatial distribution of projected 2020 annual $PM_{2.5}$ DVs in the SJV nonattainment area. Projected 2020 annual $PM_{2.5}$ DVs at every grid cell are below the threshold needed for attainment (15.04 $\mu g/m^3$), except for a few cells surrounding the Lemoore military facility, where the greater $PM_{2.5}$ levels are due to localized emissions associated with that facility. A similar $PM_{2.5}$ hotspot associated with the Lemoore military facility was observed in past SJV $PM_{2.5}$ SIPs as well. This demonstrates that all unmonitored areas within the SJV will attain the 15 $\mu g/m^3$ annual $PM_{2.5}$ standard (technically, DVs not greater than 15.04 $\mu g/m^3$ are considered as attainment) established by the USEPA in 1997, except for a small area surrounding the Lemoore military facility.

Figure 16 shows the spatial distribution of projected 2020 24-hour $PM_{2.5}$ DVs in the SJV nonattainment area. Projected 2020 24-hour $PM_{2.5}$ DVs within the SJV do not exceed 65.4 $\mu g/m^3$ except for a few grid cells surrounding the Lemoore military facility, again due to the localized emissions associated with that facility. This demonstrates that all unmonitored areas within the SJV will attain the 65 $\mu g/m^3$ 24-hour $PM_{2.5}$ standard (technically, DVs not greater than 65.4 $\mu g/m^3$ are considered as attainment) established by the USEPA in 1997, except for a small area surrounding the Lemoore military facility.

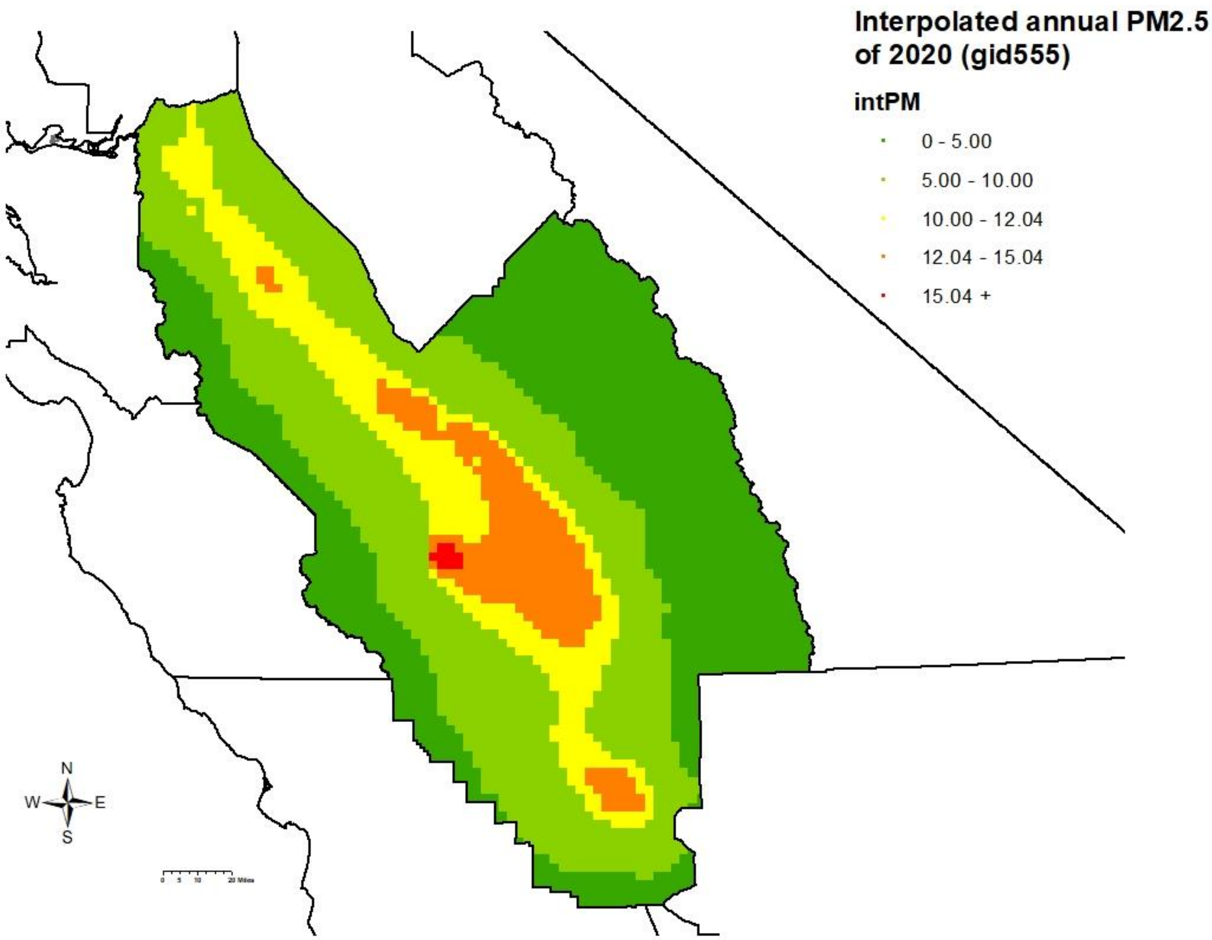

Figure 15. Spatial distribution of projected 2020 annual $PM_{2.5}$ DVs within the SJV nonattainment area. All grid cells have DVs not greater than 15.04 µg/m^3 except for a few cells surrounding the Lemoore Naval facility.

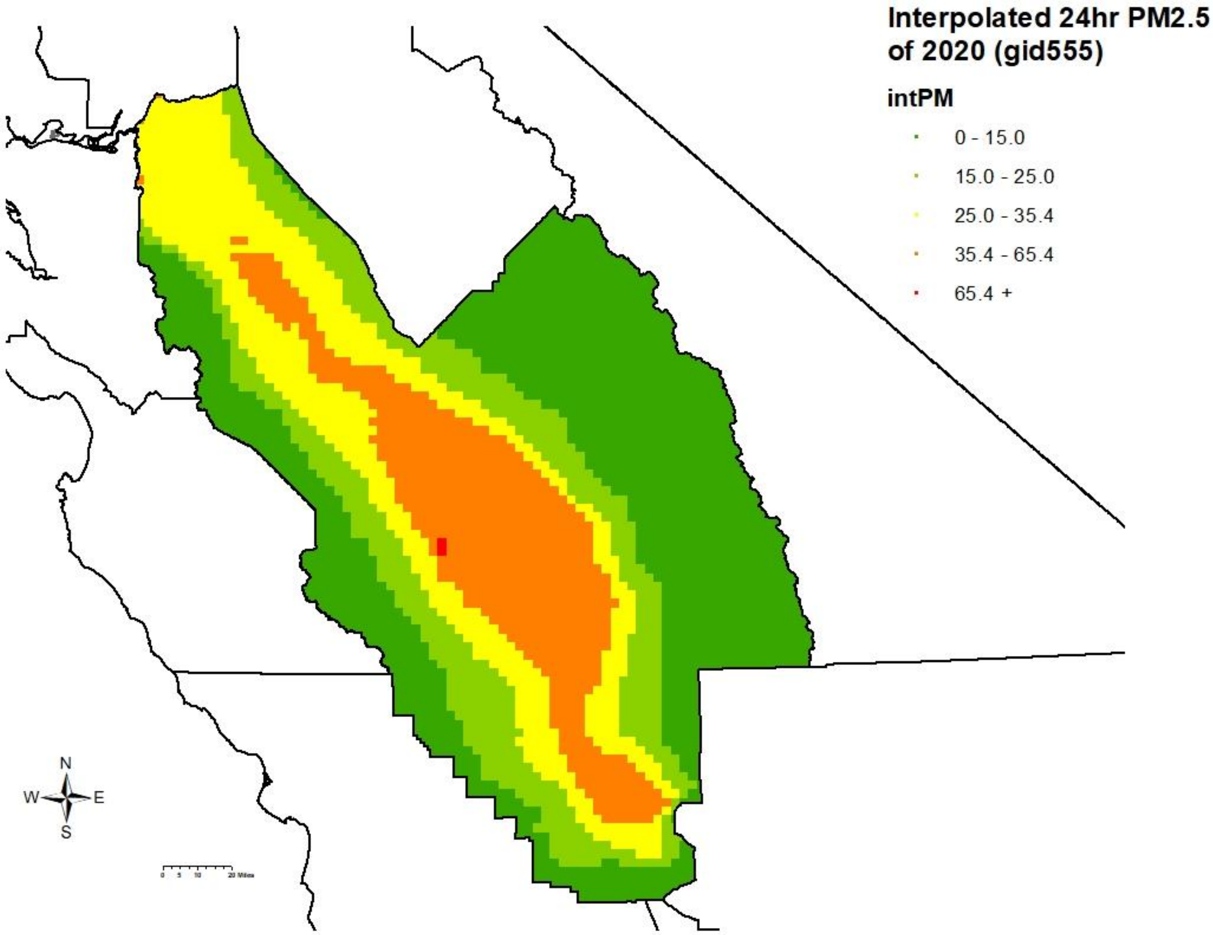

Figure 16. Spatial distribution of projected 2020 24-hour $PM_{2.5}$ DVs within the SJV nonattainment area. All grid cells have DVs not greater than 65.4 µg/m^3 except a few cells surrounding the Lemoore Naval facility.

Figure 17 shows the spatial distribution of projected 2024 24-hour $PM_{2.5}$ DVs in the SJV nonattainment area. Projected 2024 24-hour $PM_{2.5}$ DVs within the SJV do not exceed 35.4 µg/m^3 (technically, DVs not greater than 35.4 µg/m^3 are considered attainment for the 2006 35 µg/m^3 24-hour $PM_{2.5}$ standard), except for a few grid cells located to the southeast of the Fresno metropolitan area as well as a few grid cells surrounding the Lemoore Navy facility. Again, the elevated concentrations surrounding the Lemoore Naval facility are due to localized emissions associated with military operations. The area exceeding the standard to the southeast of the main Fresno metropolitan area is primarily due to elevated ammonium nitrate and organic carbon levels in the modeling system, which are likely due to a combination of transport of polluted air masses and some local emissions within the exceedance area in 2024. ARB plans to assess the elevated ammonium nitrate and organic carbon levels in the region and if appropriate, monitor $PM_{2.5}$ air quality levels.

Figure 18 shows the spatial distribution of projected 2025 annual $PM_{2.5}$ DVs in the SJV nonattainment area. Projected 2025 annual $PM_{2.5}$ DVs within the SJV are below 12.04 µg/m^3 (technically, DVs not greater than 12.04 µg/m^3 are considered attainment for the 2012 12 µg/m^3 annual $PM_{2.5}$ standard) except for a few cells surrounding the Lemoore Navy facility. Again, grid cells exceeding the standard surrounding the Lemoore Navy facility are due to localized emissions associated with the operations of that facility.

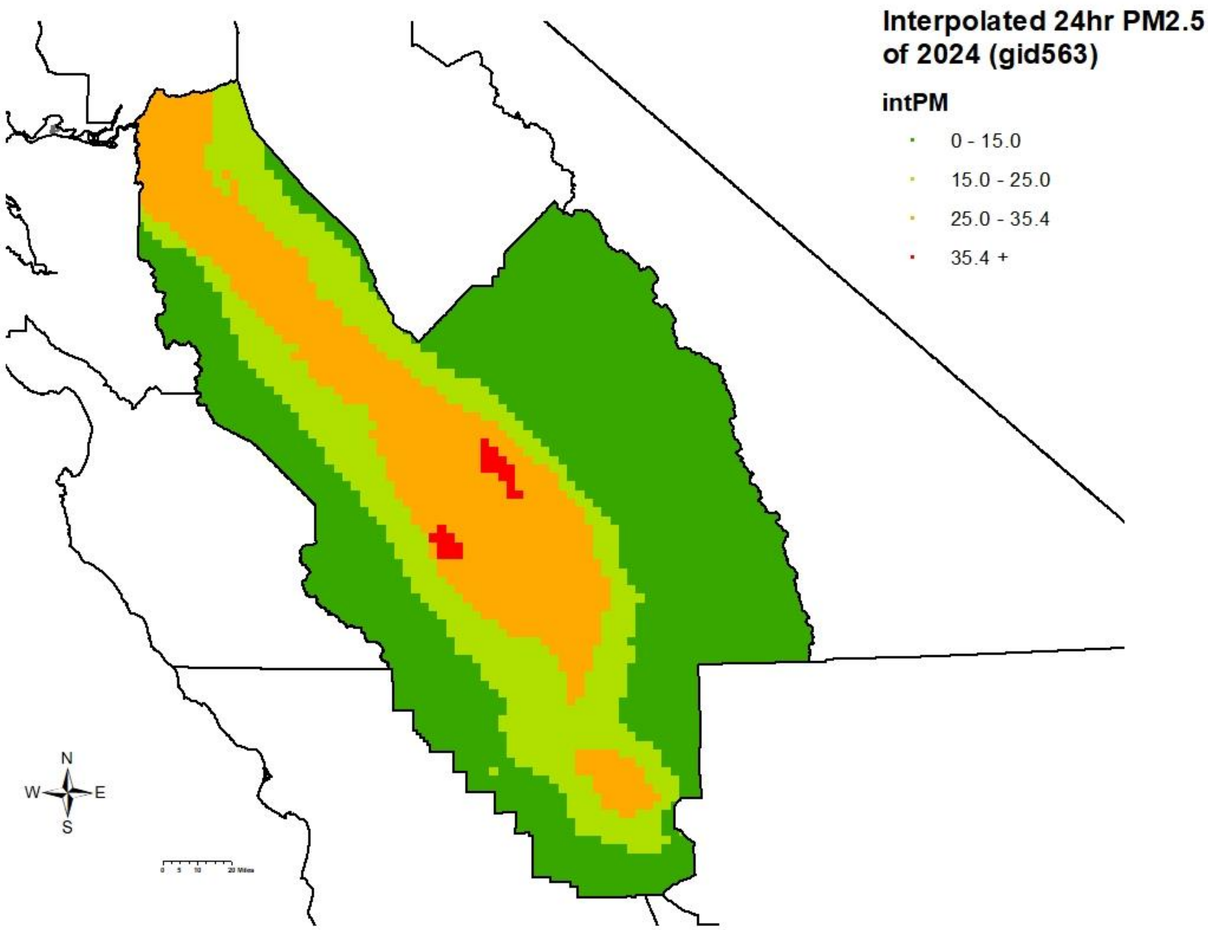

Figure 17. Spatial distribution of projected 2024 24-hour $PM_{2.5}$ DVs within the SJV nonattainment area. All grid cells have DVs not greater than 35.4 µg/m^3 except for a few cells located to the southeast of the main Fresno metropolitan area, as well as surrounding the Lemoore Naval facility.

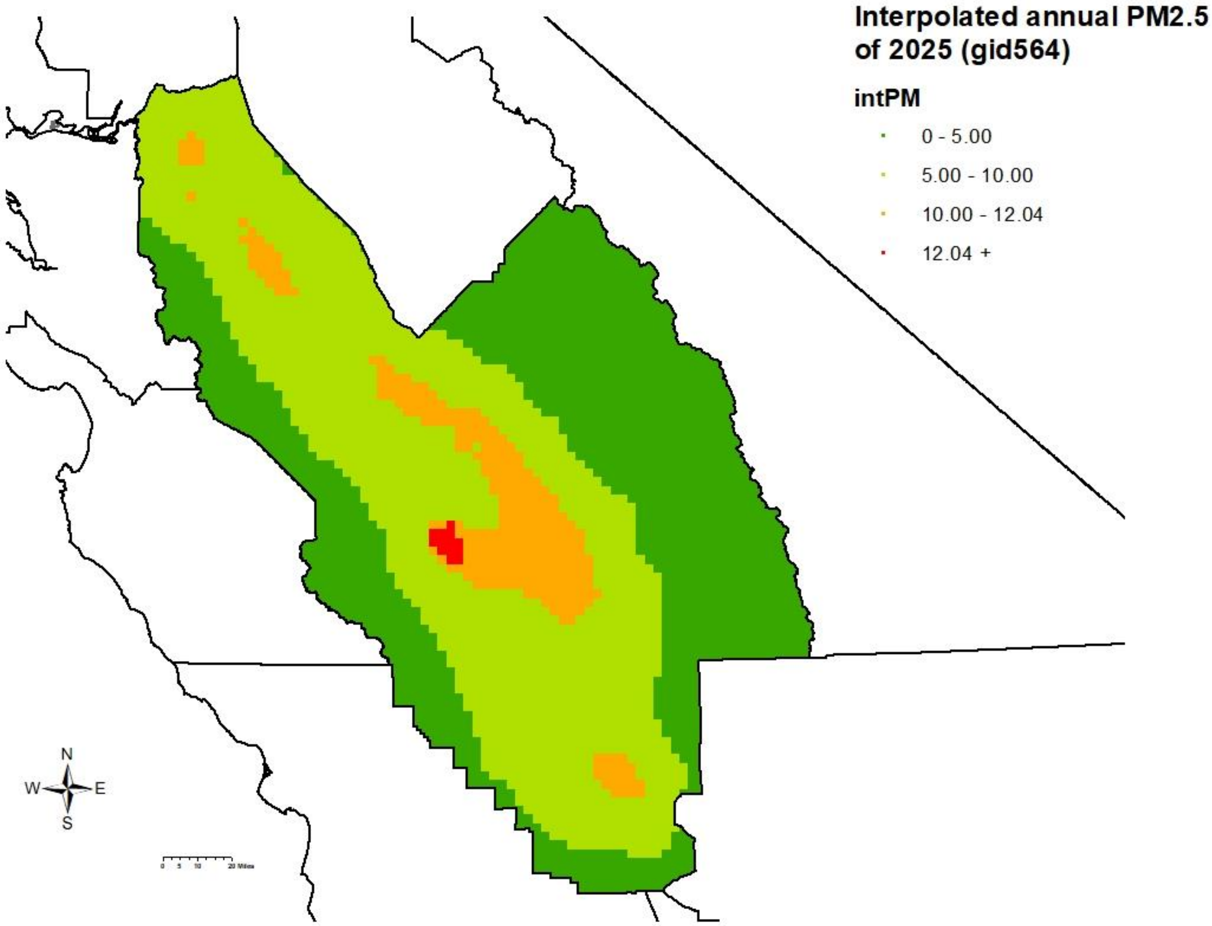

Figure 18. Spatial distribution of projected 2025 annual $PM_{2.5}$ DVs within the SJV nonattainment area. All grid cells have DVs not greater than 12.04 µg/m^3 except for a few cells surrounding the Lemoore Naval facility.

6 REFERENCES

Abt, 2014. Modeled Attainment Test Software: User's Manual. MATS available at: http://www.epa.gov/scram001/modelingapps_mats.htm.

Angevine, W. M., Eddington, L., Durkee, K., Fairall, C., Bianco, L., Brioude, J., 2012, Meteorological model evaluation for CalNex 2010, Monthly Weather Review, 140, 3885-3906.

Baker, K. R., Simon, H., Kelly, J.T., 2011, Challenges to modeling "cold pool" meteorology associated with high pollution episodes. Environmental Science and Technology, 45, 7118–9.

Baker, K. R., Misenis, C., Obland, M. D., Ferrare, R. A., Scarino, A. J., and Kelly, J. T., 2013, Evaluation of surface and upper air fine scale WRF meteorological modeling of the May and June 2010 CalNex period in California, Atmospheric Environment, 80, 299-309.

Bao, J.W., Michelson, S.A., Persson, P.O.G., Djalalova, I.V., Wilczak, J.M., 2008, Observed and WRF-simulated low-level winds in a high-ozone episode during the Central California ozone study, Journal of Applied Meteorology and Climatology, 47, 2372-2394.

Boylan, J.W. and Russell, A.G., 2006, PM and light extinction model performance metrics, goals, and criteria for three-dimensional air quality models, Atmospheric Environment, 40, 4946-4959.

CARB, 2016, Photochemical modeling for the 2016 San Joaquin Valley Annual PM2.5 State Implementation Plan, Modeling Assessment, Prepared by California Air Resources Board and San Joaquin Valley Air Pollution Control District for United States Environmental Protection Agency Region IX, available at http://www.valleyair.org/Air_Quality_Plans/docs/PM25-2016/a.pdf

Chen, J.J., Lu, J., Avise, J.C., DaMassa, J.A., Kleeman, M.J., Kaduwela, A.P., 2014, Seasonal modeling of PM2.5 in California's San Joaquin Valley, Atmospheric Environment, 92, 182-190.

Daly, C., Conklin, D., Unsworth, M., 2009, Local atmospheric decoupling in complex topography alters climate change impacts. International Journal of Climatology, 30, 1857–1864.

Emmons, L. K., et al., 2010, Impact of Mexico City emissions on regional air quality from MOZART-4 simulations, Atmospheric Chemistry and Physics, 10, 6195-6212.
Fast, J. D., et al., 2012, Transport and mixing patterns over Central California during the carbonaceous aerosol and radiative effects study (CARES), Atmospheric Chemistry and Physics, 12, 1759-1783, doi:10.5194/acp-12-1759-2012.

Fosberg, M.A., Schroeder, M.J., 1966, Marine air penetration in Central California, Journal of Applied Meteorology, 5, 573-589.

Frank, N.H., 2006, Retained nitrate, hydrated sulfates, and carbonaceous mass in federal reference method fine particulate matter for six eastern U.S. cities, Journal of Air & Waste Management Association, 56, 500-511.

Gillies, R. R., S. Wang, and M. R. Booth, 2010, Atmospheric scale interaction on wintertime intermountain west low-level inversions, Weather Forecasting, 25, 1196 – 1210.

Hu, J., Howard, C. J., Mitloehner, F., Green, P. G., Kleeman, M. J., 2012, Mobile Source and Livestock Feed Contributions to Regional Ozone Formation in Central California, Environmental Science & Technology, 46, 2781-2789.

Jackson, B.S., Chau, D., Gurer, K., Kaduwela, A., 2006, Comparison of ozone simulations using MM5 and CALMET/MM5 hybrid meteorological fields for the July/August 2000 CCOS episode, Atmospheric Environment, 40, 2812-2822.

Kelly, J. T., et al., 2014, Fine-scale simulation of ammonium and nitrate over the South Coast Air Basin and San Joaquin Valley of California during CalNex-2010, Journal of Geophysical Research, 119, 3600-3614, doi:10.1002/2013JD021290.

Kleeman, M.J., Ying, Q., Kaduwela, A., 2005, Control strategies for the reduction of airborne particulate nitrate in California's San Joaquin Valley, Atmospheric Environment, 39, 5325-5341.

Lurmann, F.W., Brown, S.G., McCarthy, M.C., Roberts, P.T., 2006, Processes Influencing Secondary Aerosol Formation in the San Joaquin Valley during Winter, Journal of Air and Waste Management Association, 56, 1679-1693.

Markovic, M. Z., VandenBoer, T. C., Baker, K. R., Kelly, J. T., Murphy, J. G., 2014, Measurements and modeling of the inorganic chemical composition of fine particulate matter and associated precursor gases in California's San Joaquin Valley during CalNex 2010, Journal of Geophysical Research - Atmosphere,119, 6853–6866, doi:10.1002/2013JD021408.

Meng, Z., Dabdub, D., Seinfeld, J.H., 1997, Chemical coupling between atmospheric ozone and particulate matter, Science, 277, 116-119.

Parworth, C.L., Young, D.E., Kim, H., Zhang, X., Cappa, C.D., Collier, S., Zhang, Q., 2017, Wintertime water-soluble aerosol composition and particle water content in Fresno, California, Journal of Geophysical Research, Atmosphere, 10.1002/2016JD026173.

Prabhakar, G., Parworth, C., Zhang, X., Kim, H., Young, D., Beyersdorf, A.J., Ziemba, L.D., Nowak, J.B., Bertram, T.H., Faloona, I.C., Zhang, Q., Cappa, C.D., 2017, Observational assessment of the role of nocturnal residual-layer chemistry in determining daytime surface particulate nitrate concentrations, Atmospheric Chemistry Physics, https://doi.org/10.5194/acp-17-14747-2017.

Pun, B.K., Balmori, R.T.F., Seigneur, C., 2009. Modeling wintertime particulate matter formation in central California, Atmospheric Environment 43, 402-409.

Pusede, S.E., et al., 2016, On the effectiveness of nitrogen oxide reductions as a control over ammonium nitrate aerosol, Atmospheric Chemistry Physics, 16, 2575-2596.

Rogers, R.E., Deng, A., Stauffer, D. Gaudet, B.J., Jia, Y., Soong, S.-T., Tanrikulu, S., 2013, Application of the Weather Research and Forecasting model for air quality modeling in the San Francisco Bay area, Journal of Applied Meteorology and Climatology, 52, 1953-1973.

Simon, H., Baker, K.R., and Phillips, S., 2012, Compilation and interpretation of photochemical model performance statistics published between 2006 and 2012, Atmospheric Environment, 61, 124-139.

Skamarock, W. C., J. B. Klemp, J. Dudhia, D. O. Gill, D. M. Barker, W. Wang, and J. G. Powers, 2005: A description of the Advanced Research WRF Version 2. NCAR Tech Notes-468+STR.

U.S. EPA, 2014, Draft Modeling Guidance for Demonstrating Attainment of Air Quality Goals for Ozone, PM2.5 and Regional Haze, available at http://www.epa.gov/scram001/guidance/guide/Draft_O3-PM-RH_Modeling_Guidance-2014.pdf

U.S. EPA, 2016, PM2.5 Precursor Demonstration Guidance, available at https://www.epa.gov/sites/production/files/2016-11/documents/transmittal_memo_and_draft_pm25_precursor_demo_guidance_11_17_16.pdf.

West, J.J., Ansari, A.S., Pandis, S.N., 1999, Marginal PM2.5: Nonlinear aerosol mass response to sulfate reductions in the eastern United States, Journal of the Air & Waste Management Association, 49, 1415-1424.

Whiteman, C. D., Zhong, S., Shaw, W. J., Hubbe, J. M., Bian, X., Mittelstadt, J., 2001, Cold pools in the Columbia Basin. Weather Forecasting, 16, 432–447.

SUPPLEMENTAL MATERIALS

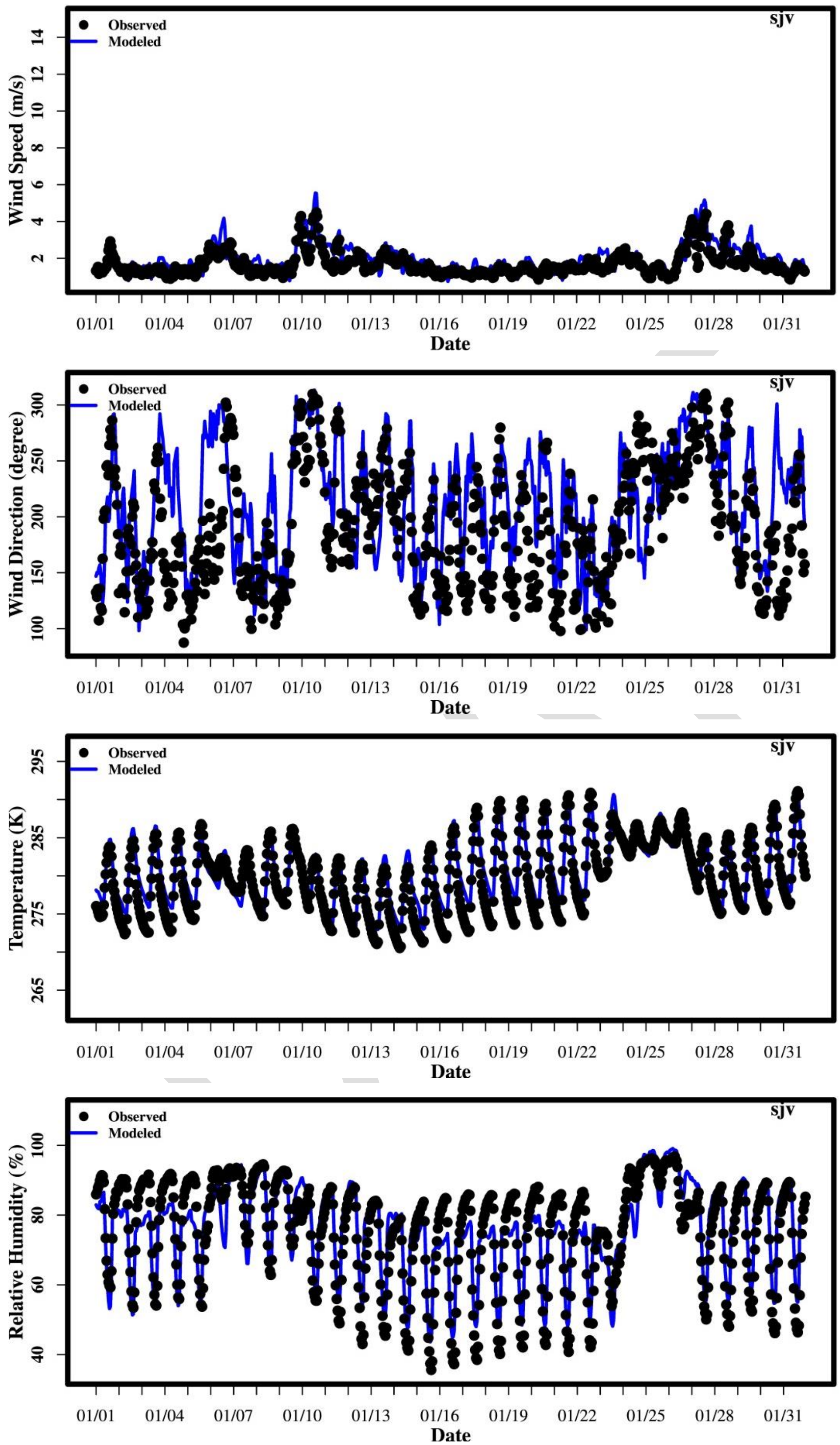

Figure S. 1 Time series of wind speed, direction, temperature and relative humidity for San Joaquin Valley in January 2013.

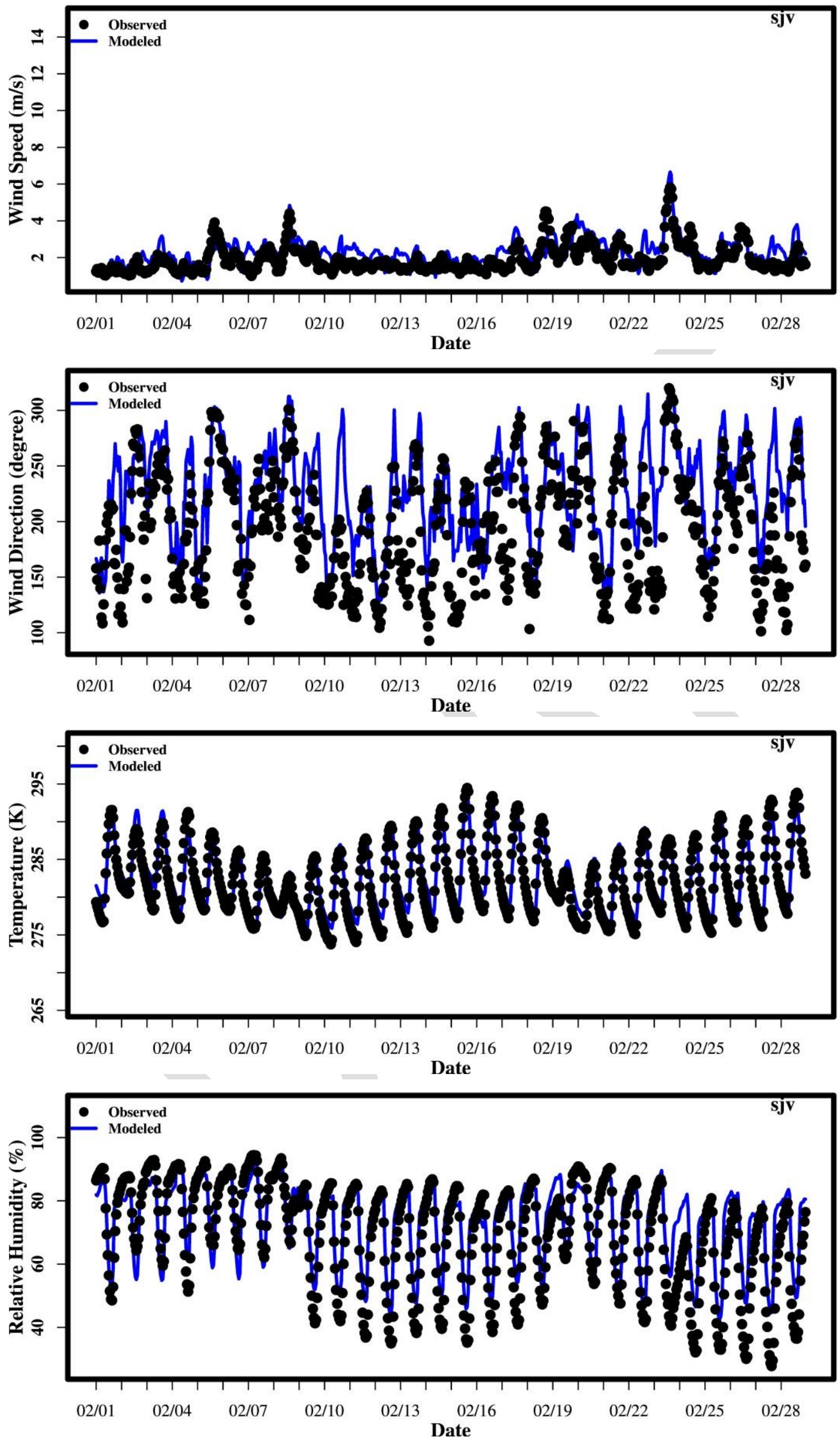

Figure S. 2 Time series of wind speed, direction, temperature and relative humidity for San Joaquin Valley in February 2013.

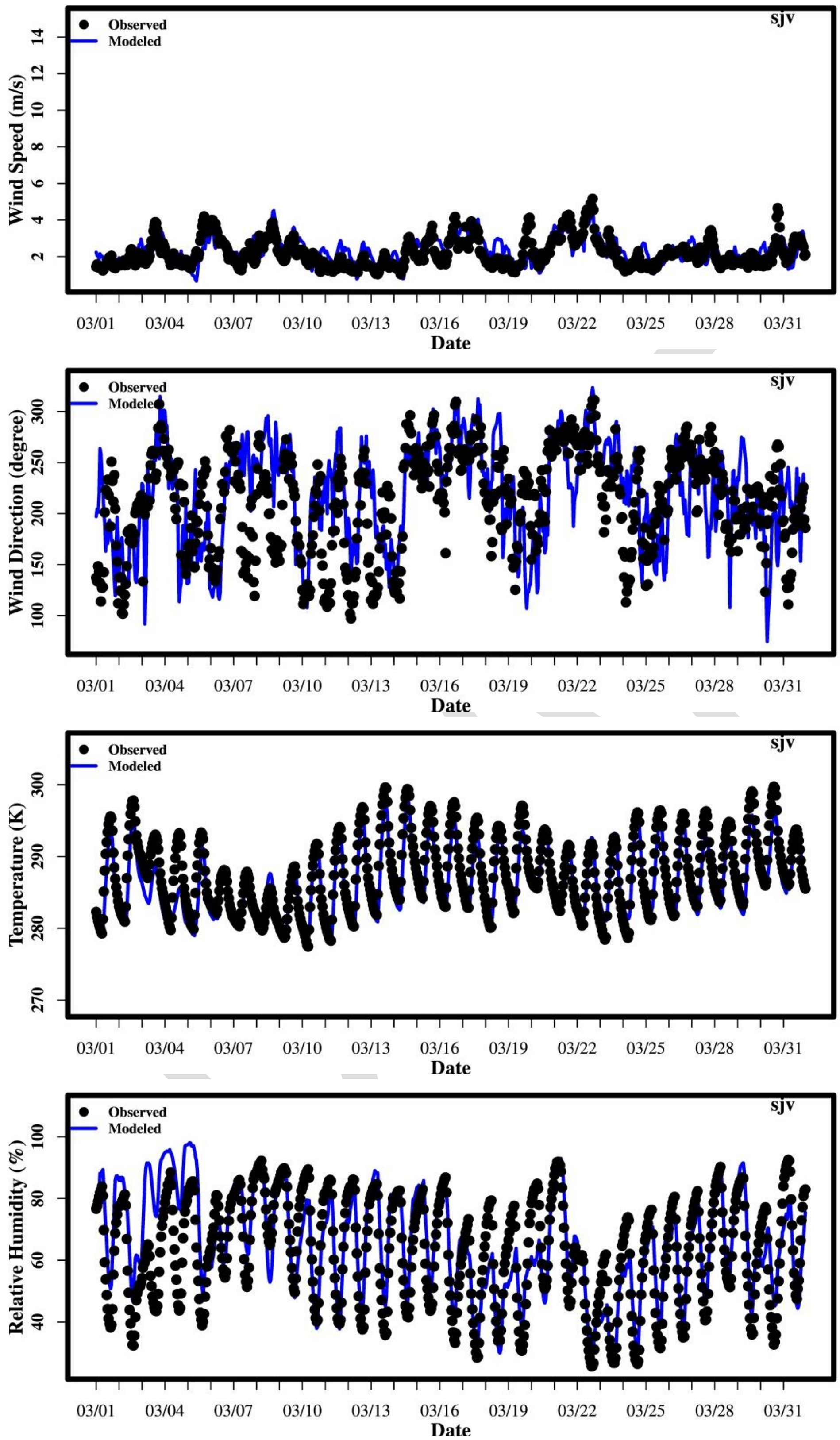

Figure S. 3 Time series of wind speed, direction, temperature and relative humidity for San Joaquin Valley in March 2013.

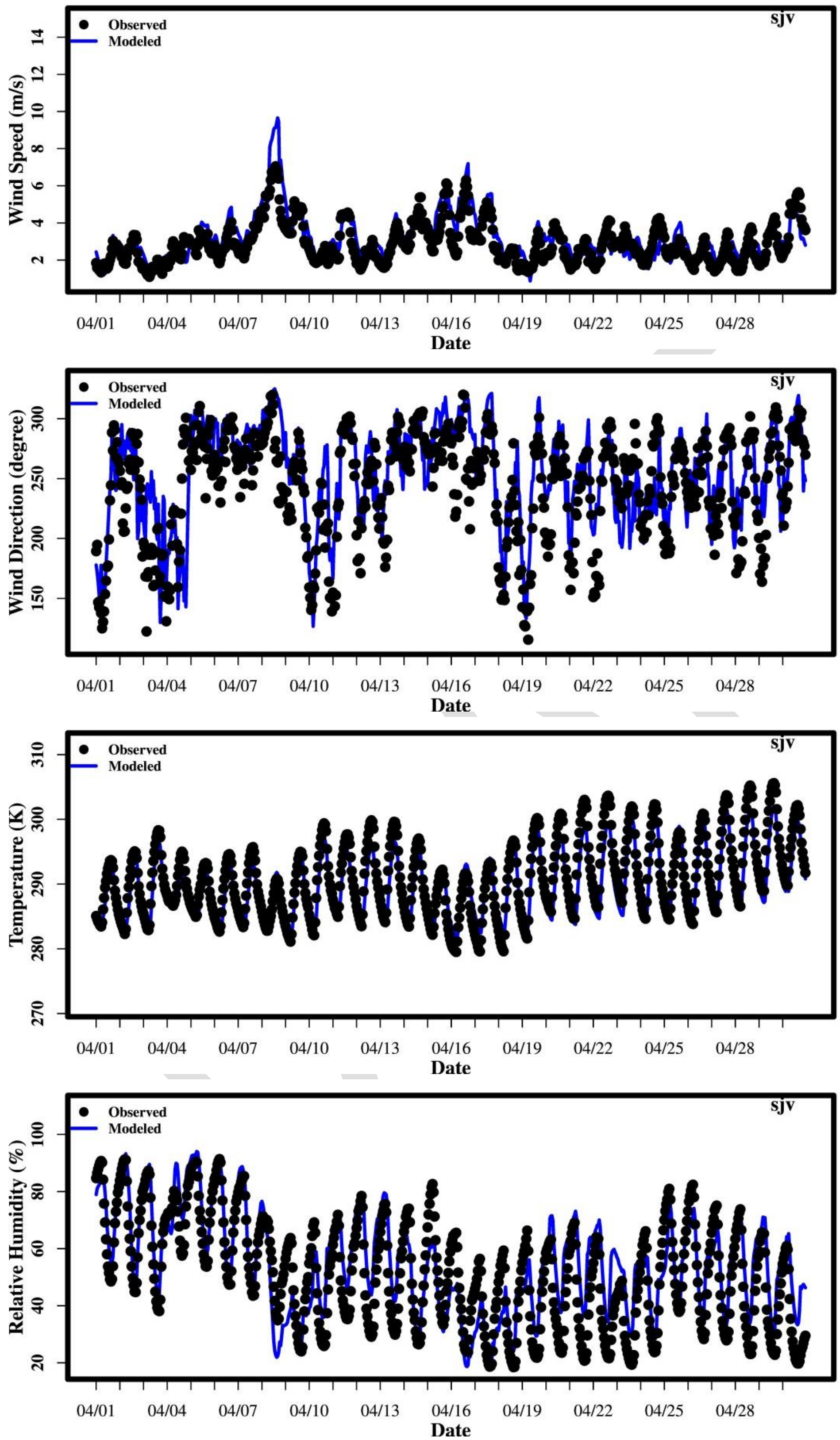

Figure S. 4 Time series of wind speed, direction, temperature and relative humidity for San Joaquin Valley in April 2013.

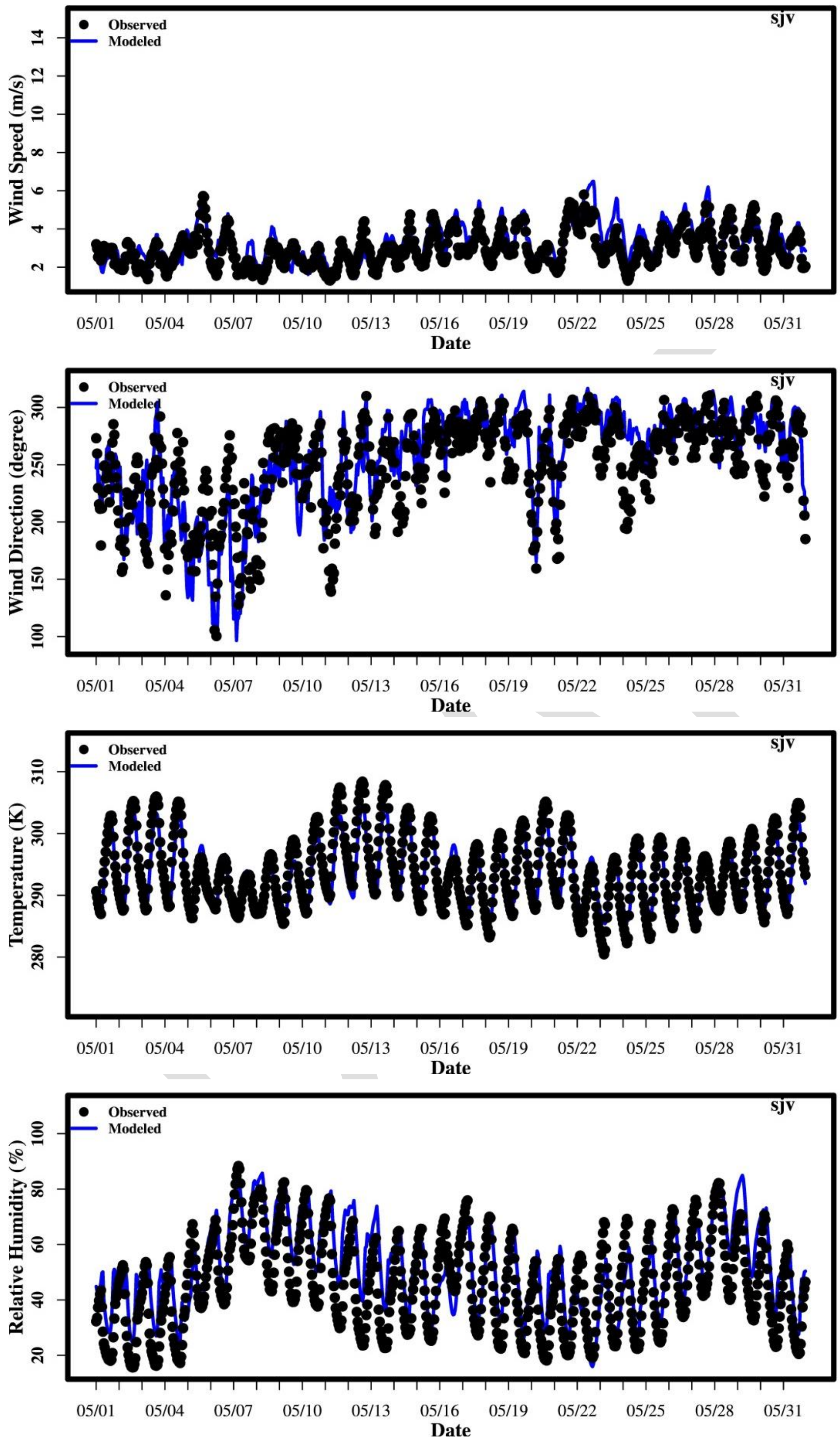

Figure S. 5 Time series of wind speed, direction, temperature and relative humidity for San Joaquin Valley in May 2013.

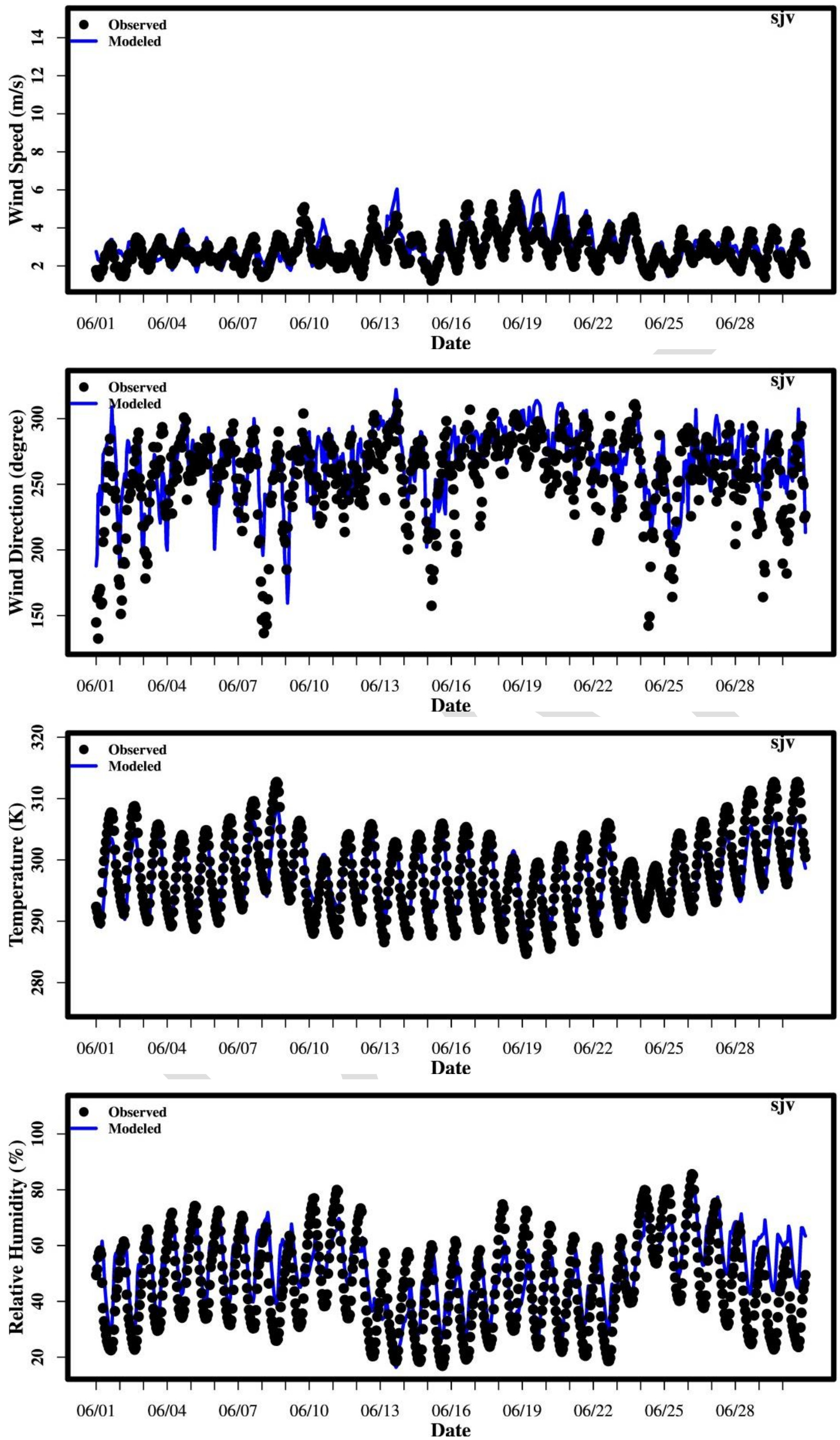

Figure S. 6 Time series of wind speed, direction, temperature and relative humidity for San Joaquin Valley in June 2013.

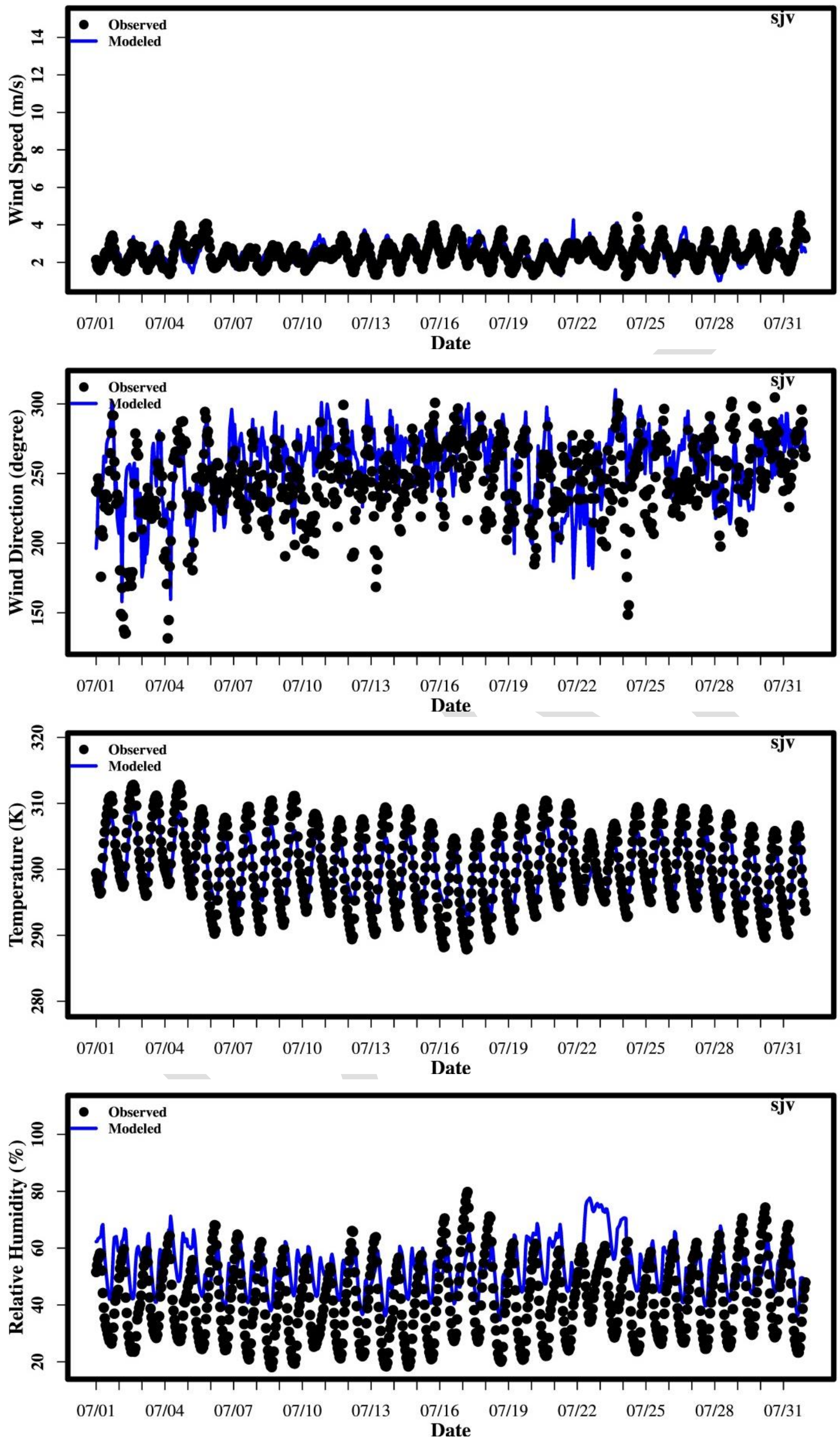

Figure S. 7 Time series of wind speed, direction, temperature and relative humidity for San Joaquin Valley in July 2013.

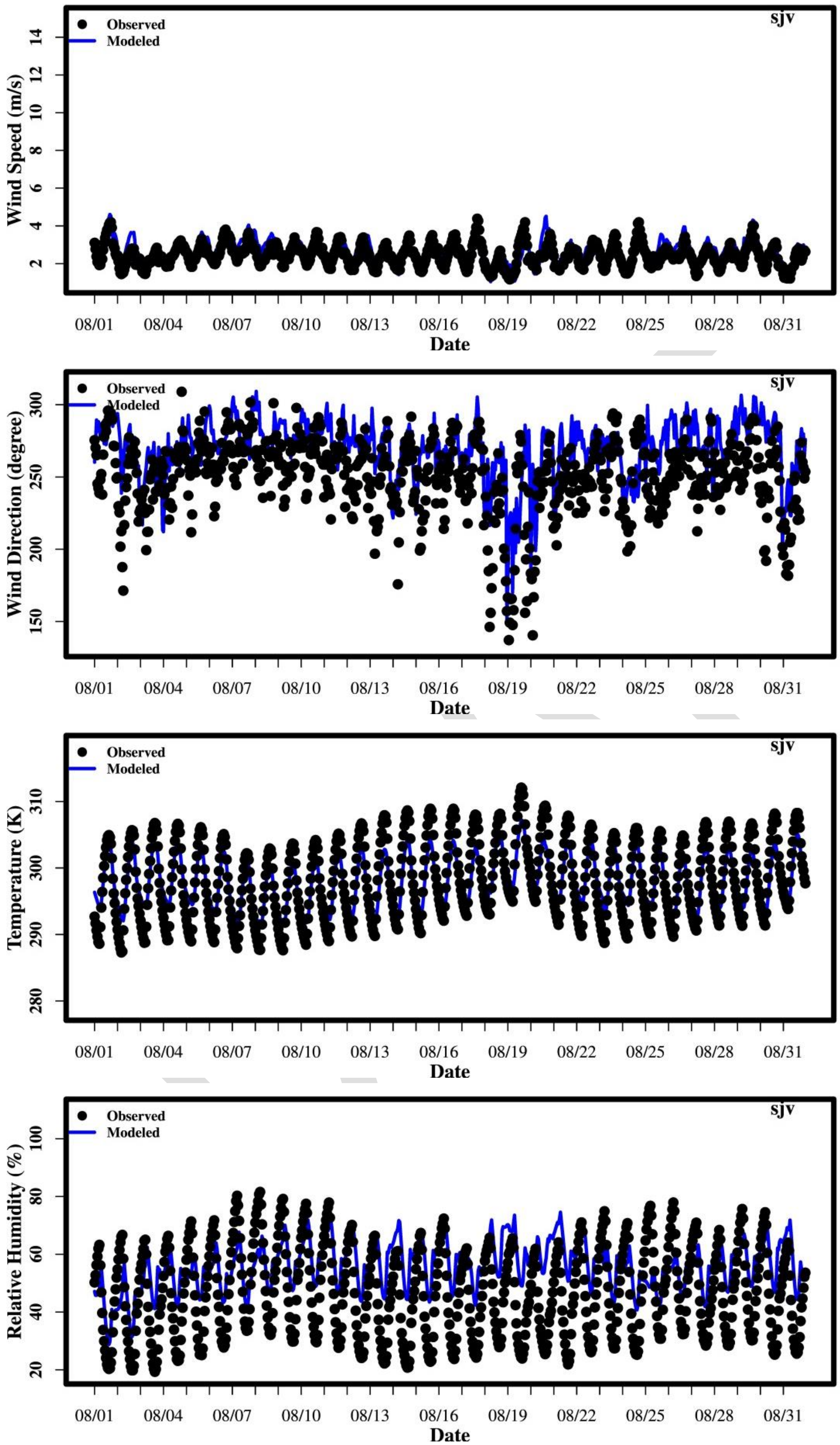

Figure S. 8 Time series of wind speed, direction, temperature and relative humidity for San Joaquin Valley in August 2013.

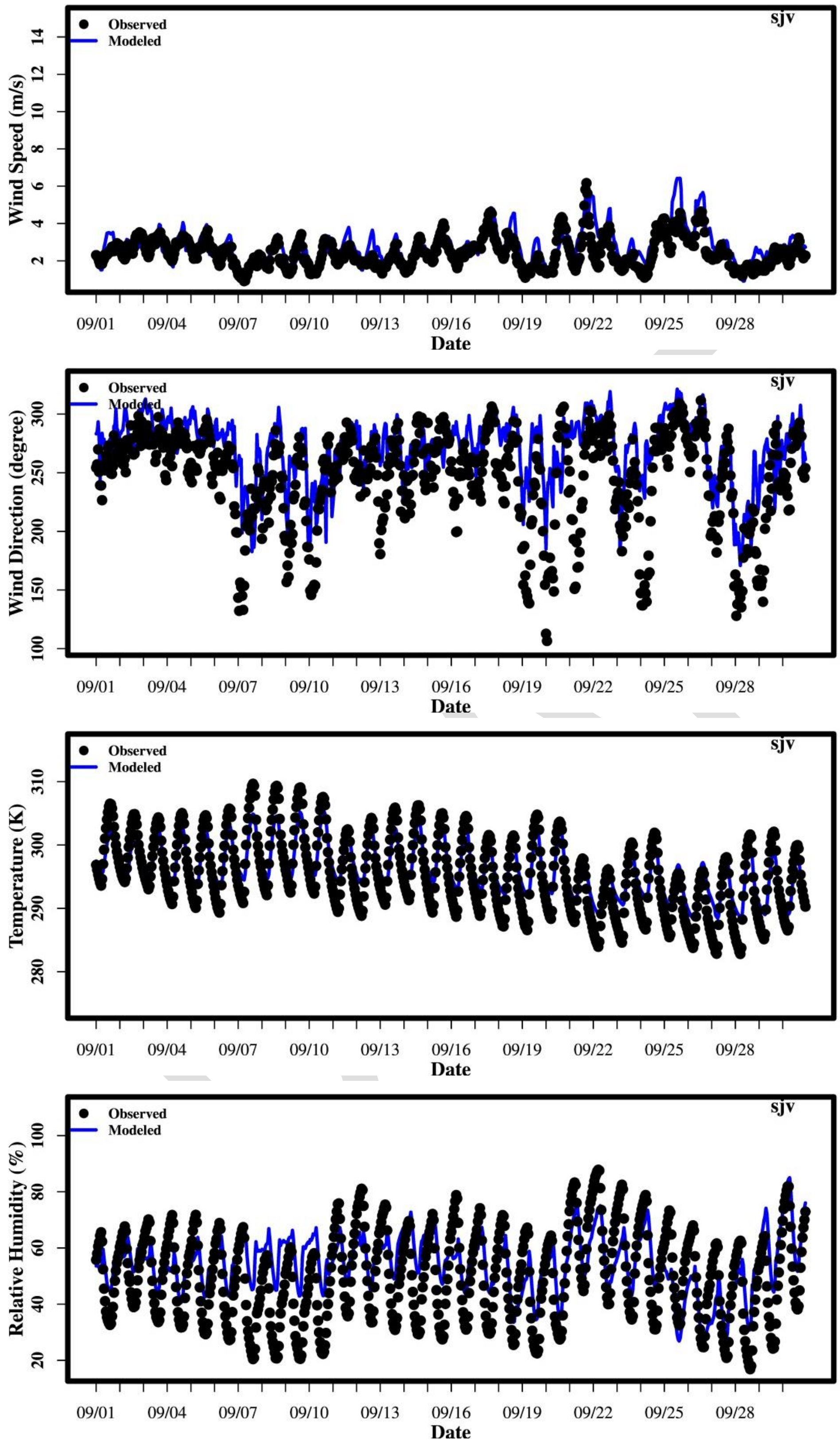

Figure S. 9 Time series of wind speed, direction, temperature and relative humidity for San Joaquin Valley in September 2013.

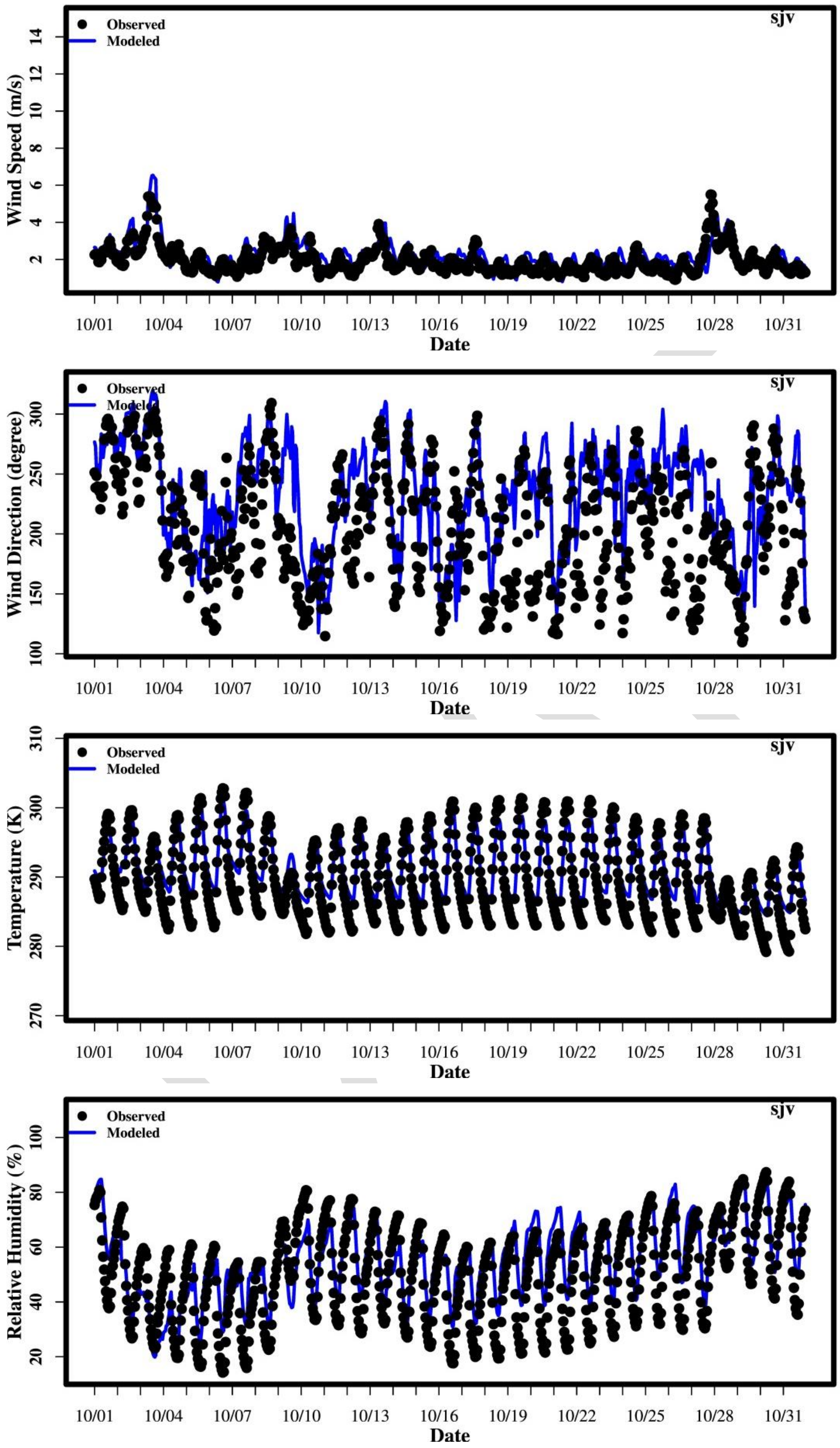

Figure S. 10 Time series of wind speed, direction, temperature and relative humidity for San Joaquin Valley in October 2013.

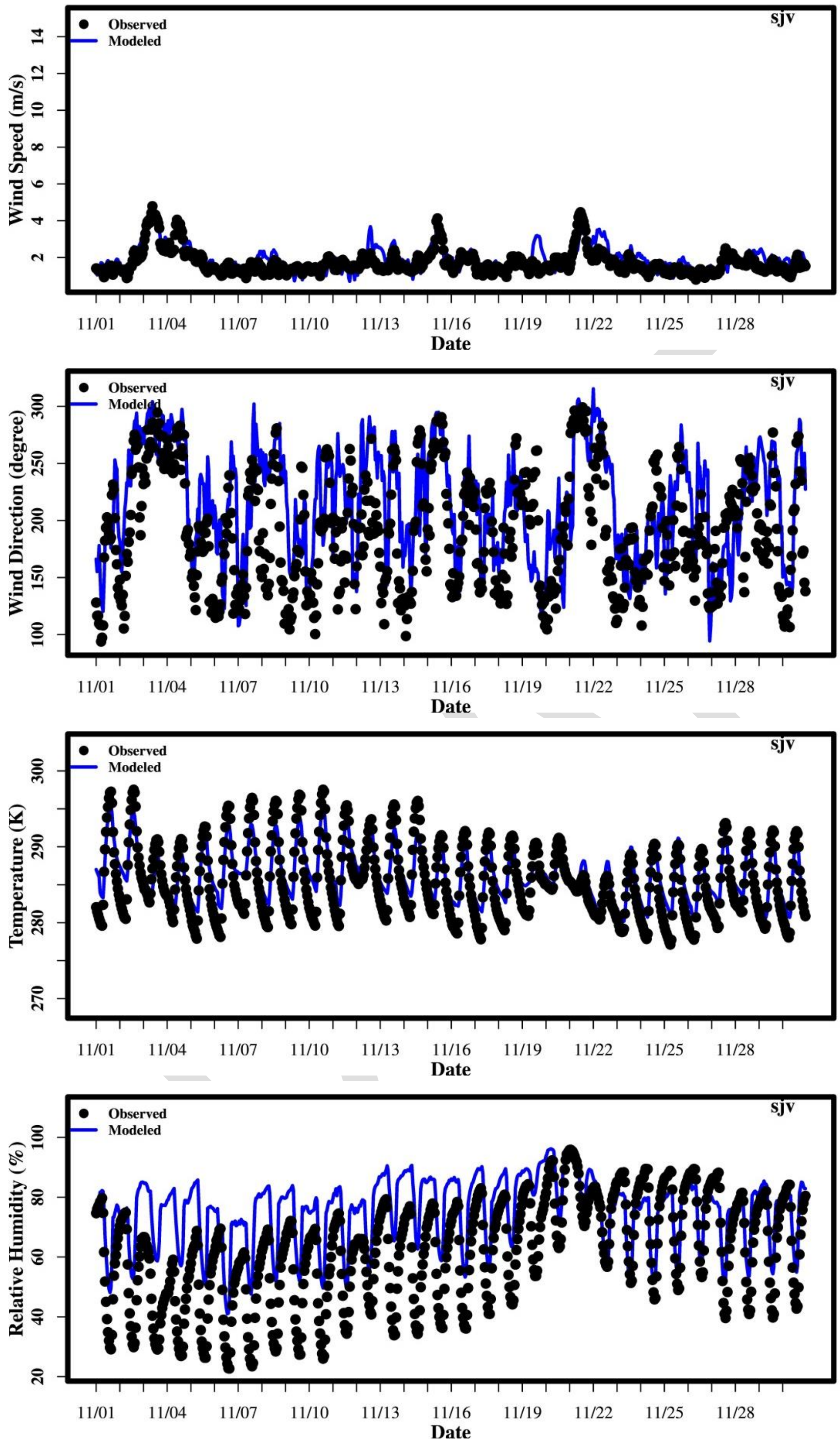

Figure S. 11 Time series of wind speed, direction, temperature and relative humidity for San Joaquin Valley in November 2013.

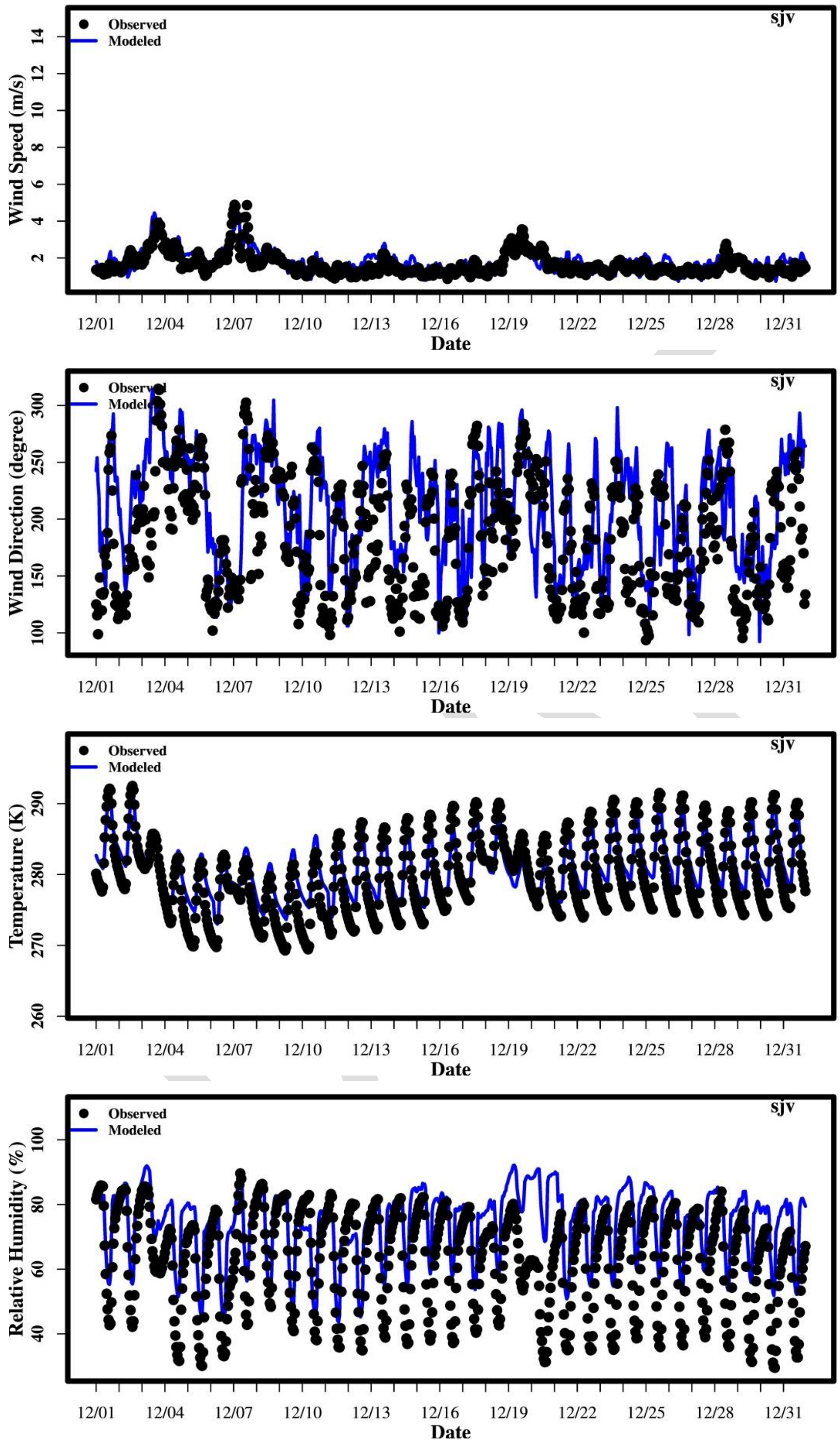

Figure S. 12 Time series of wind speed, direction, temperature and relative humidity for San Joaquin Valley in December 2013.

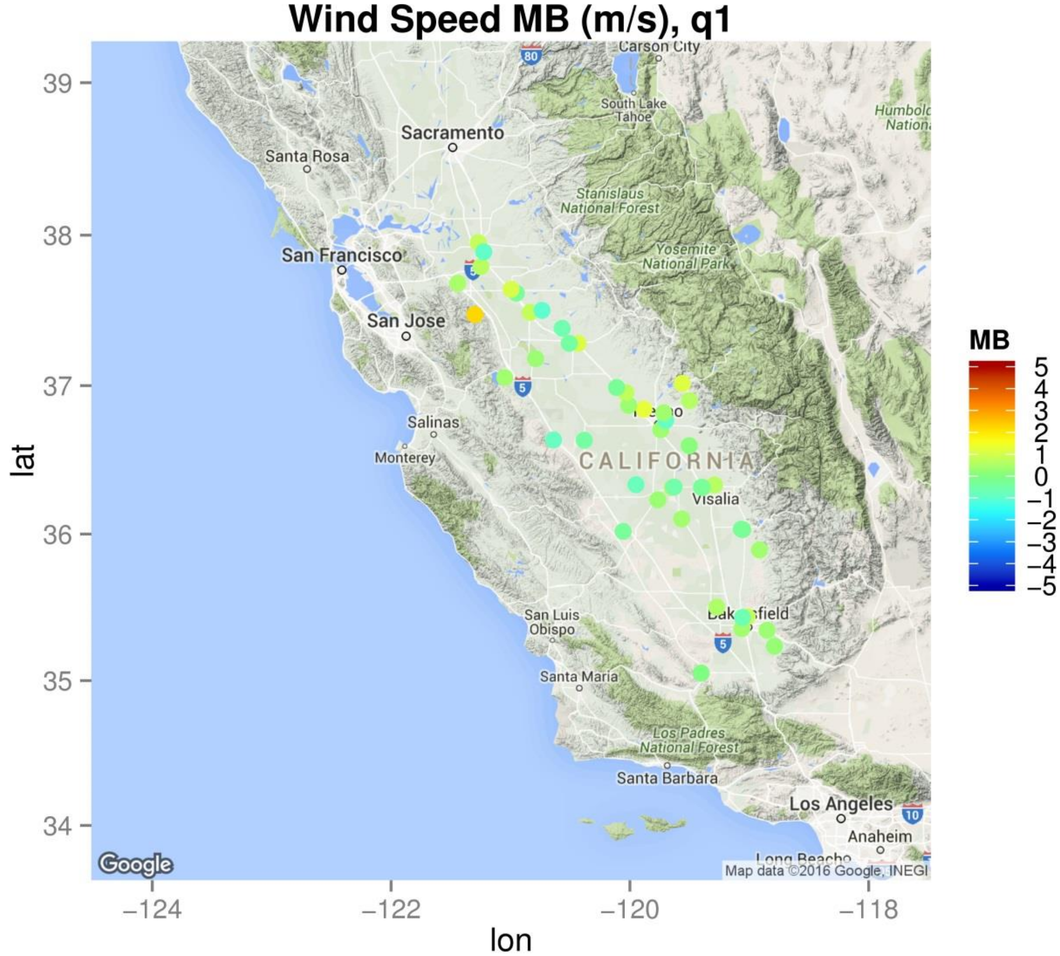

Figure S. 13 Hourly wind speed mean error in the first quarter of 2013

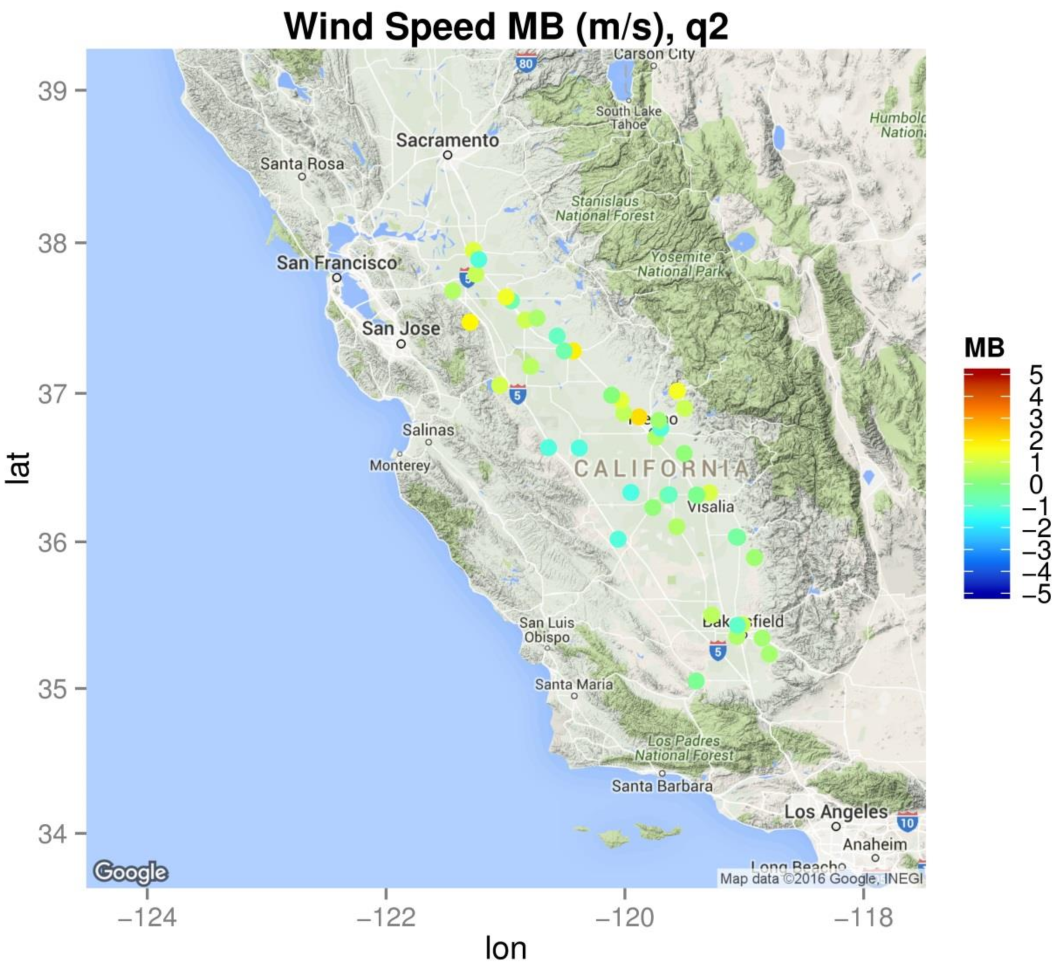

Figure S. 14 Hourly wind speed mean bias in the second quarter of 2013

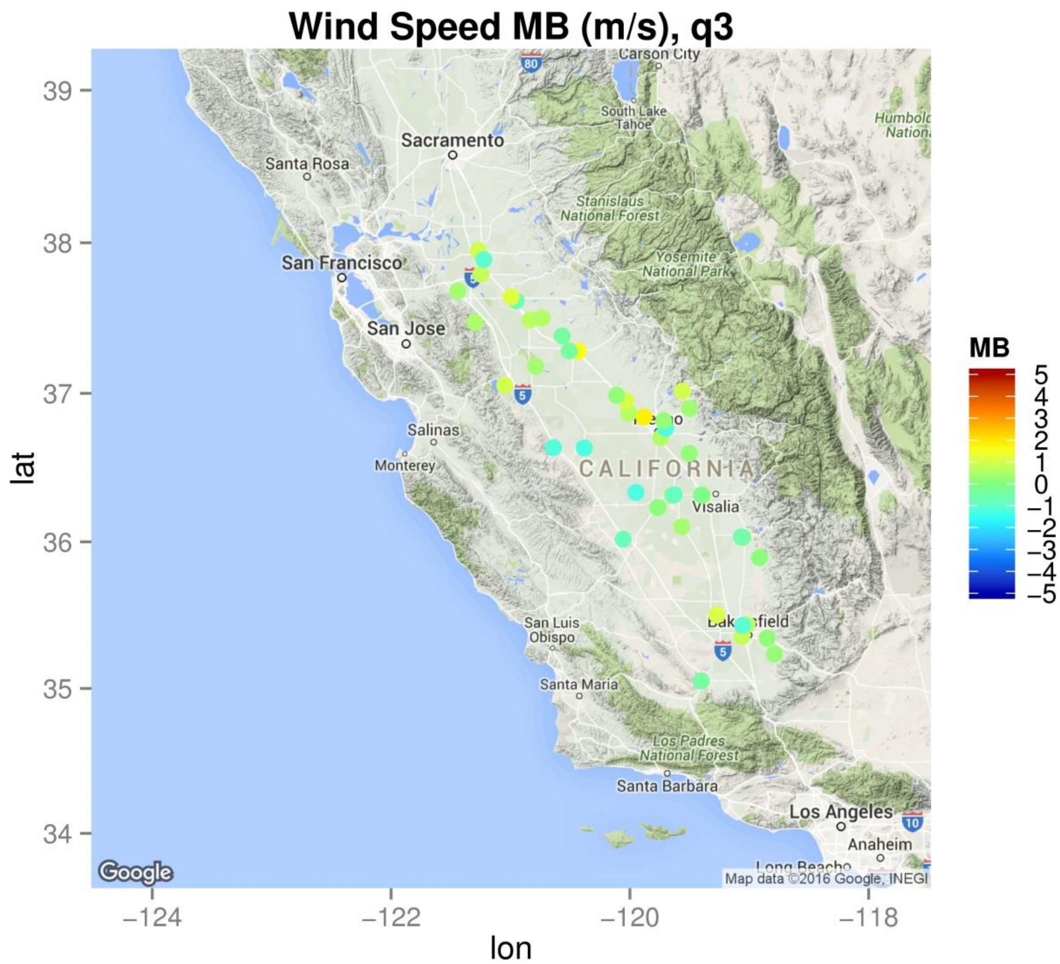

Figure S. 15 Hourly wind speed mean bias in the third quarter of 2013

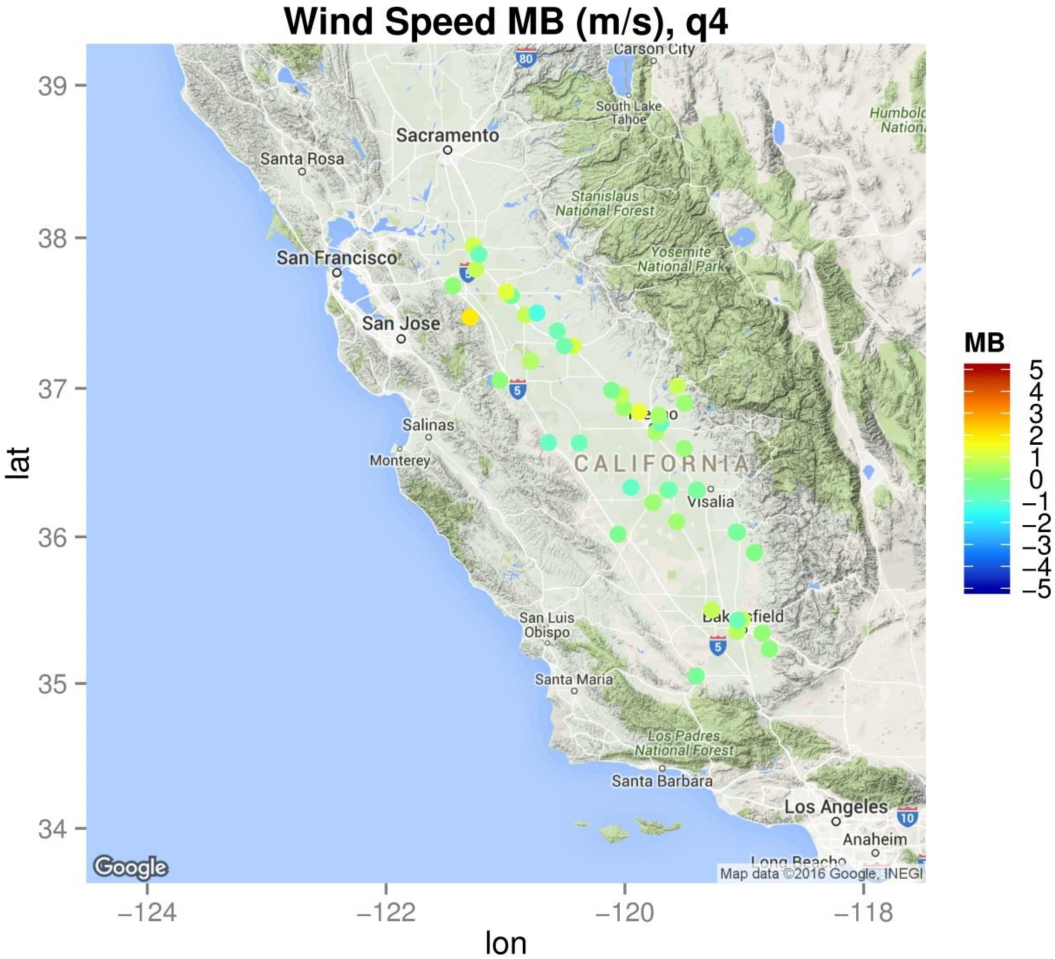

Figure S. 16 Hourly wind speed mean bias in the fourth quarter of 2013

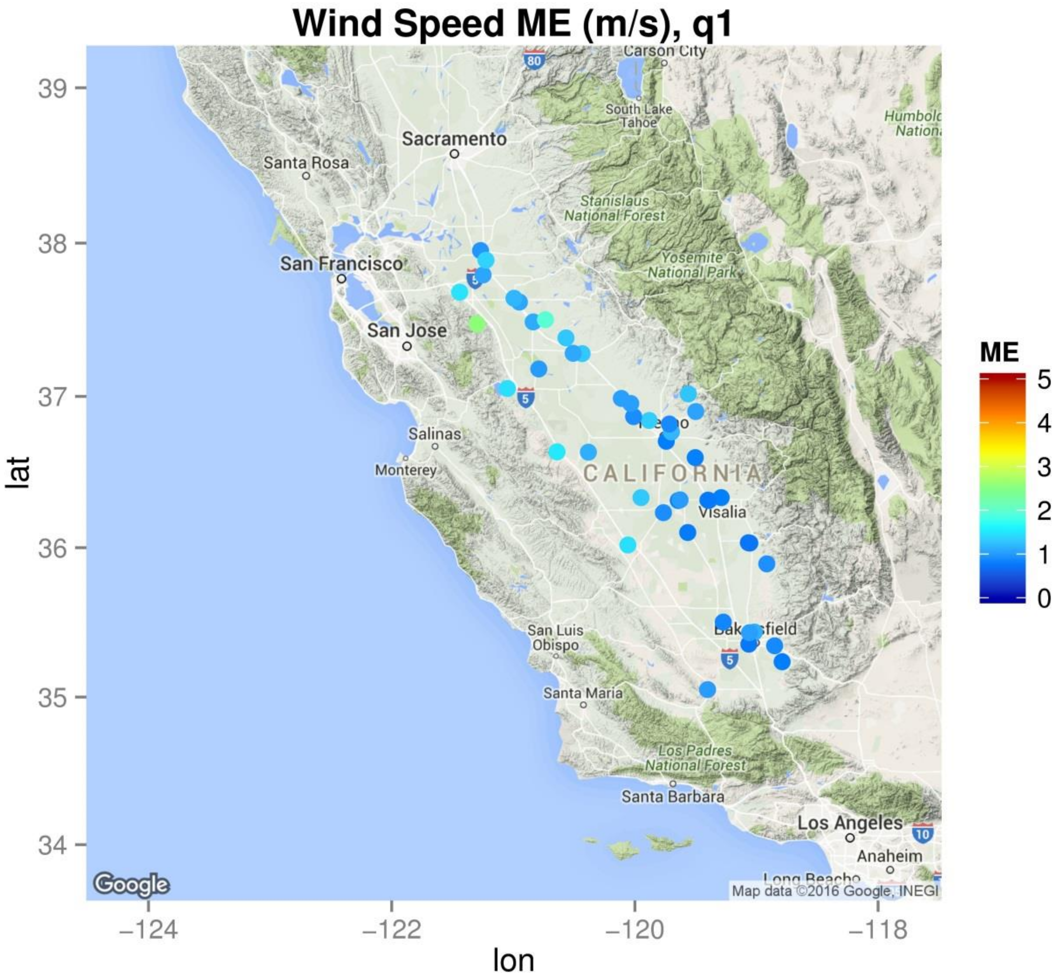

Figure S. 17 Hourly wind speed mean error in the first quarter of 2013

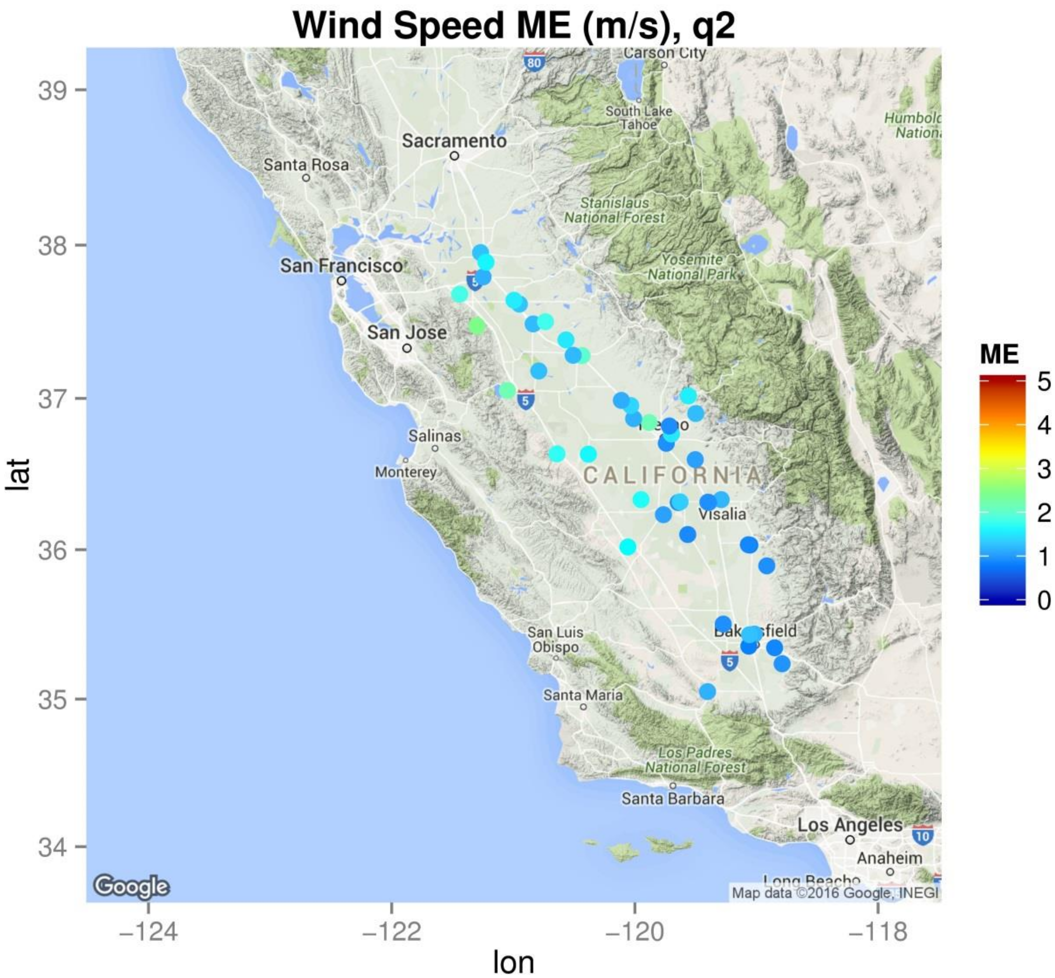

Figure S. 18 Hourly wind speed mean error in the second quarter of 2013

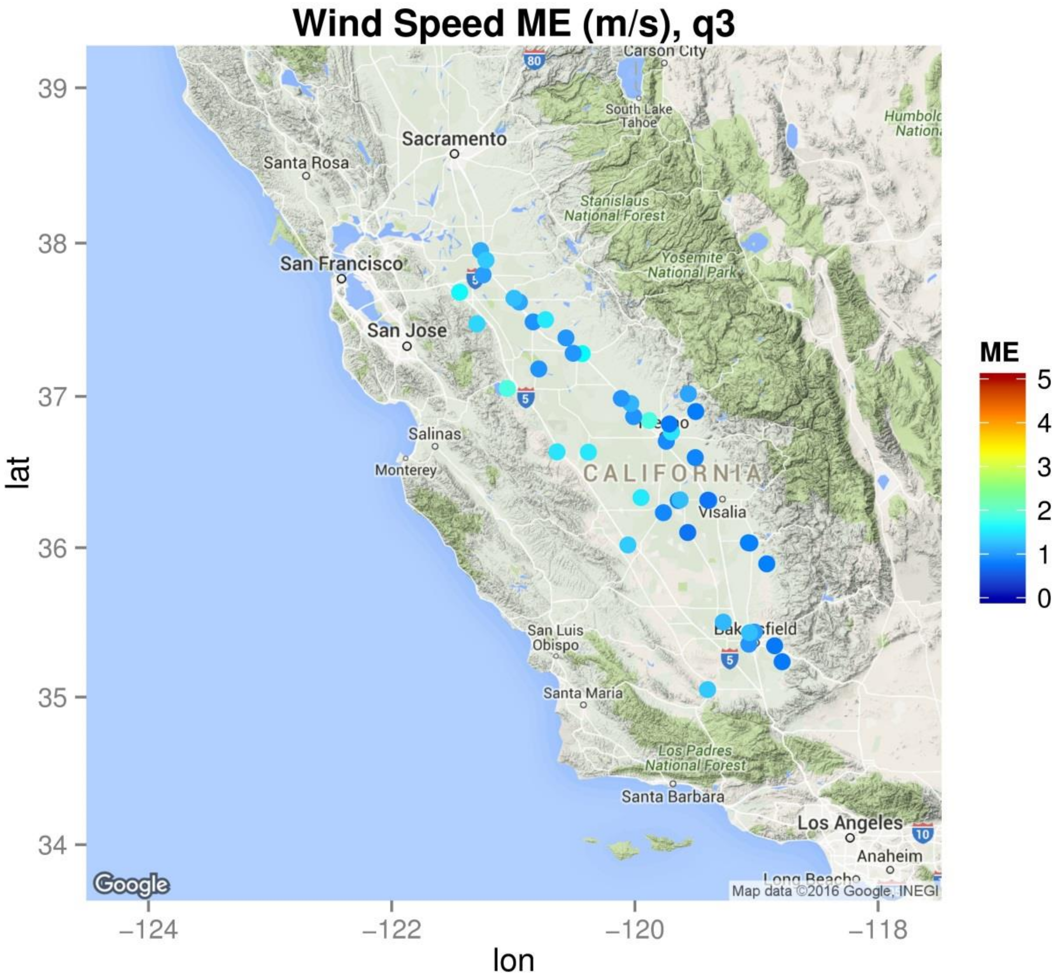

Figure S. 19 Hourly wind speed mean error in the third quarter of 2013

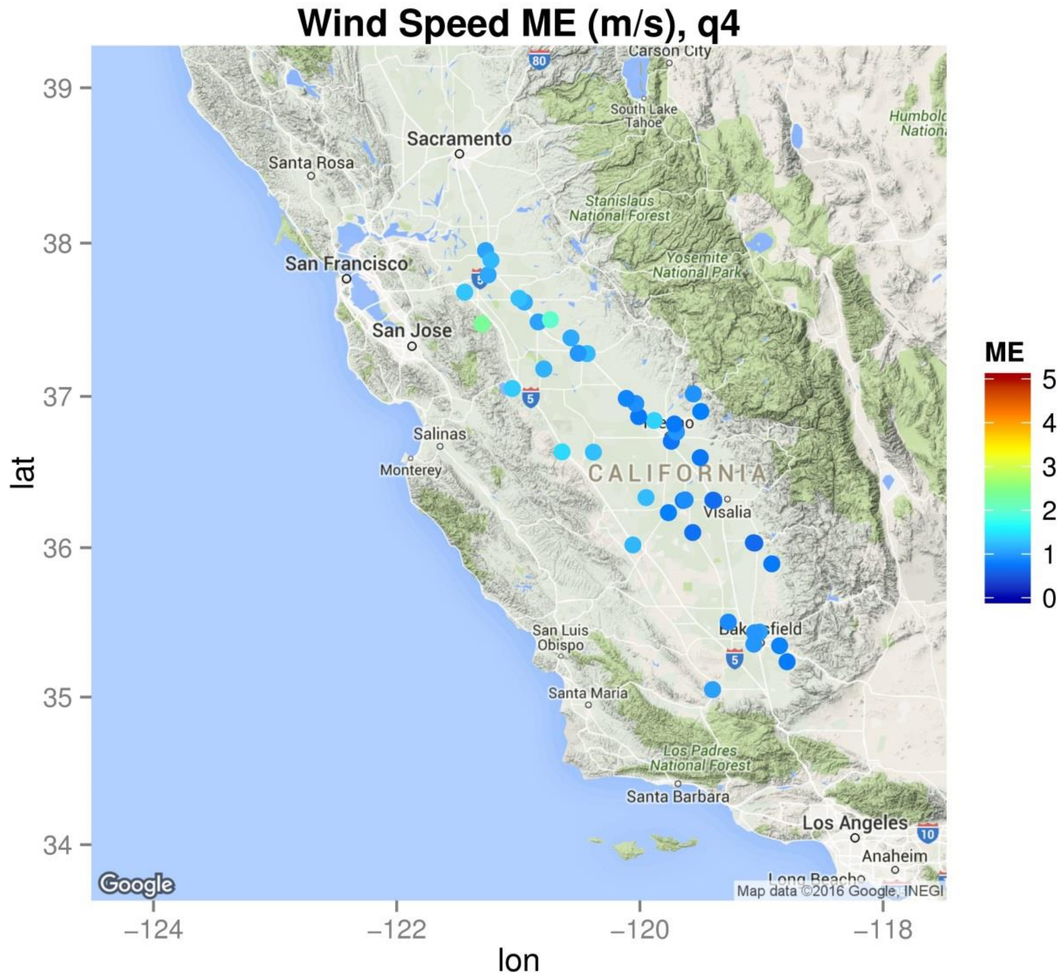

Figure S. 20 Hourly wind speed mean error in the fourth quarter of 2013

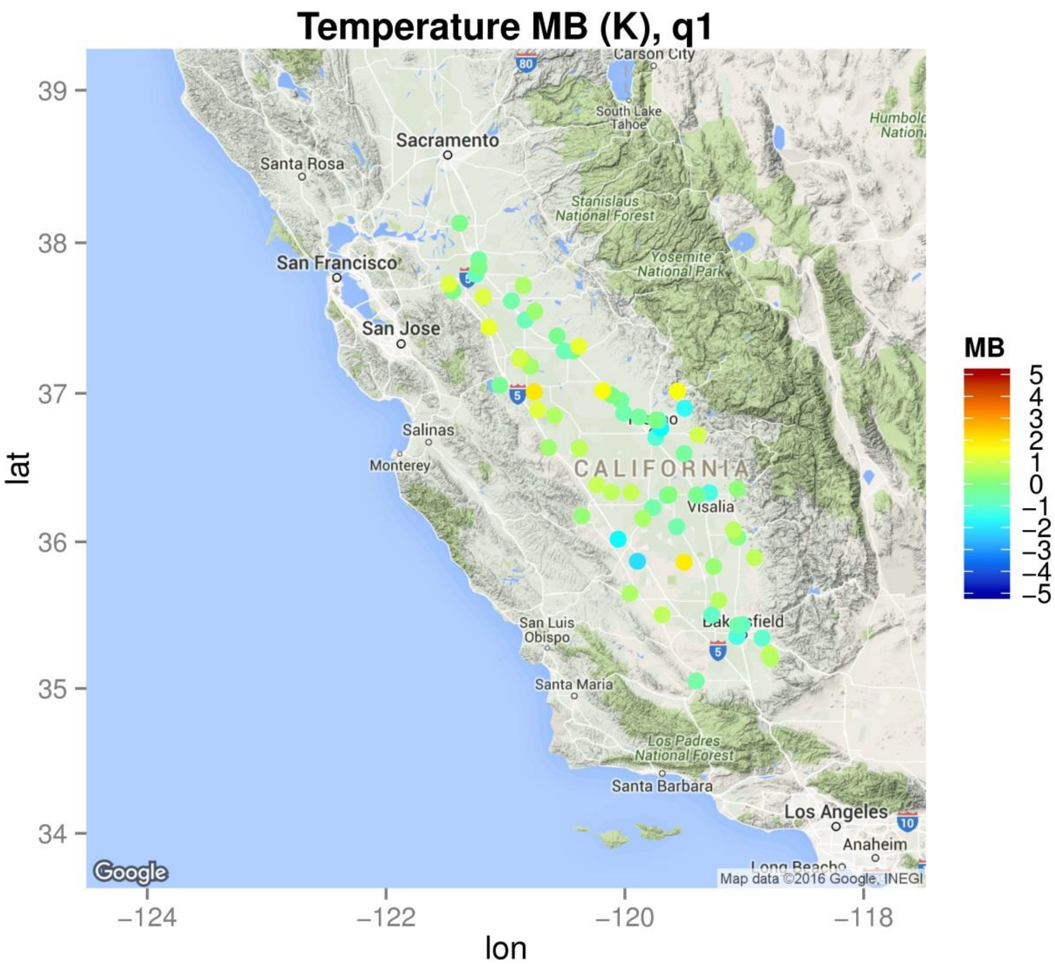

Figure S. 21 Hourly temperature mean bias in the first quarter of 2013

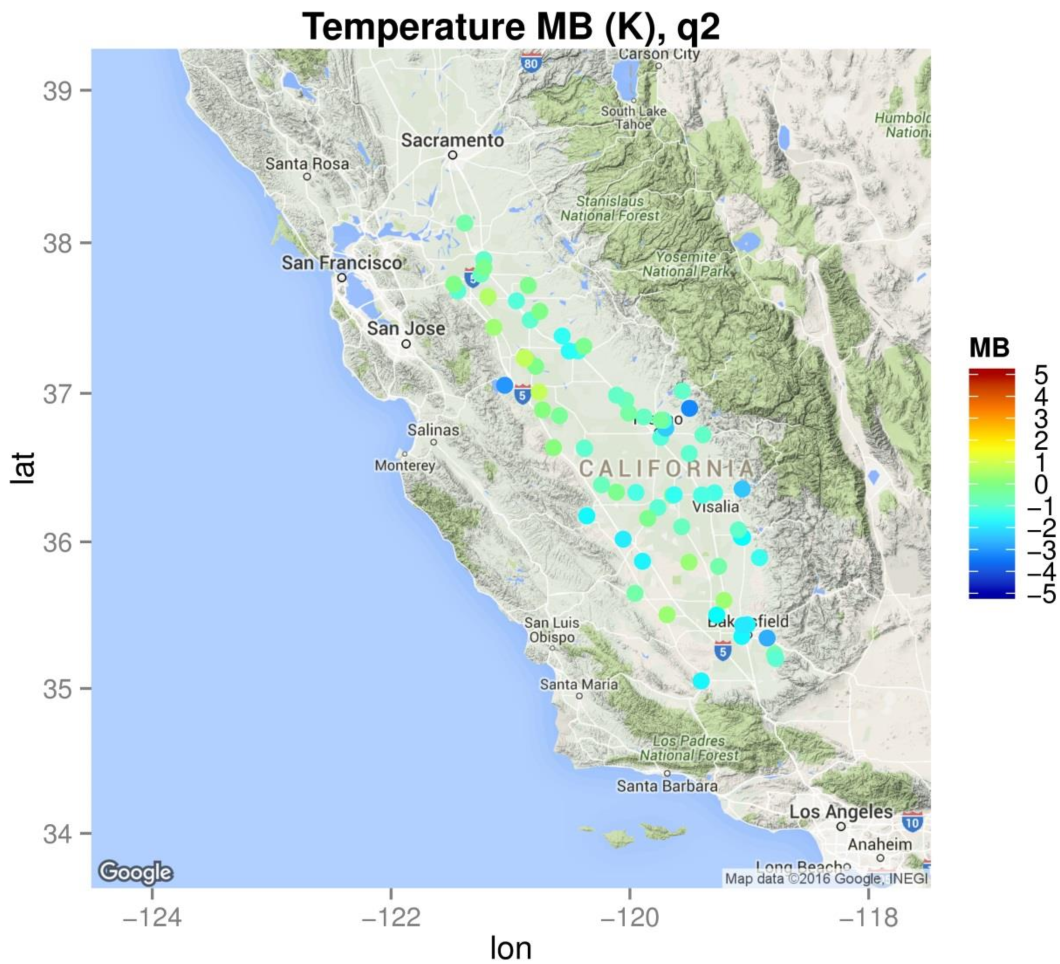

Figure S. 22 Hourly temperature mean bias in the second quarter of 2013

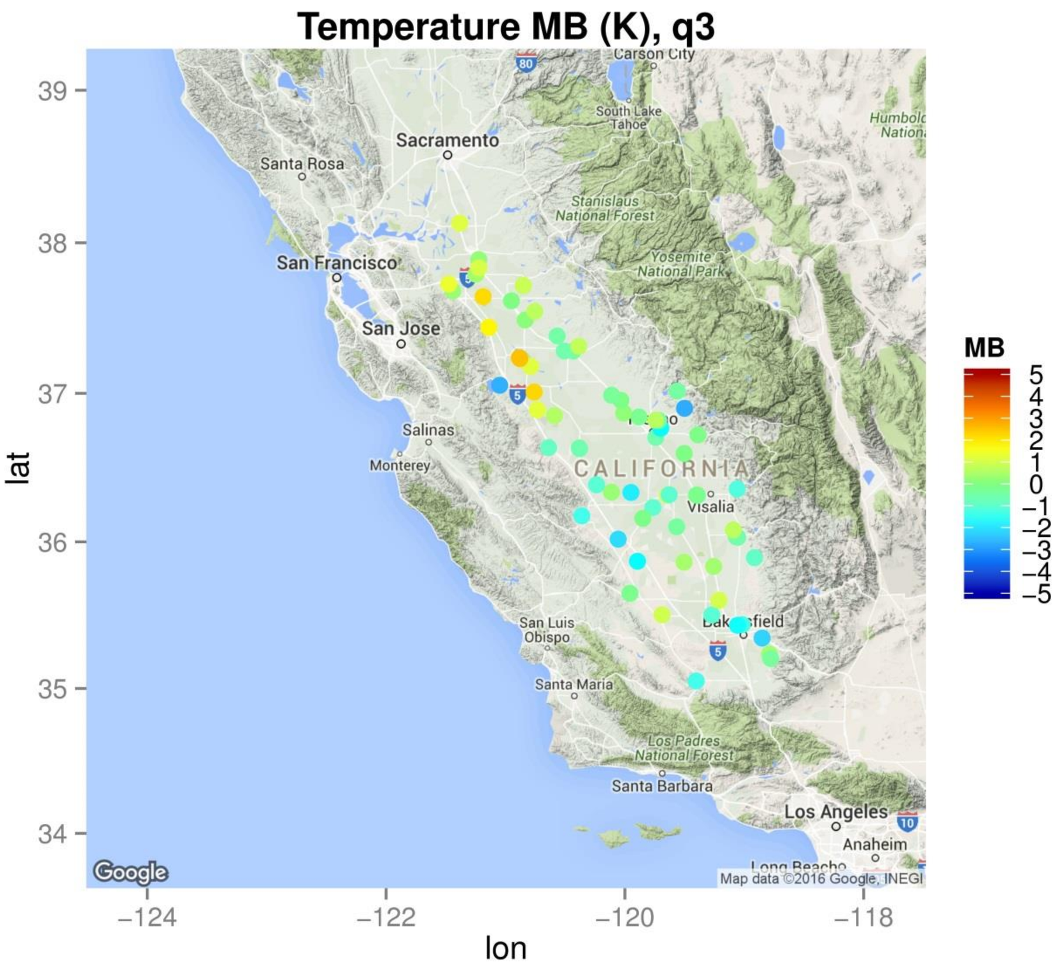

Figure S. 23 Hourly temperature mean bias in the third quarter of 2013

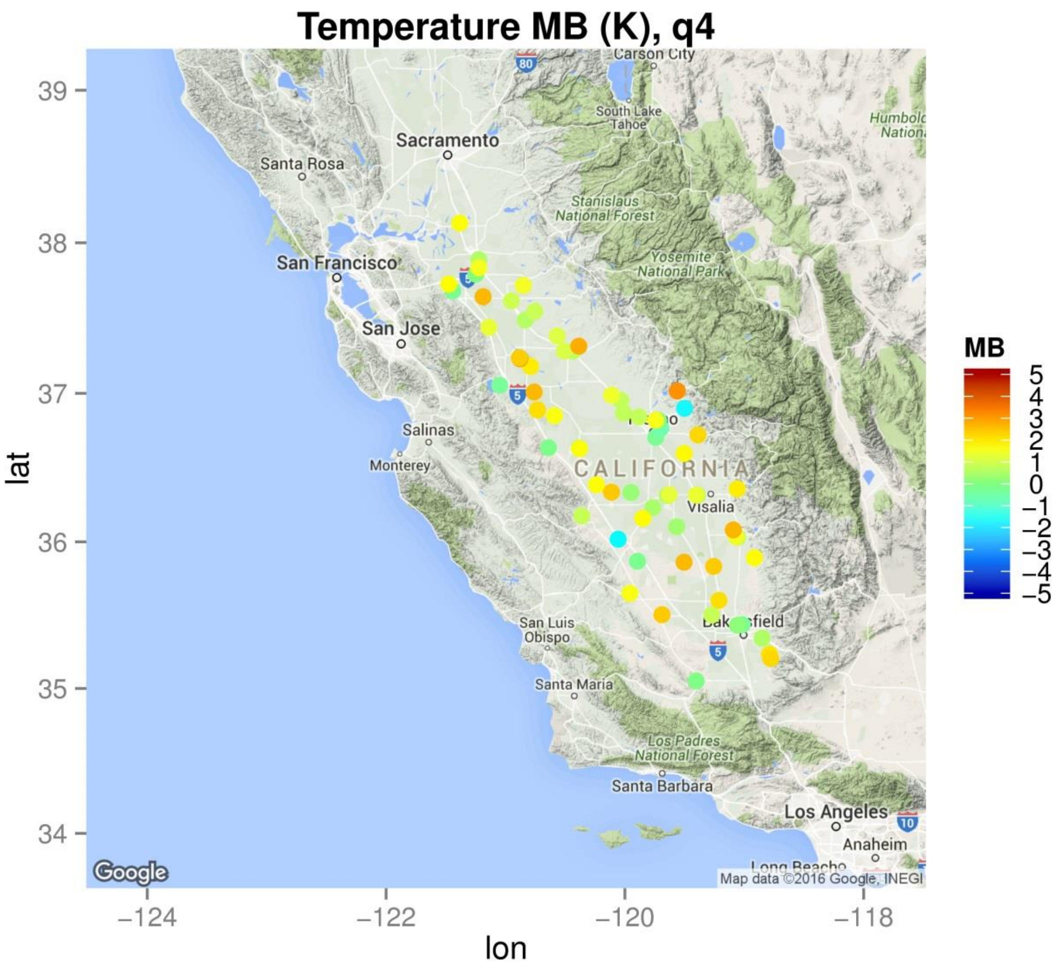

Figure S. 24 Hourly temperature mean bias in the fourth quarter of 2013

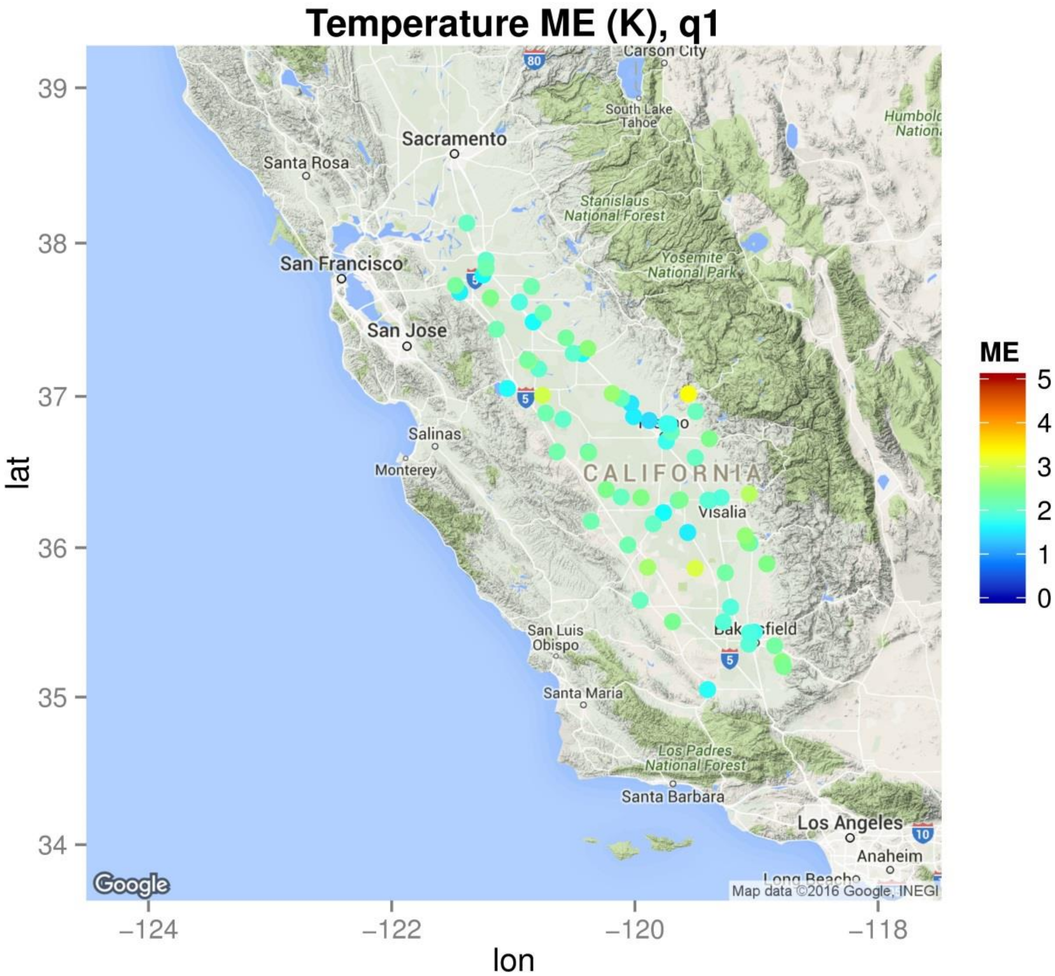

Figure S. 25 Hourly temperature mean error in the first quarter of 2013

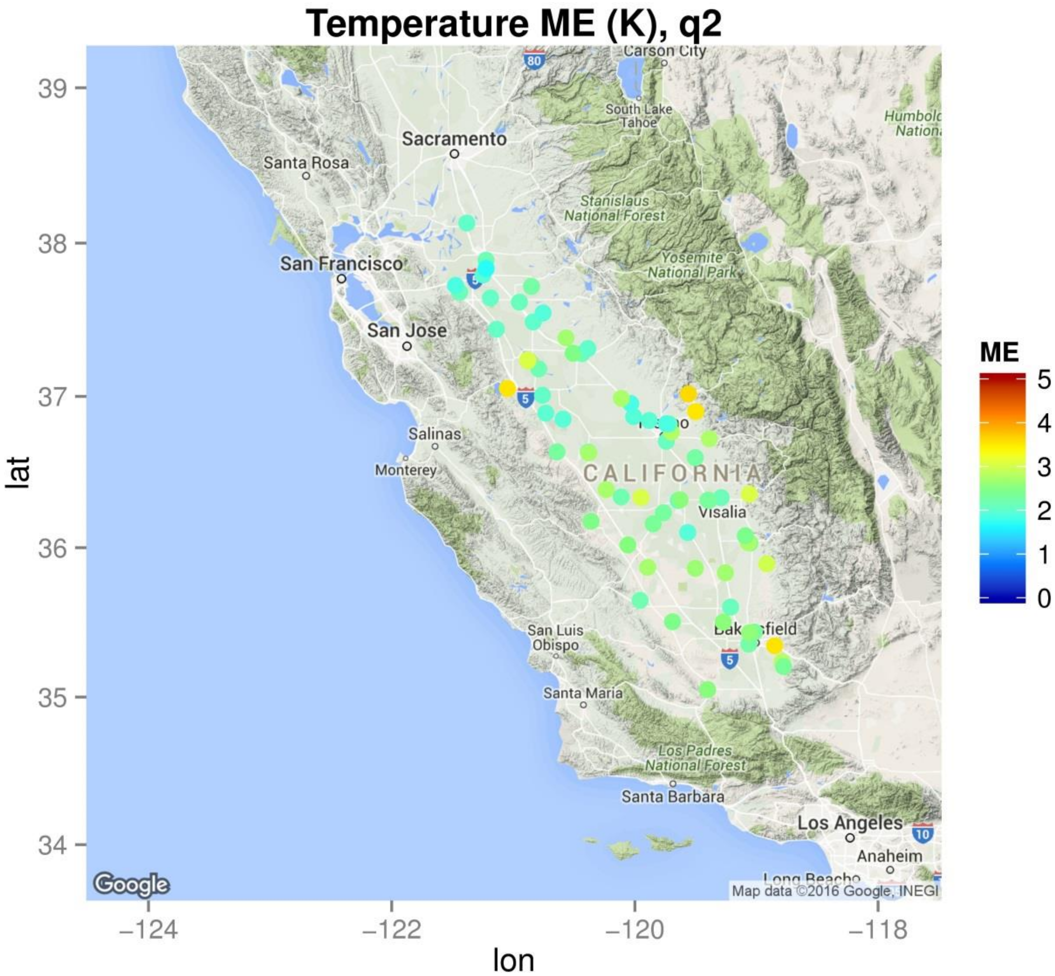

Figure S. 26 Hourly temperature mean error in the second quarter of 2013

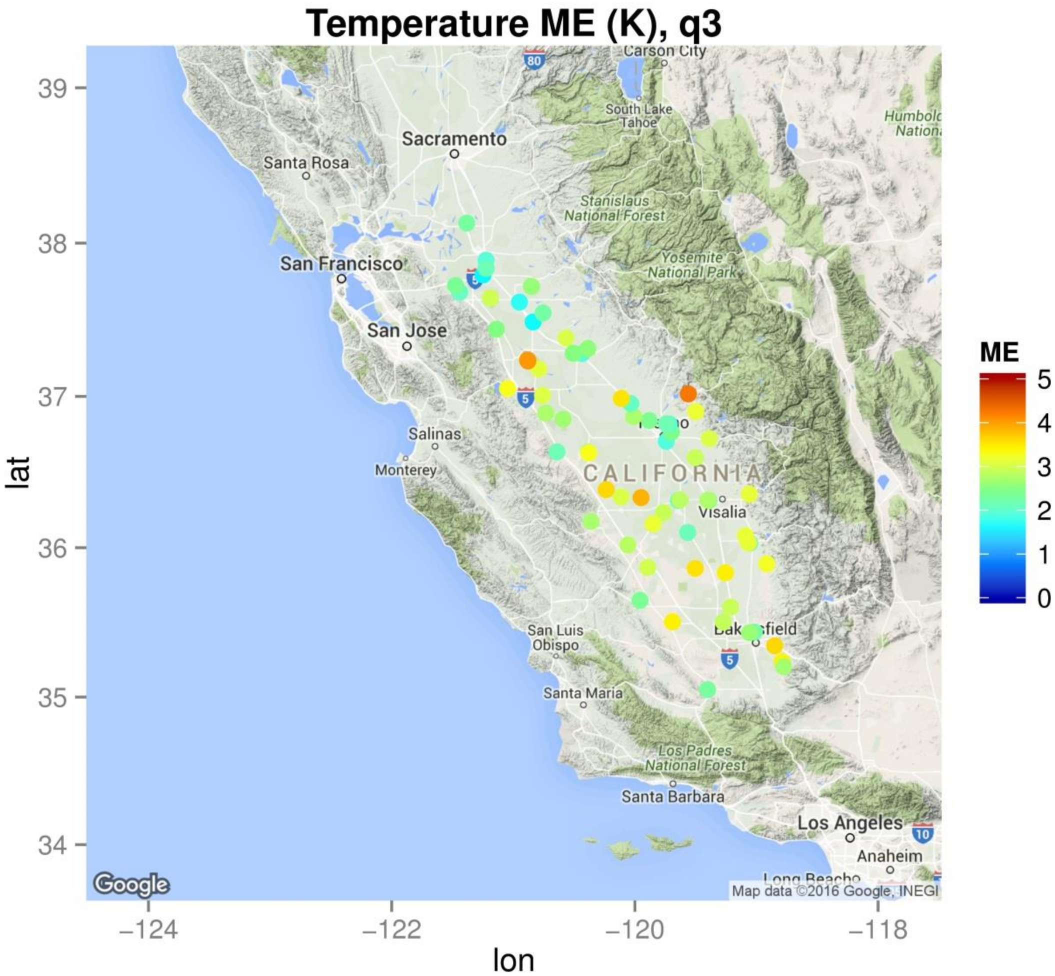

Figure S. 27 Hourly temperature mean error in the third quarter of 2013

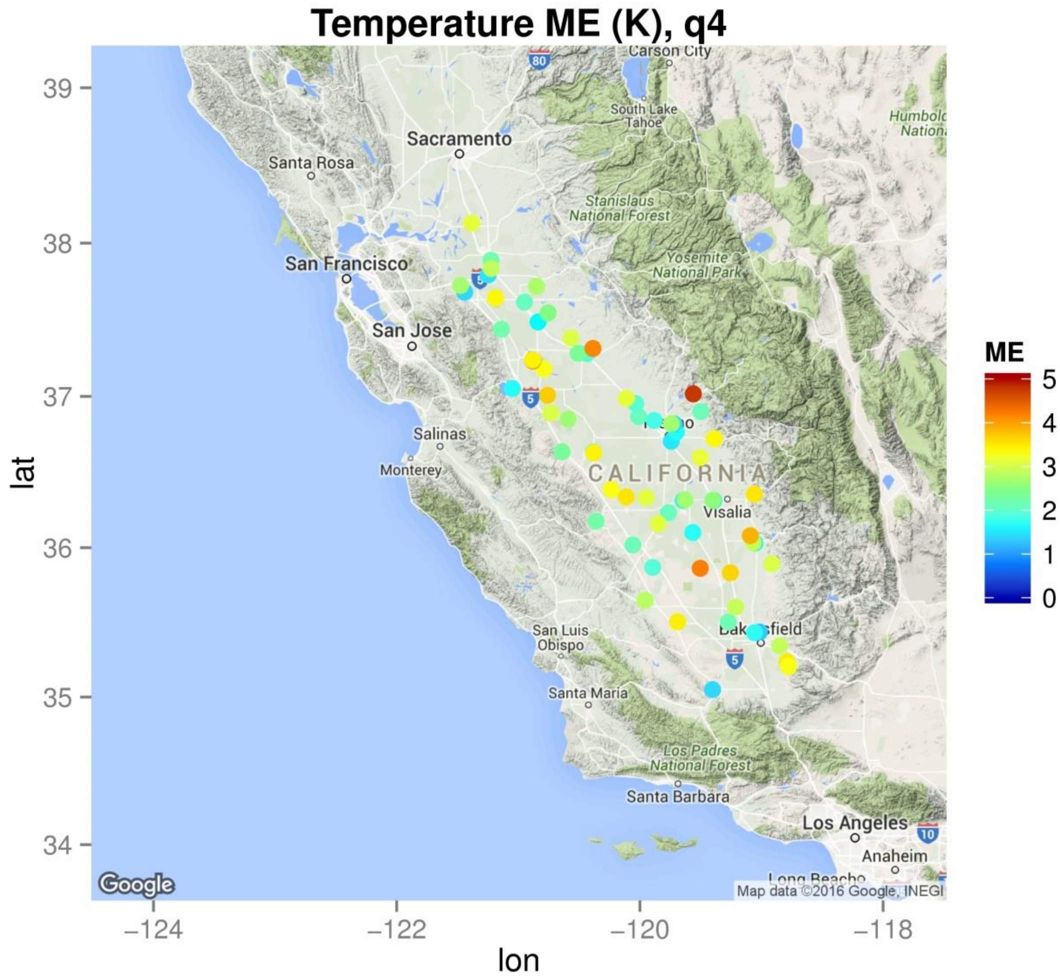

Figure S. 28 Hourly temperature mean error in the fourth quarter of 2013

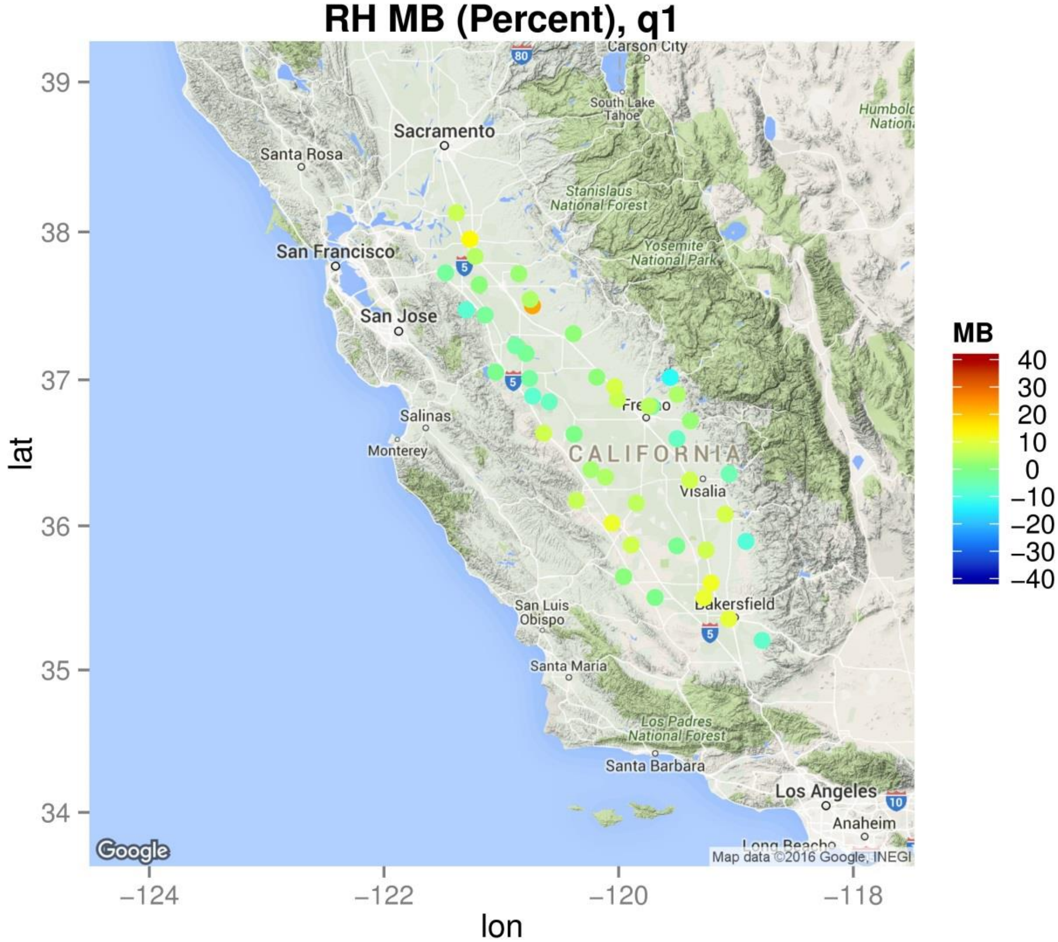

Figure S. 29 Hourly relative humidity mean bias in the first quarter of 2013

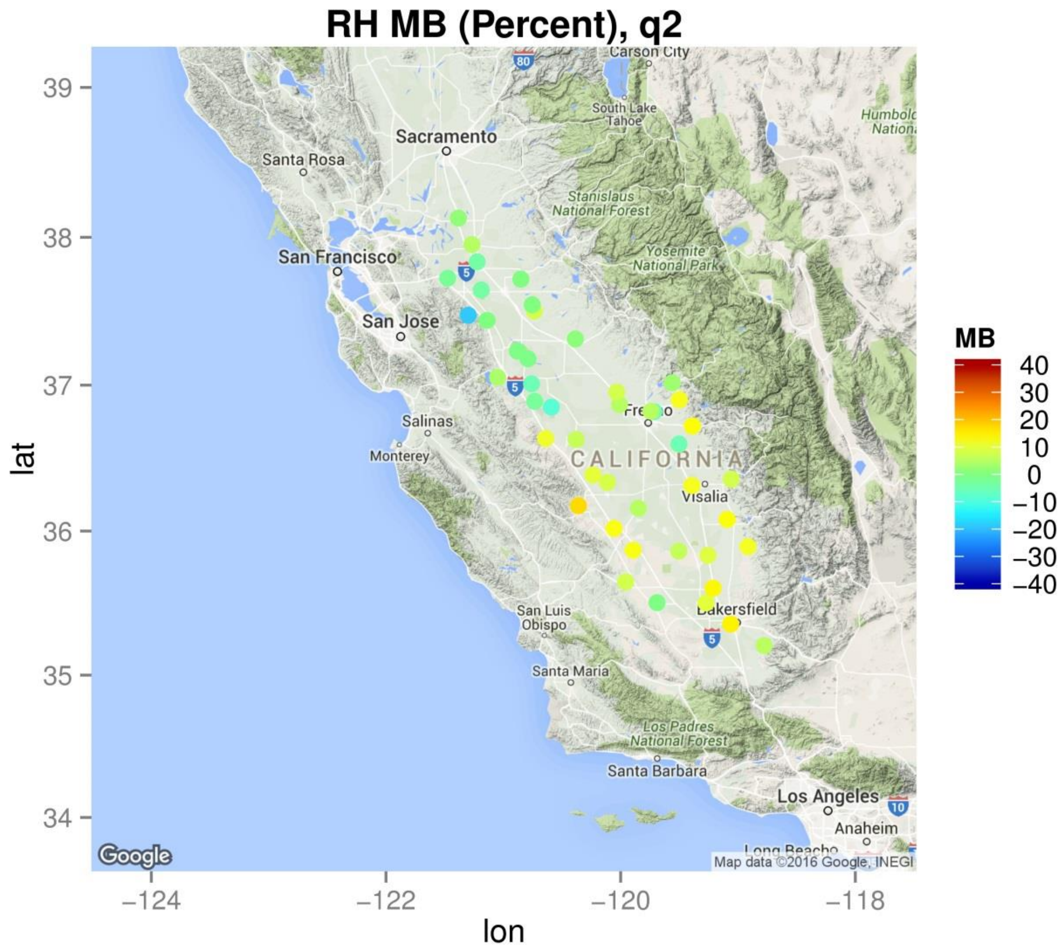

Figure S. 30 Hourly relative humidity mean bias in the second quarter of 2013

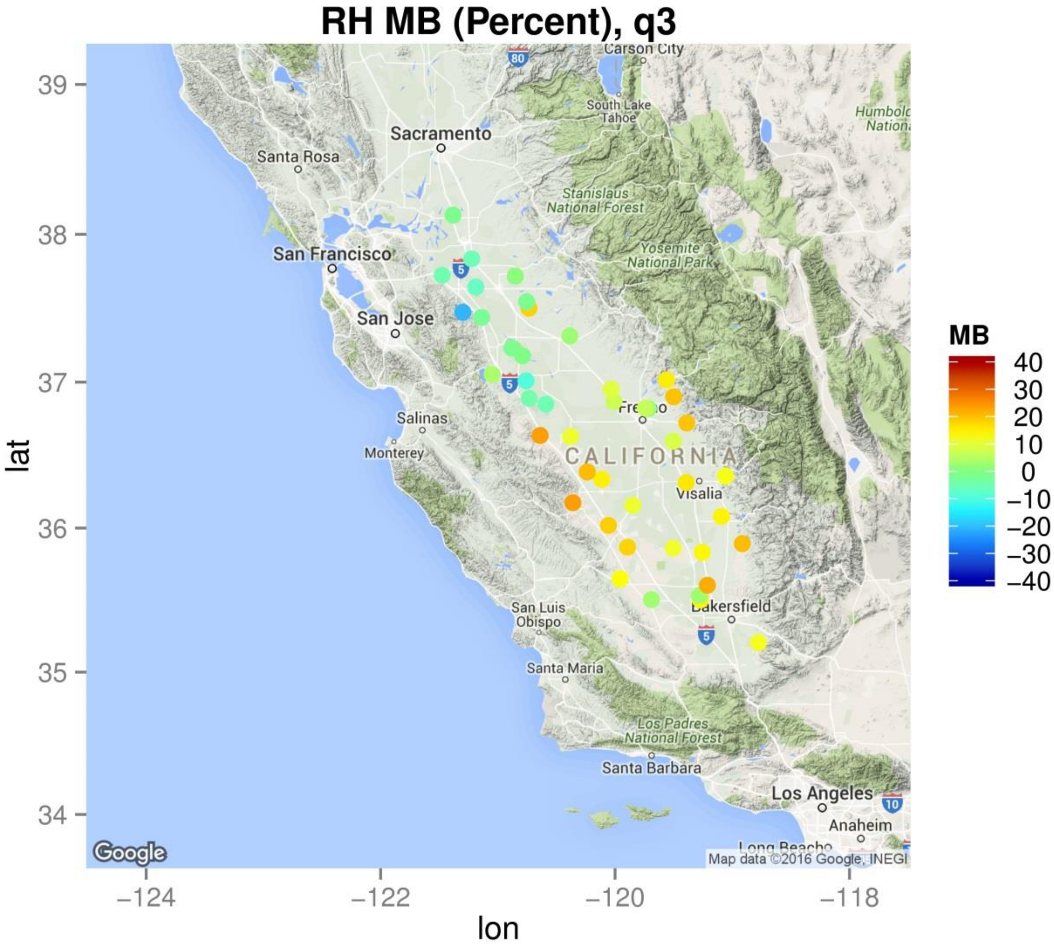

Figure S. 31 Hourly relative humidity mean bias in the third quarter of 2013

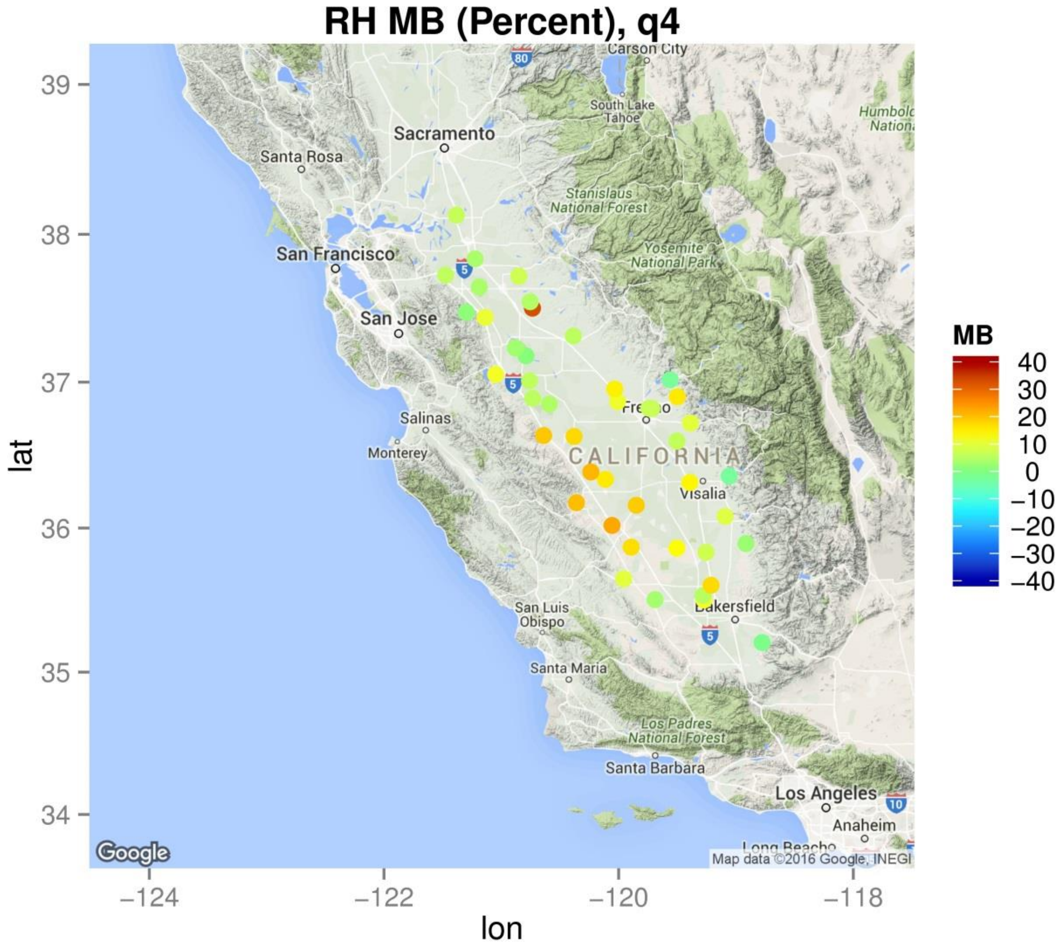

Figure S. 32 Hourly relative humidity mean bias in the fourth quarter of 2013

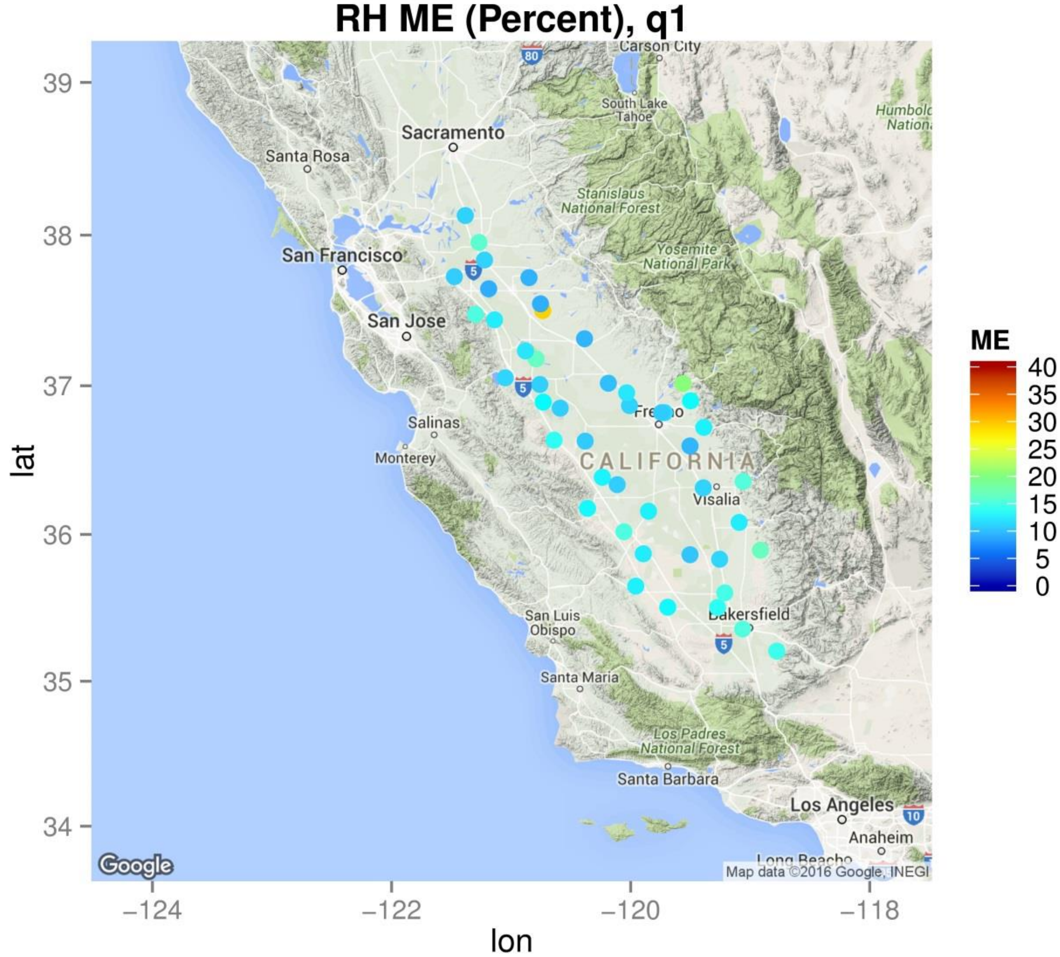

Figure S. 33 Hourly relative humidity mean error in the first quarter of 2013

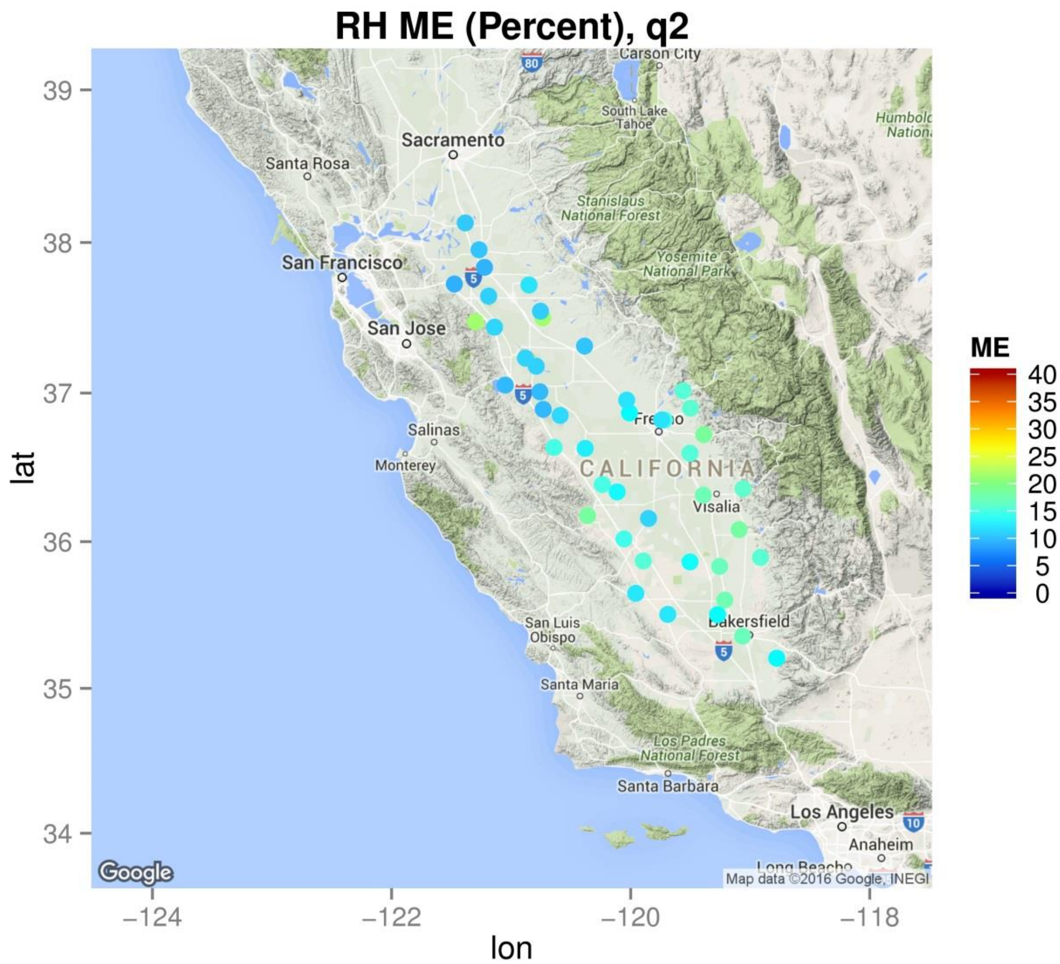

Figure S. 34 Hourly relative humidity mean error in the second quarter of 2013

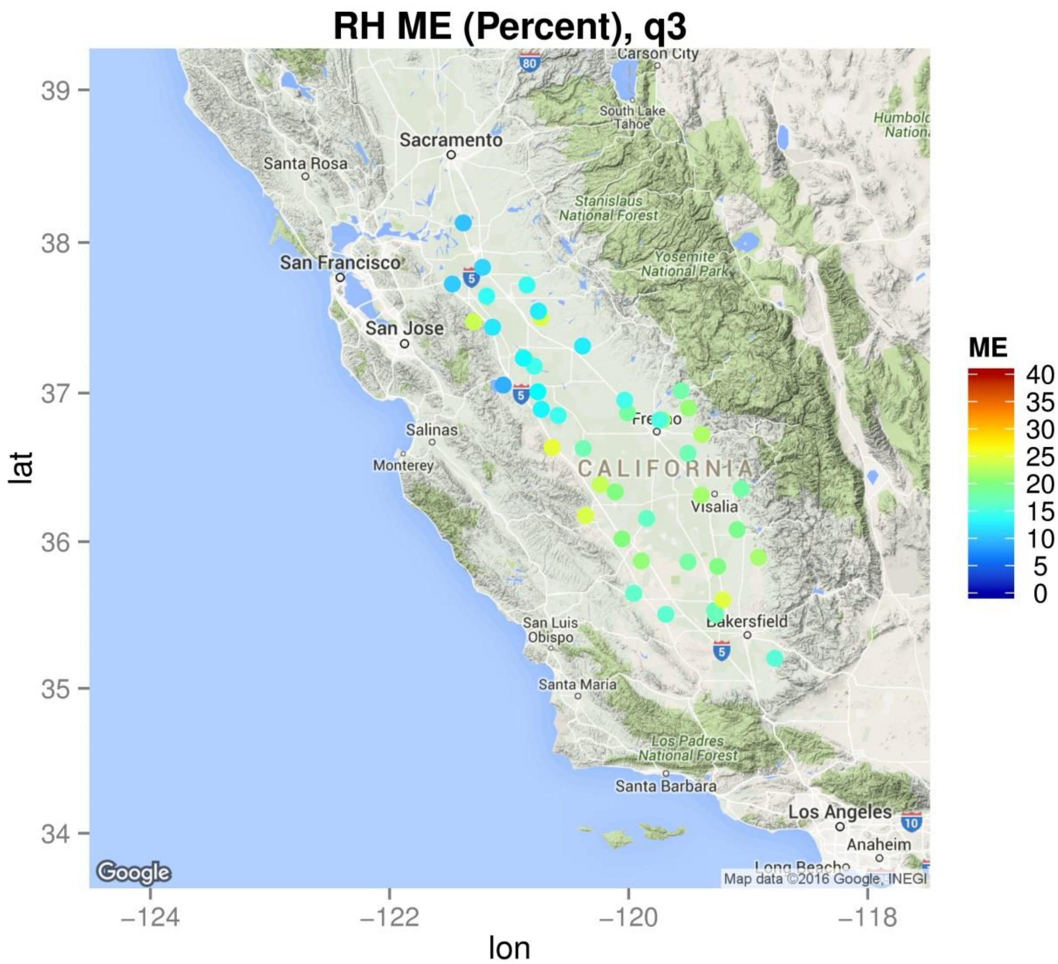

Figure S. 35 Hourly relative humidity mean error in the third quarter of 2013

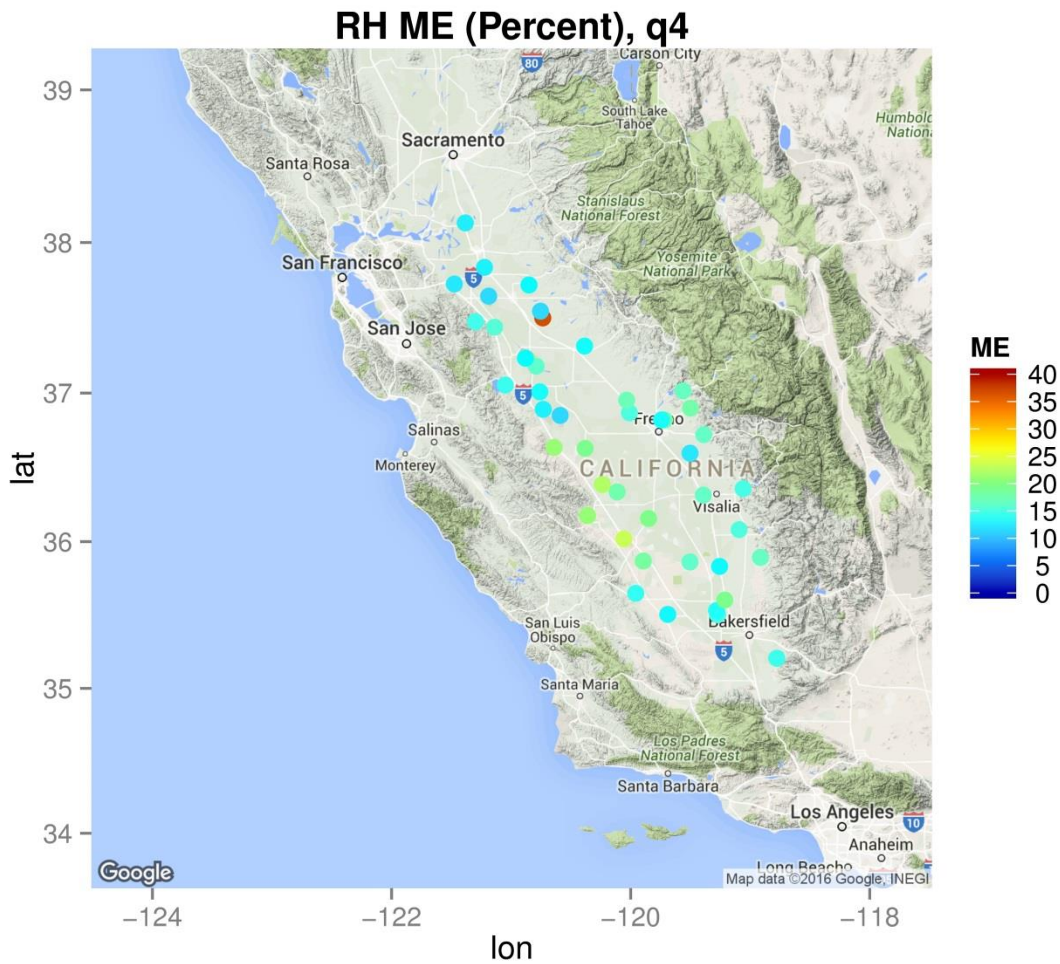

Figure S. 36 Hourly relative humidity mean error in the fourth quarter of 2013

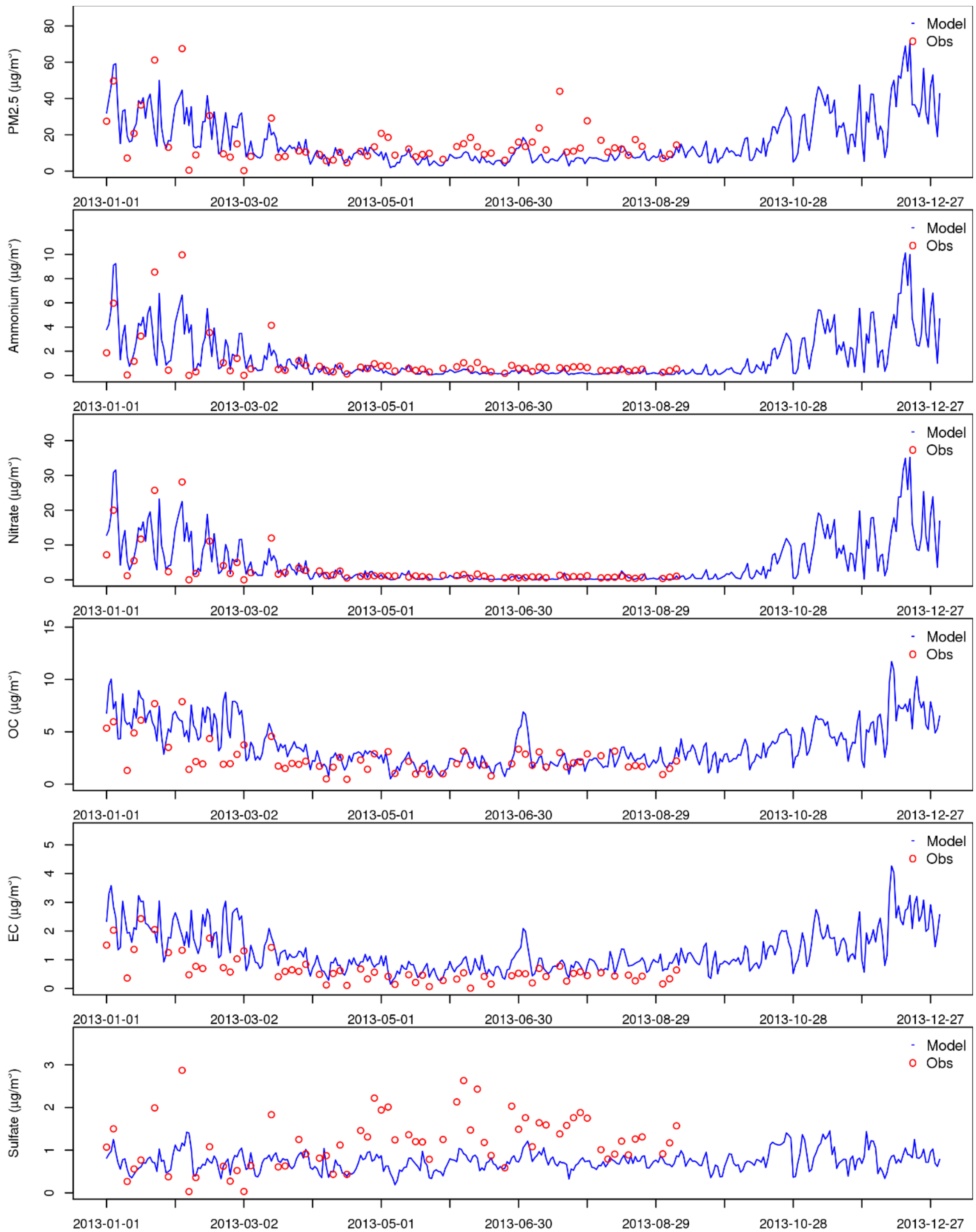

Figure S. 37 Comparison of time series of observed (from CSN measurement) and modeled $PM_{2.5}$ species at Bakersfield

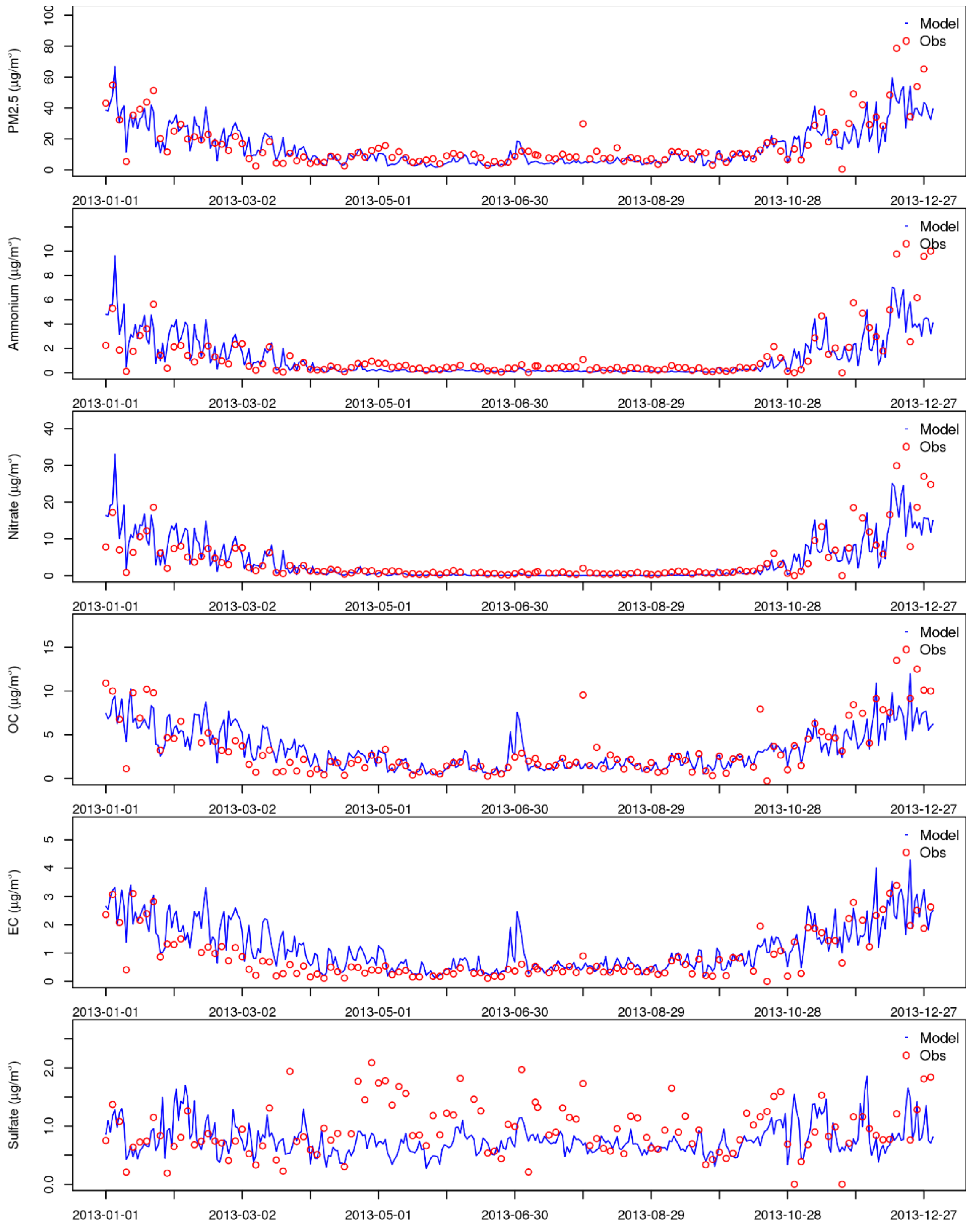

Figure S. 38 Comparison of time series of observed (from CSN measurement) and modeled $PM_{2.5}$ species at Fresno

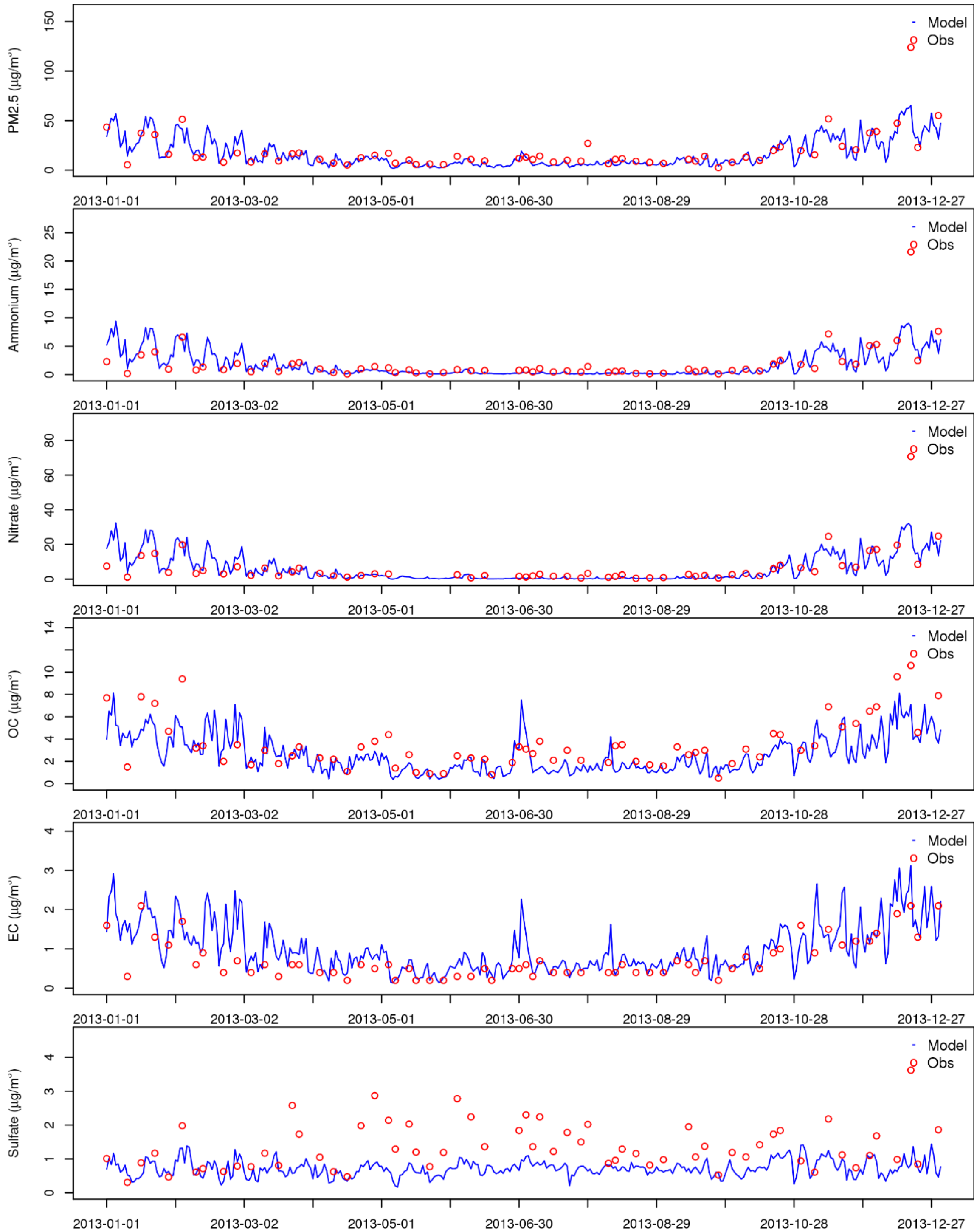

Figure S. 39 Comparison of time series of observed (from CSN measurement) and modeled $PM_{2.5}$ species at Visalia

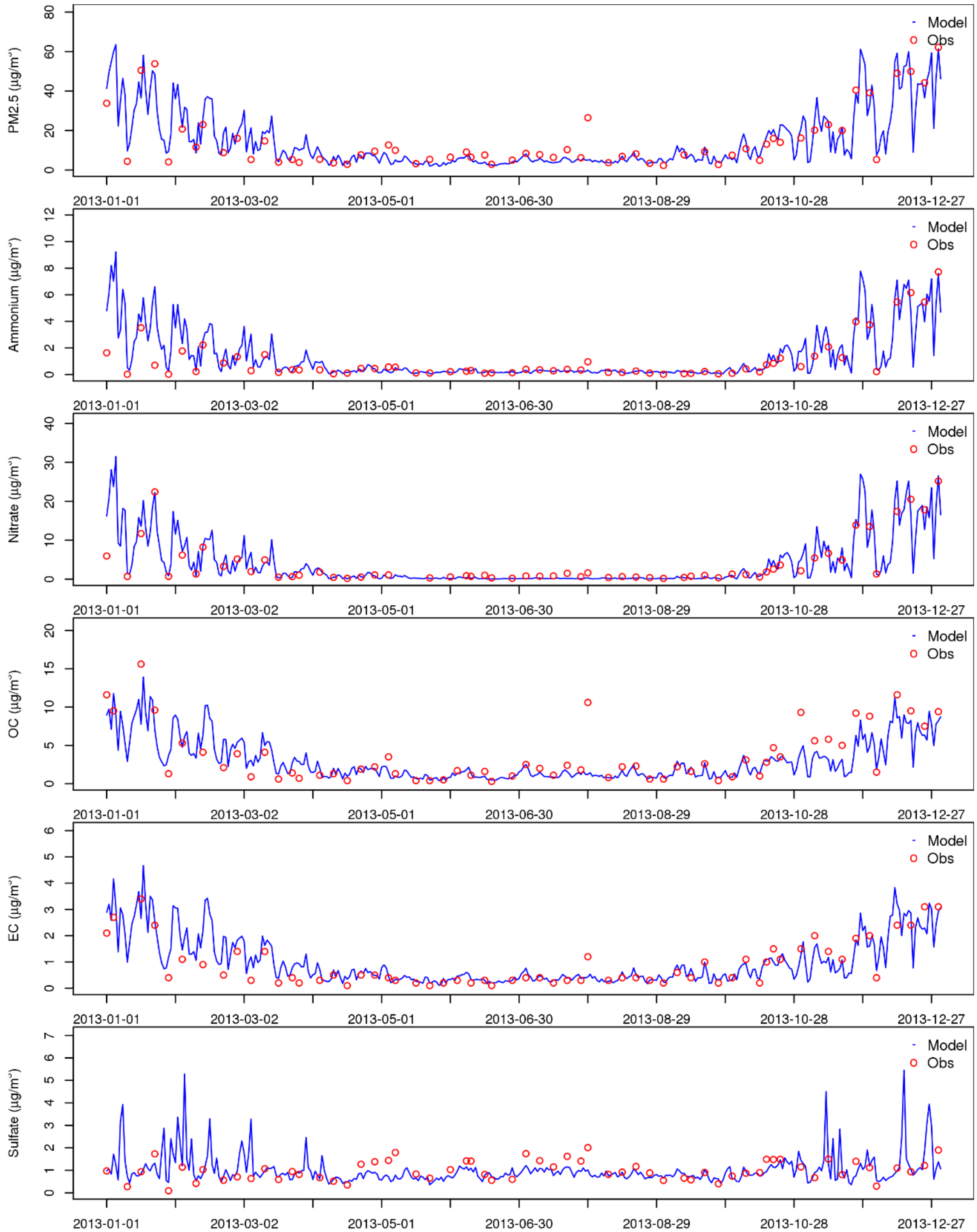

Figure S. 40 Comparison of time series of observed (from CSN measurement) and modeled $PM_{2.5}$ species at Modesto

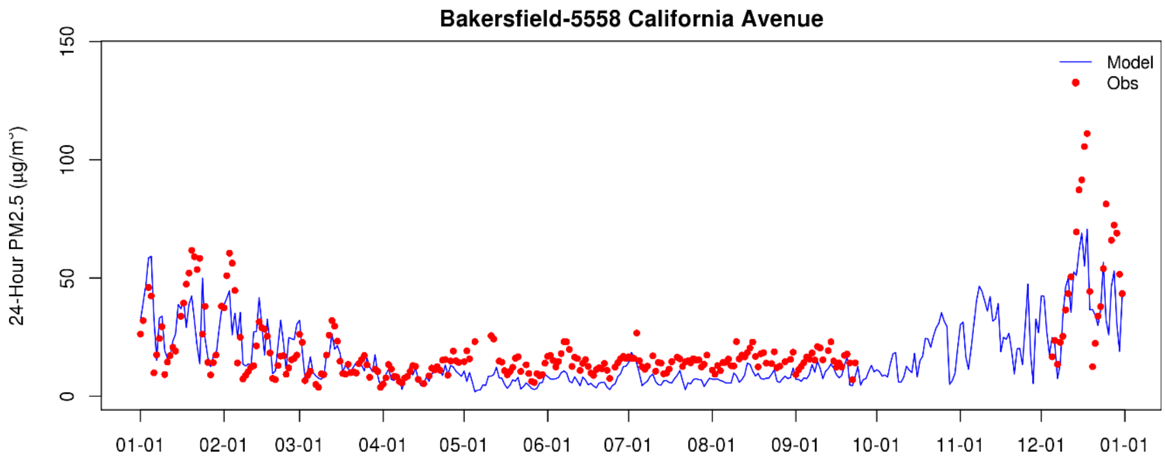

Figure S. 41 Observed and modeled 24-hour average $PM_{2.5}$ at Bakersfield – California Avenue.

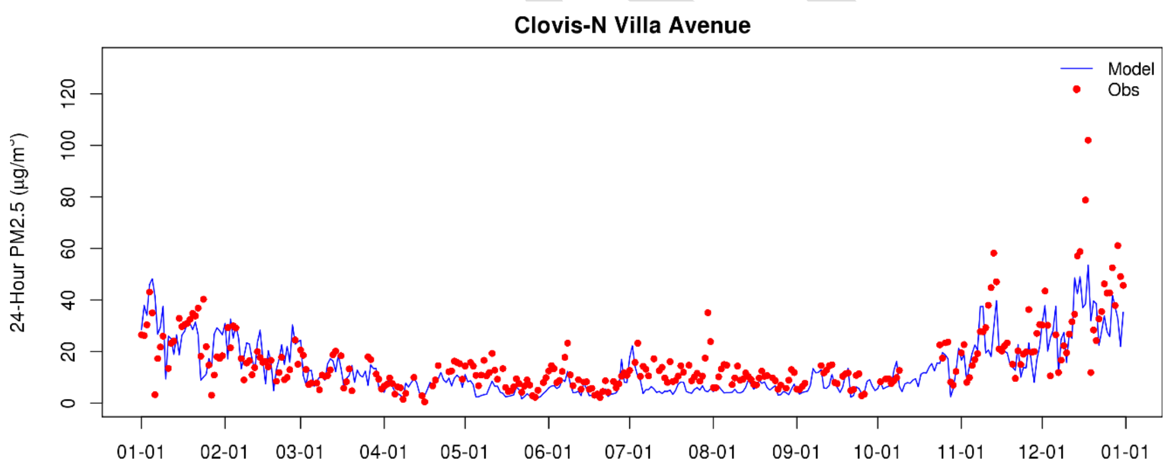

Figure S. 42 Observed and modeled 24-hour average $PM_{2.5}$ at Clovis – Villa Avenue

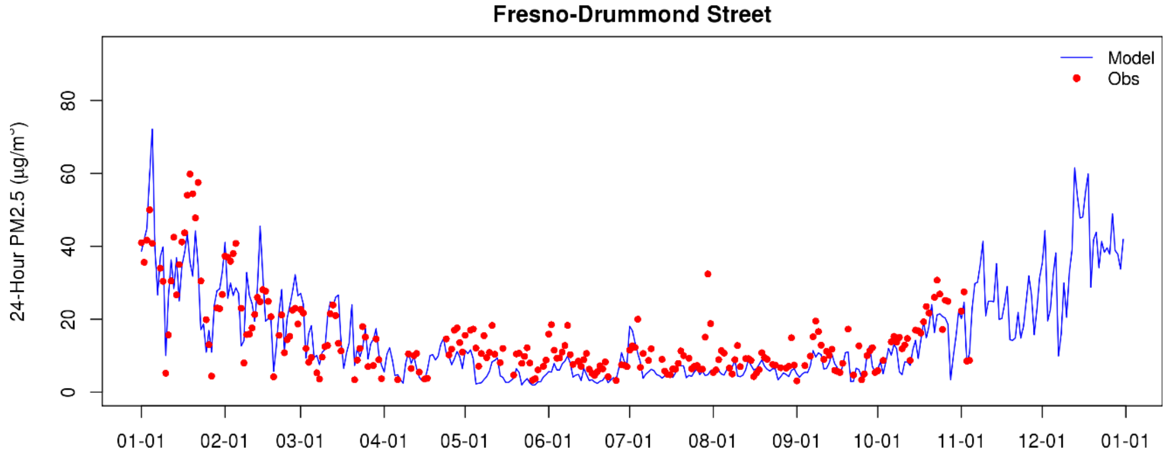

Figure S. 43 Observed and modeled 24-hour average $PM_{2.5}$ at Fresno – Drummond Street

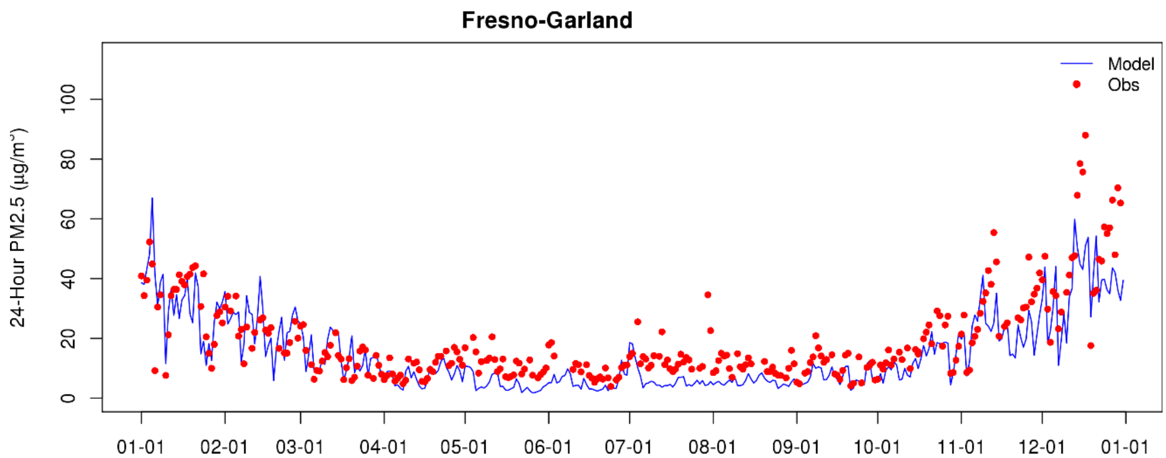

Figure S. 44 Observed and modeled 24-hour average $PM_{2.5}$ at Fresno – Garland

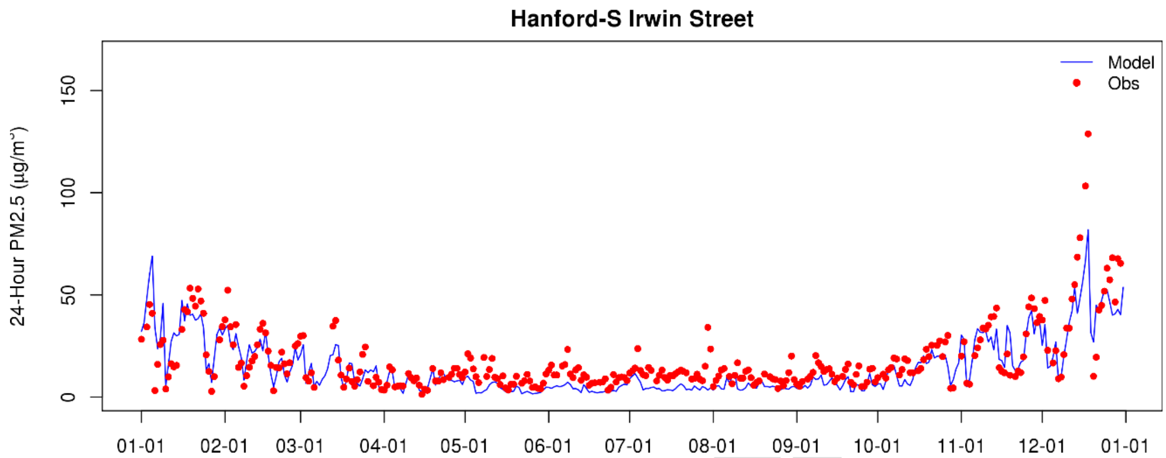

Figure S. 45 Observed and modeled 24-hour average $PM_{2.5}$ at Hanford – Irwin Street

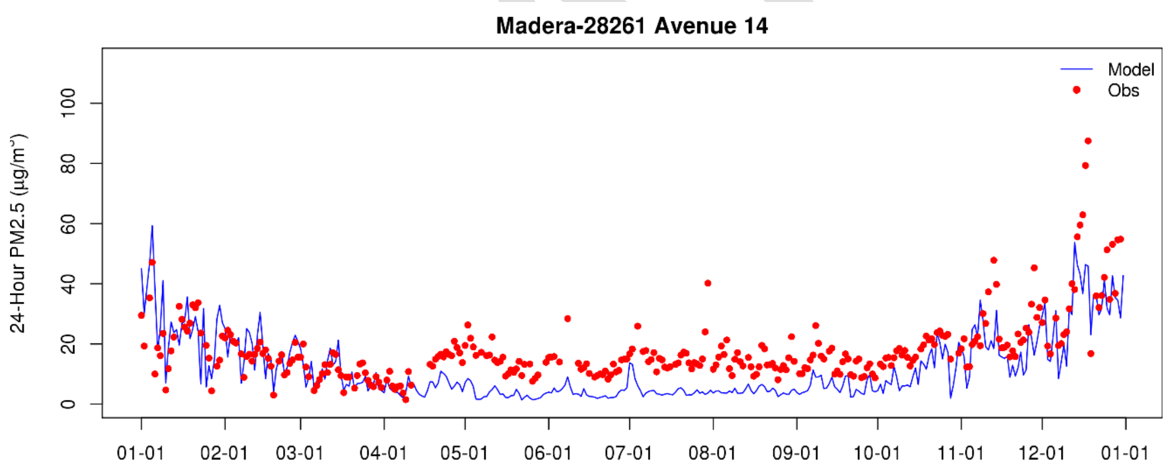

Figure S. 46 Observed and modeled 24-hour average $PM_{2.5}$ at Madera – Avenue 14

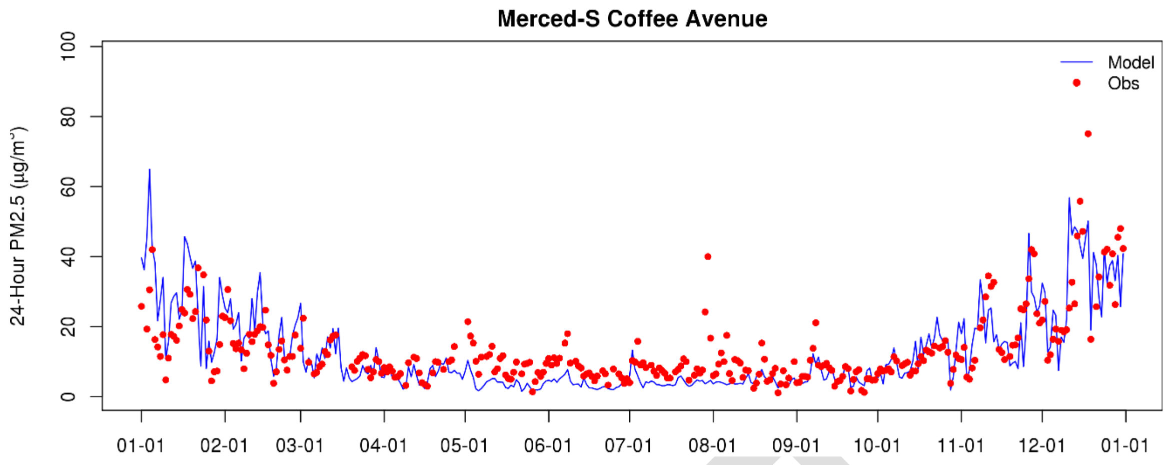

Figure S. 47 Observed and modeled 24-hour average $PM_{2.5}$ at Merced – S Coffee Avenue

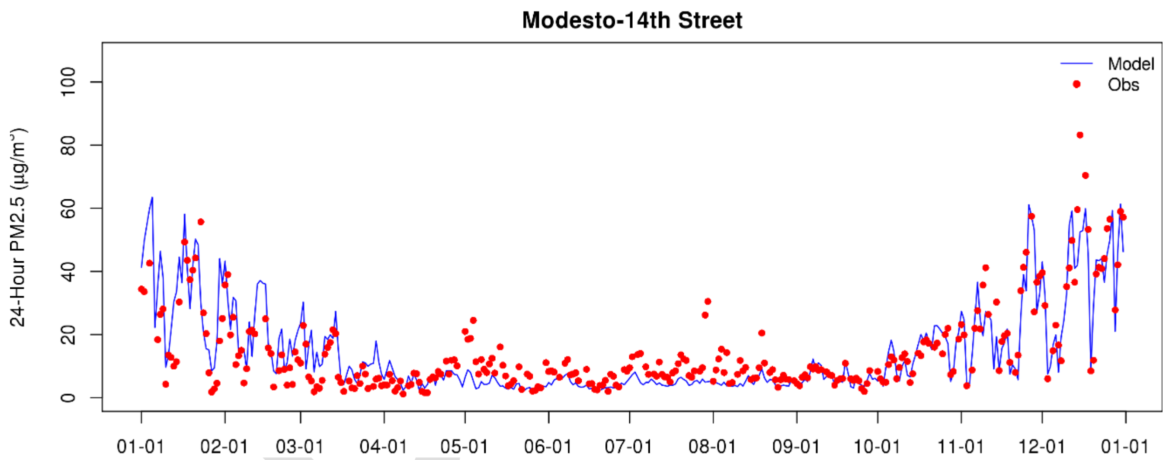

Figure S. 48 Observed and modeled 24-hour average $PM_{2.5}$ at Modesto – 14th Street

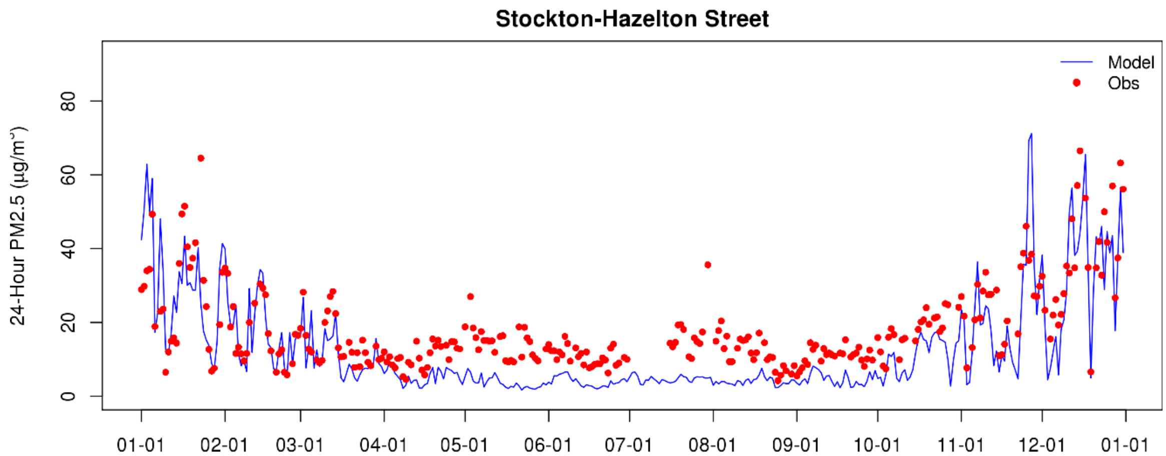

Figure S. 49 Observed and modeled 24-hour average $PM_{2.5}$ at Stockton – Hazelton Street

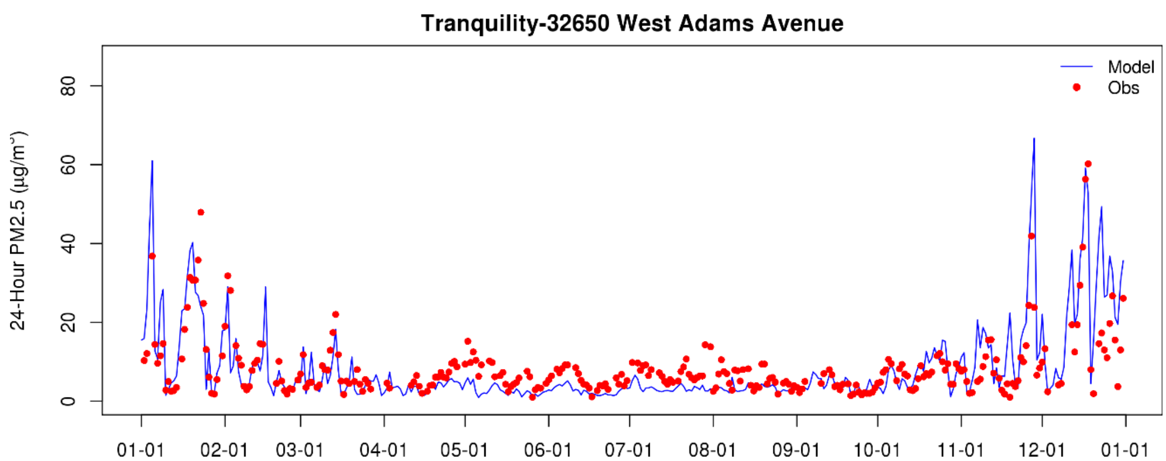

Figure S. 50 Observed and modeled 24-hour average $PM_{2.5}$ at Tranquility – West Adams Avenue

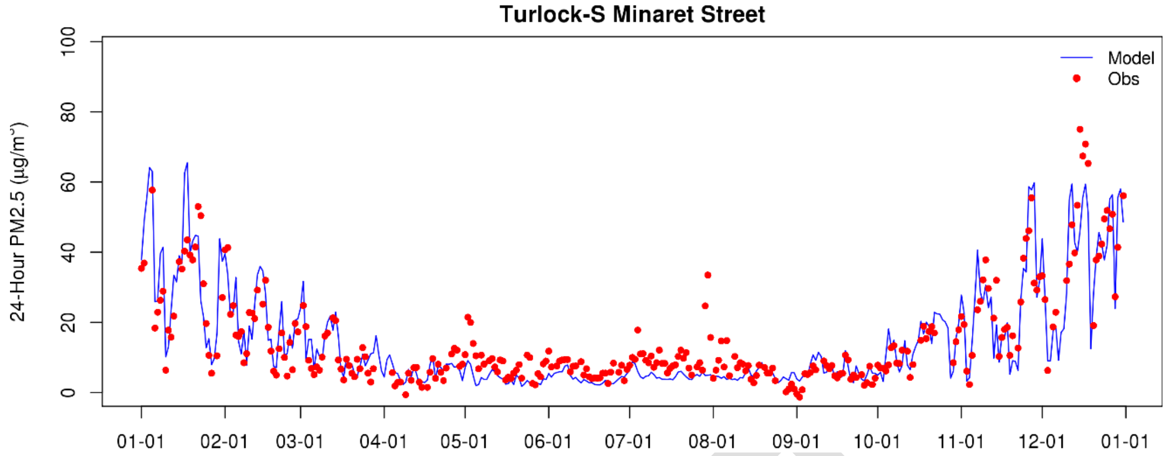

Figure S. 51 Observed and modeled 24-hour average $PM_{2.5}$ at Turlock – Minaret Street

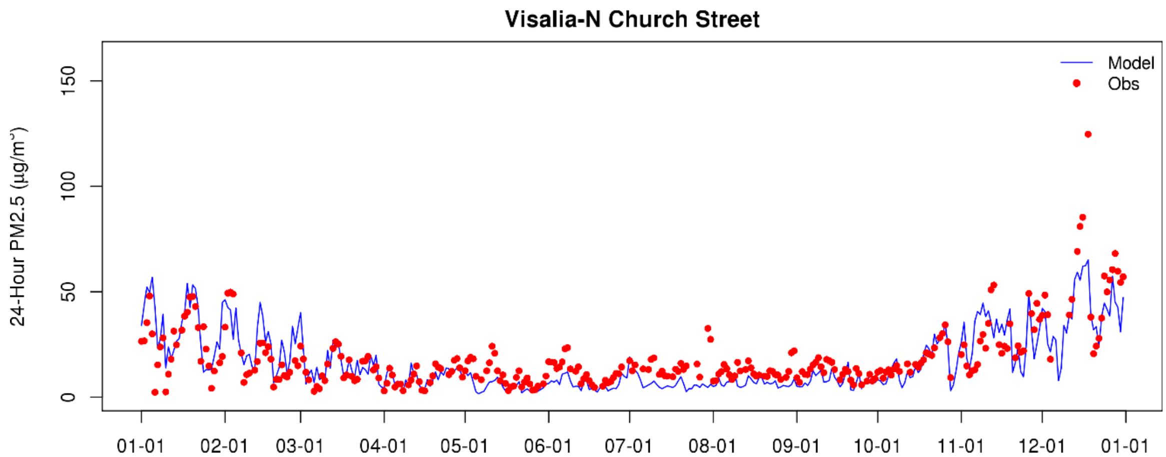

Figure S. 52 Observed and modeled 24-hour average $PM_{2.5}$ at Visalia – Church Street

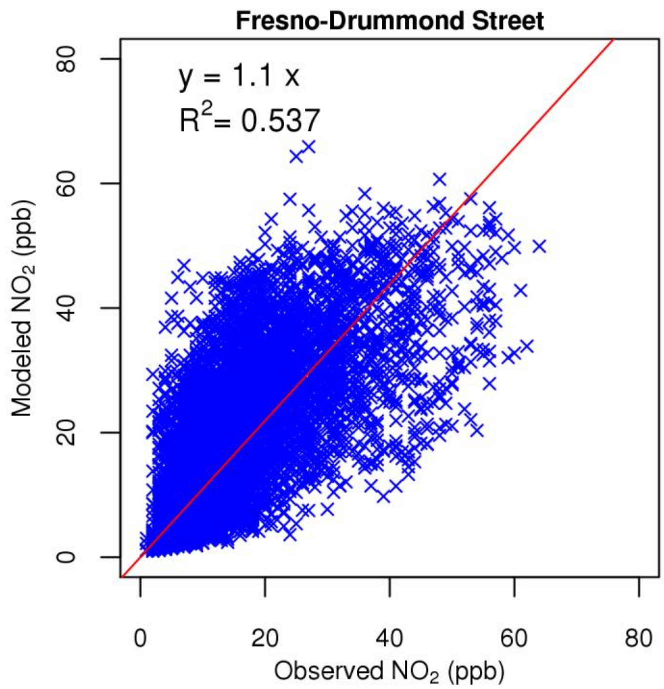

Figure S. 53 Scattering plot of observed and modeled 1-hour NO_2 mixing ratio at Fresno – Drummond Street

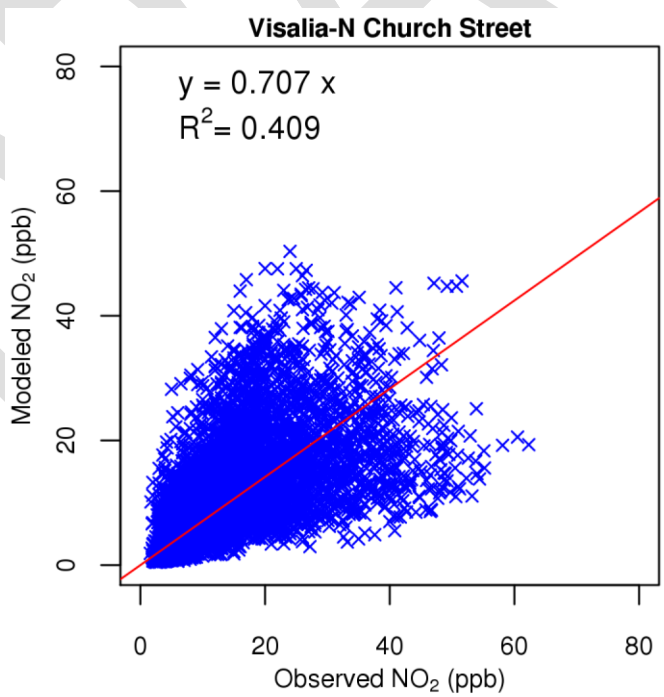

Figure S. 54 Scattering plot of observed and modeled 1-hour NO_2 mixing ratio at Visalia

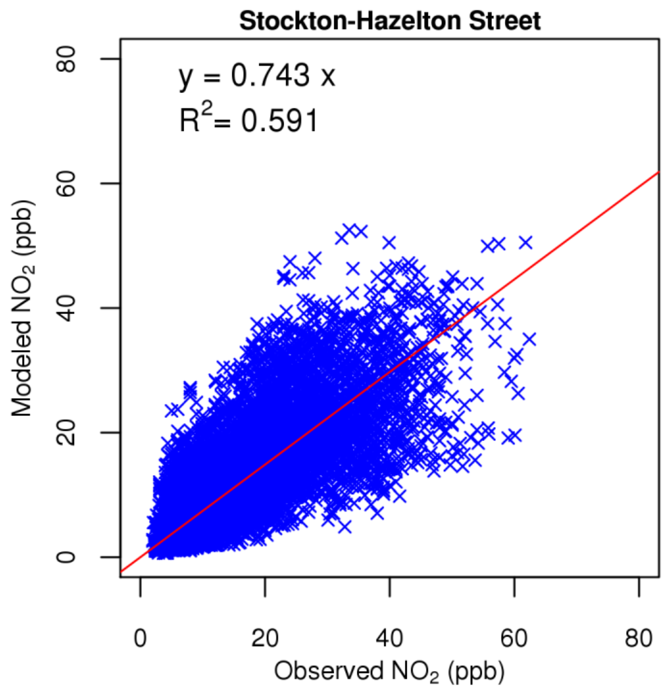

Figure S. 55 Scattering plot of observed and modeled 1-hour NO_2 mixing ratio at Stockton

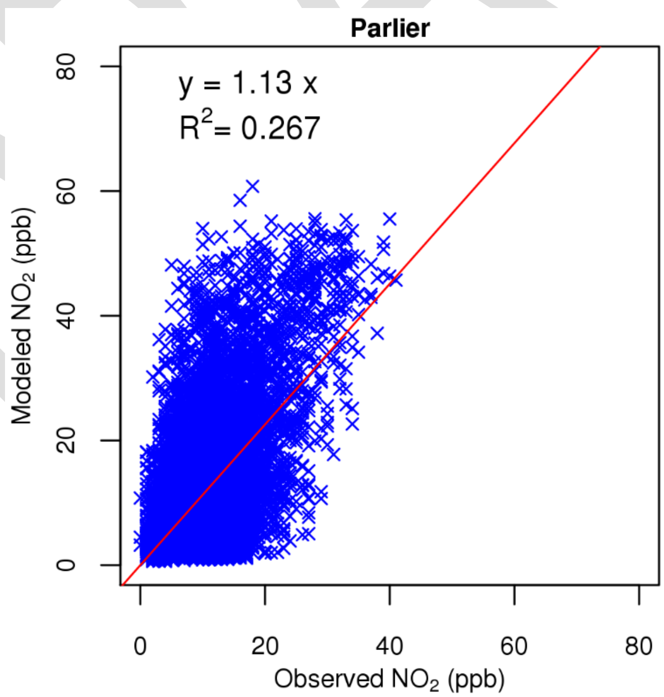

Figure S. 56 Scattering plot of observed and modeled 1-hour NO_2 mixing ratio at Parlier

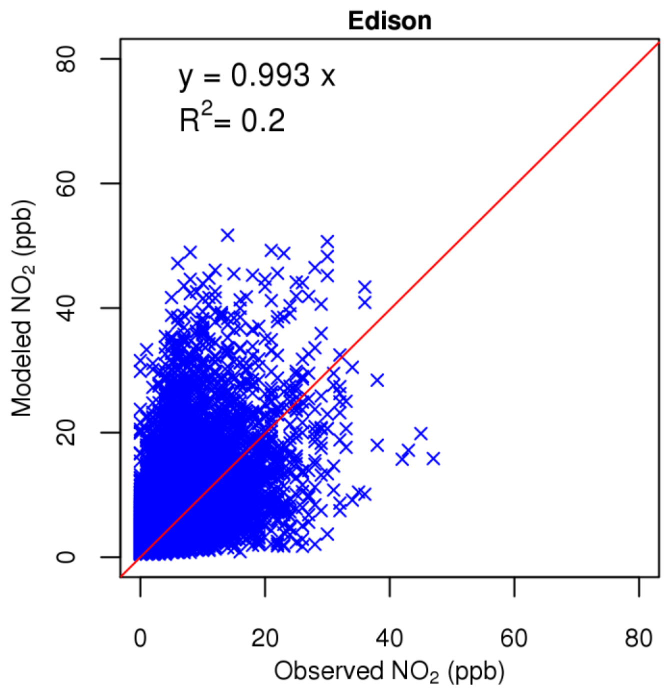

Figure S. 57 Scattering plot of observed and modeled 1-hour NO_2 mixing ratio at Edison

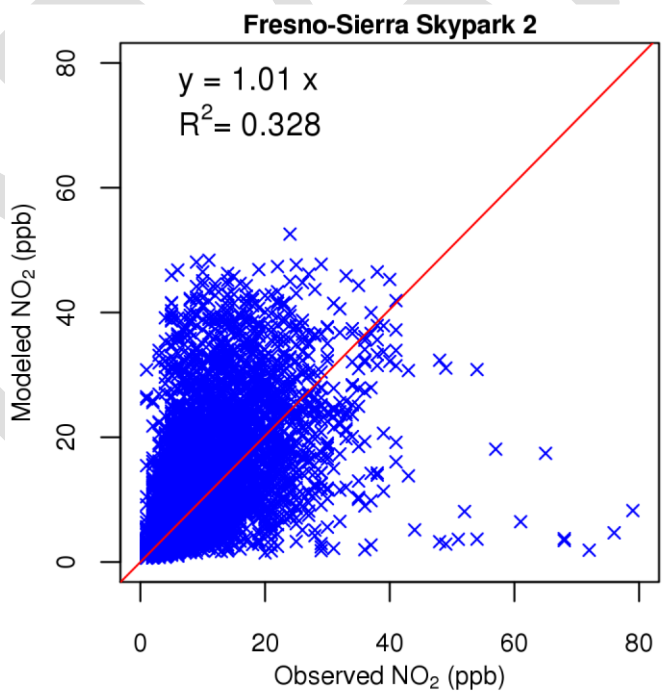

Figure S. 58 Scattering plot of observed and modeled 1-hour NO_2 mixing ratio at Fresno – Sierra Sky Park

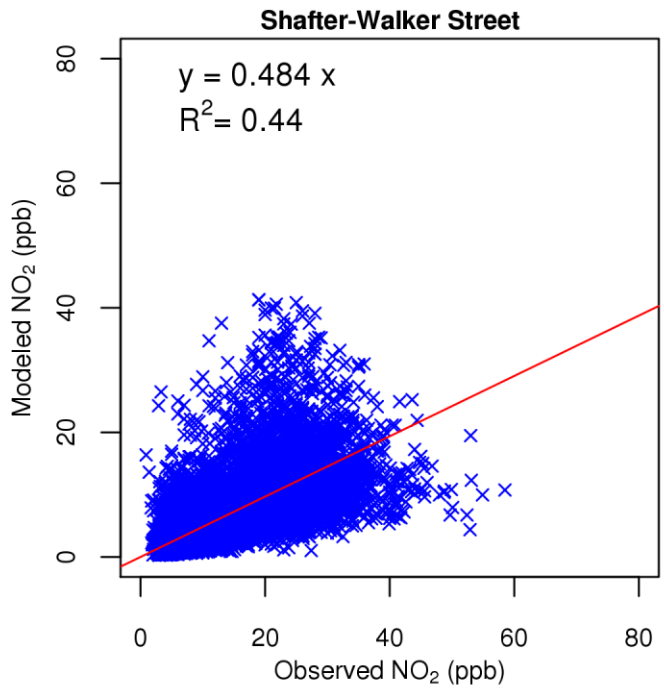

Figure S. 59 Scattering plot of observed and modeled 1-hour NO_2 mixing ratio at Shafter

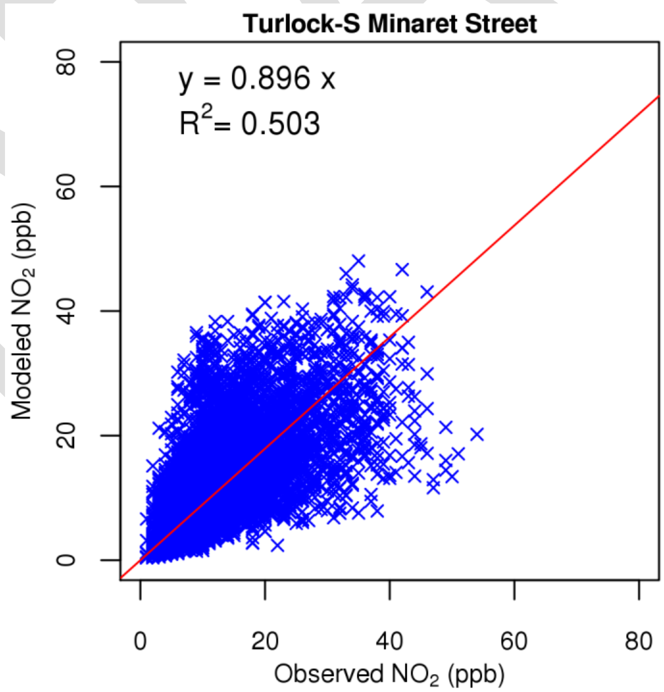

Figure S. 60 Scattering plot of observed and modeled 1-hour NO_2 mixing ratio at Turlock

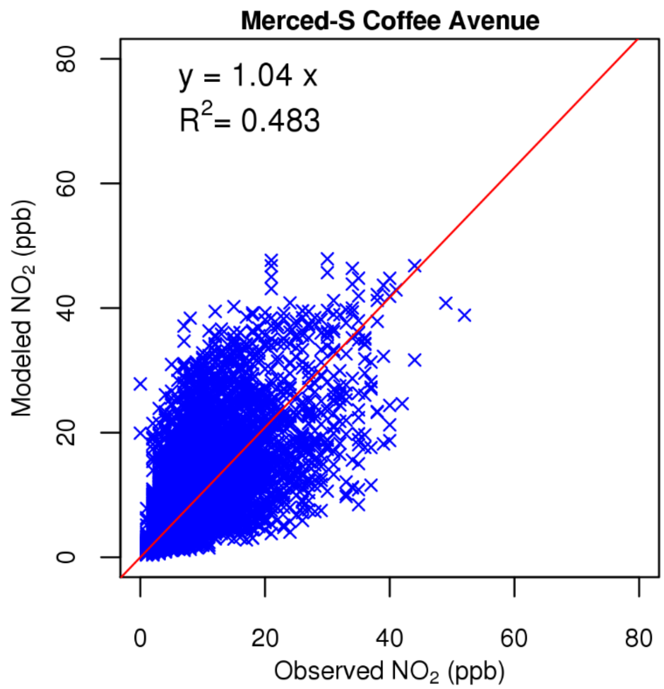

Figure S. 61 Scattering plot of observed and modeled 1-hour NO_2 mixing ratio at Merced

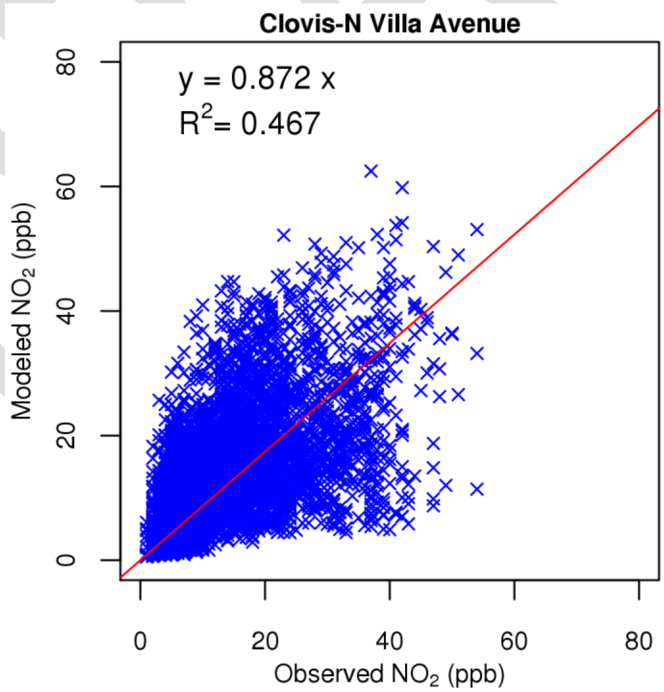

Figure S. 62 Scattering plot of observed and modeled 1-hour NO_2 mixing ratio at Clovis

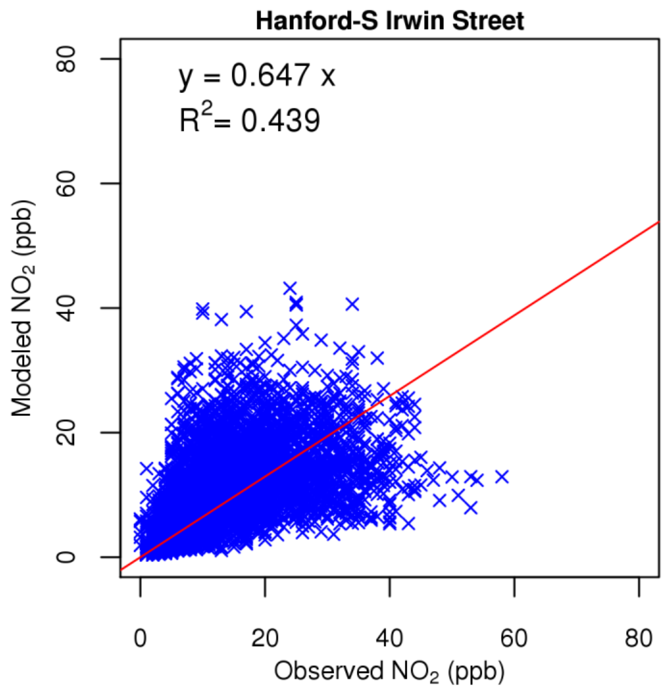

Figure S. 63 Scattering plot of observed and modeled 1-hour NO_2 mixing ratio at Hanford

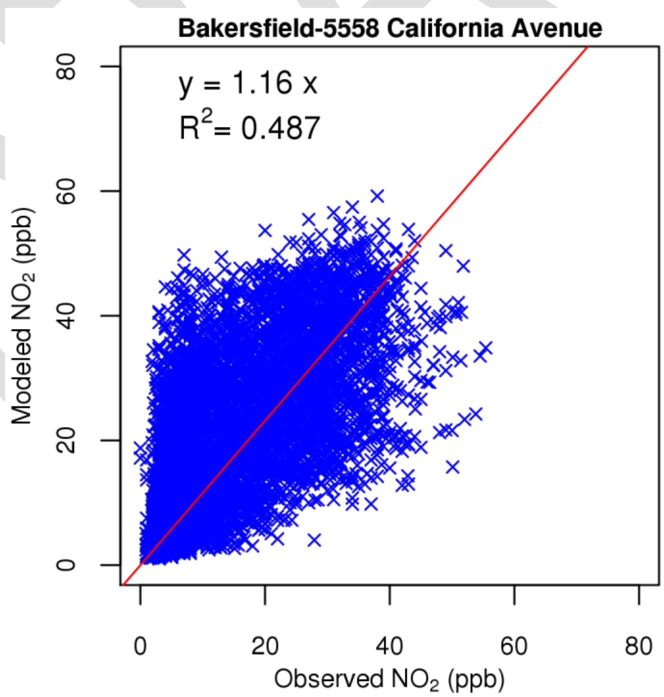

Figure S. 64 Scattering plot of observed and modeled 1-hour NO_2 mixing ratio at Bakersfield – California Avenue

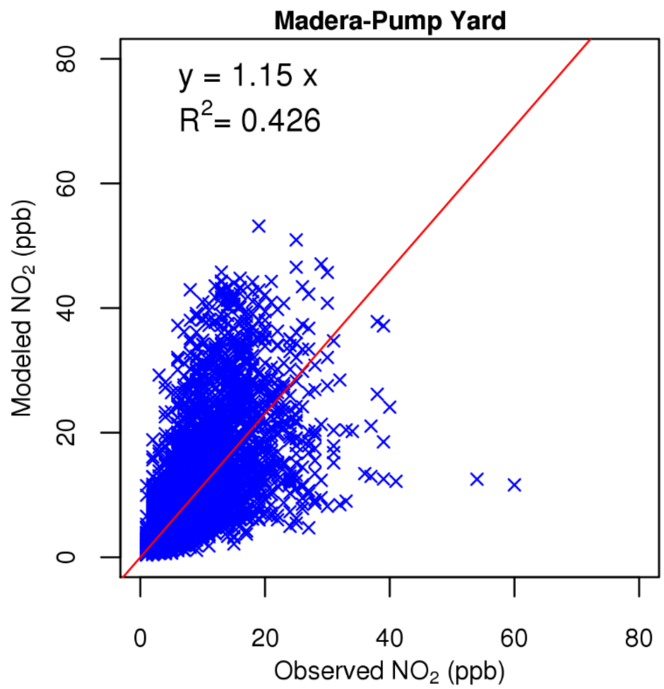

Figure S. 65 Scattering plot of observed and modeled 1-hour NO_2 mixing ratio at Madera

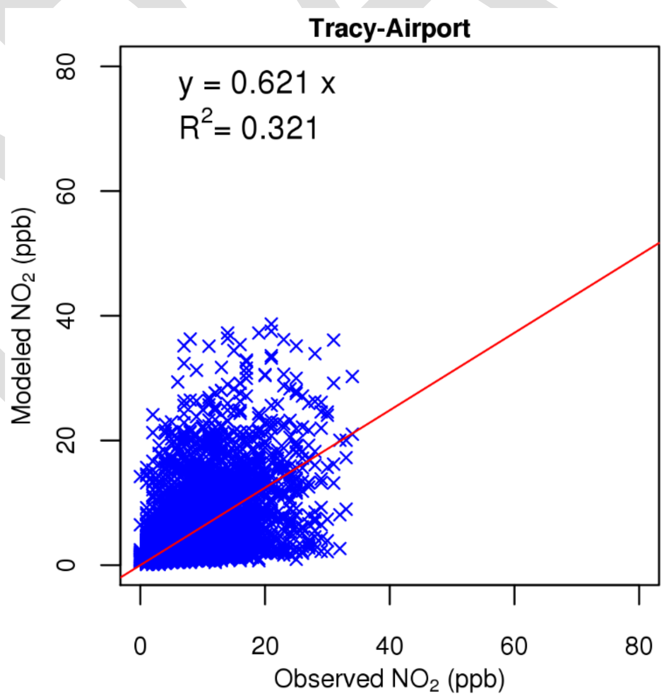

Figure S. 66 Scattering plot of observed and modeled 1-hour NO_2 mixing ratio at Tracy

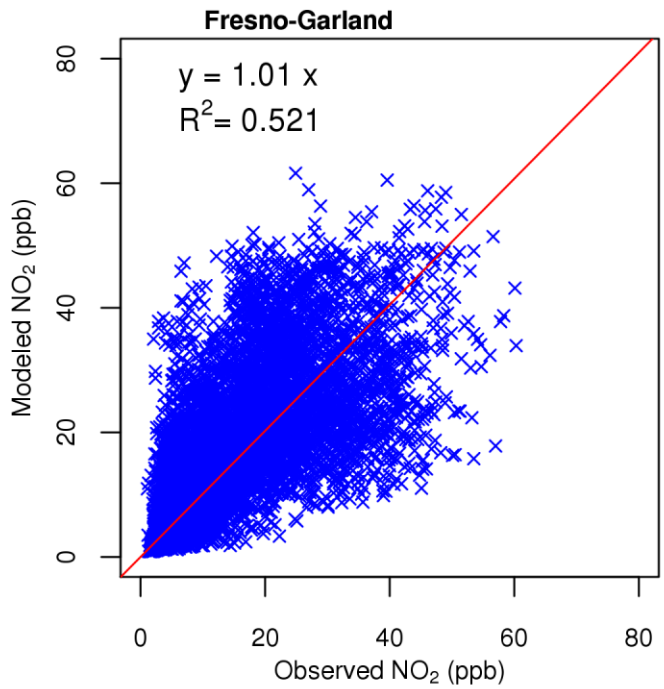

Figure S. 67 Scattering plot of observed and modeled 1-hour NO_2 mixing ratio at Fresno – Garland

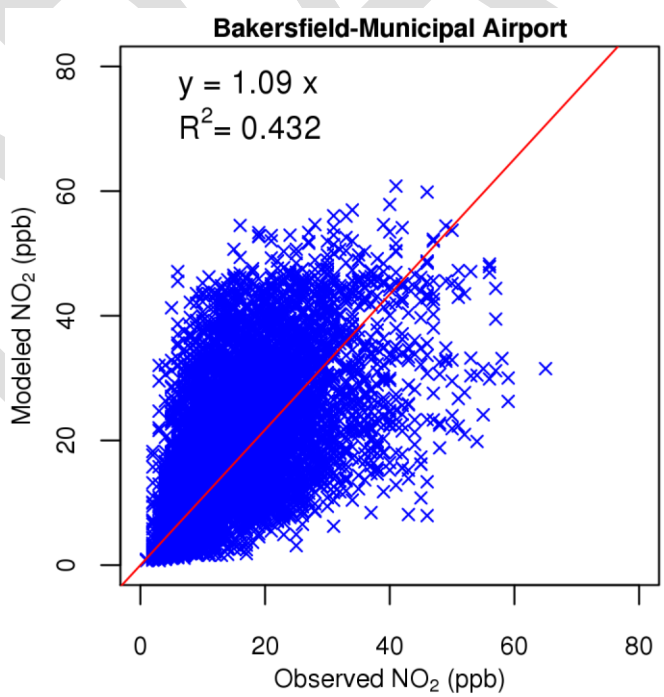

Figure S. 68 Scattering plot of observed and modeled 1-hour NO_2 mixing ratio at Bakersfield – Municipal Airport

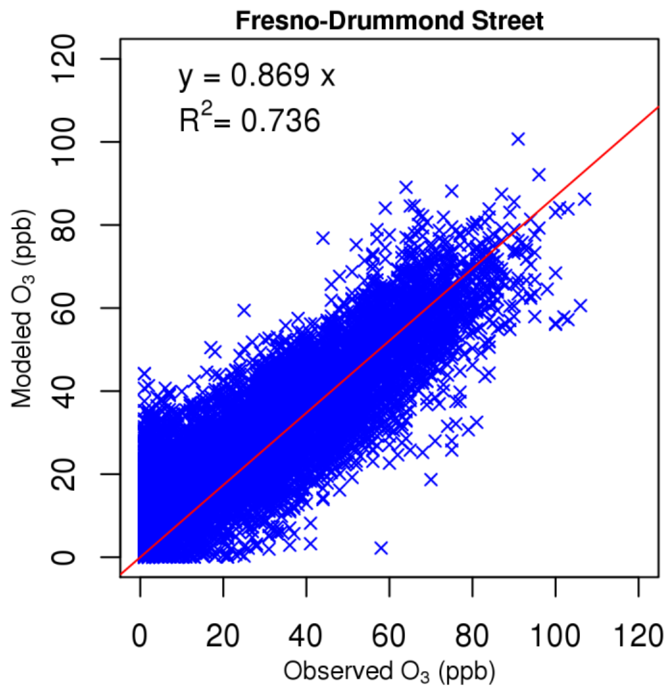

Figure S. 69 Scattering plot of observed and modeled 1-hour O_3 mixing ratio at Fresno – Drummond Street

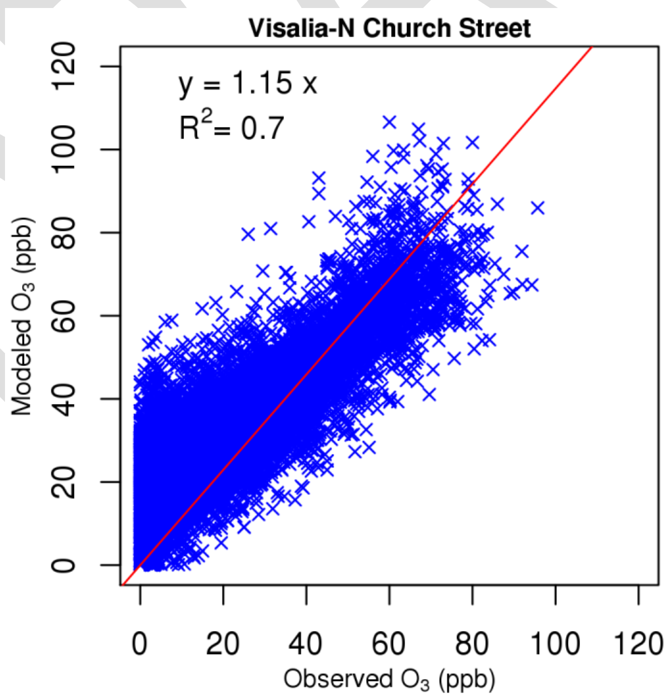

Figure S.70 Scattering plot of observed and modeled 1-hour O_3 mixing ratio at Visalia

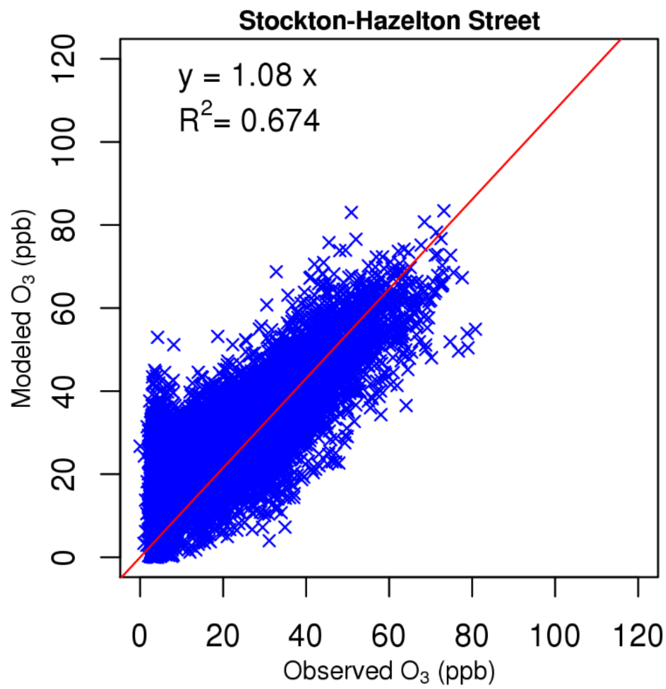

Figure S. 71 Scattering plot of observed and modeled 1-hour O_3 mixing ratio at Stockton

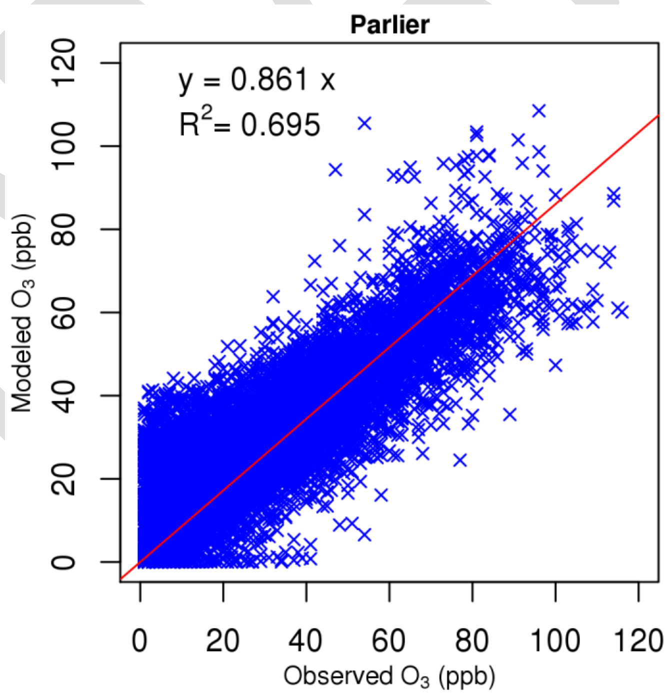

Figure S. 72 Scattering plot of observed and modeled 1-hour O_3 mixing ratio at Parlier

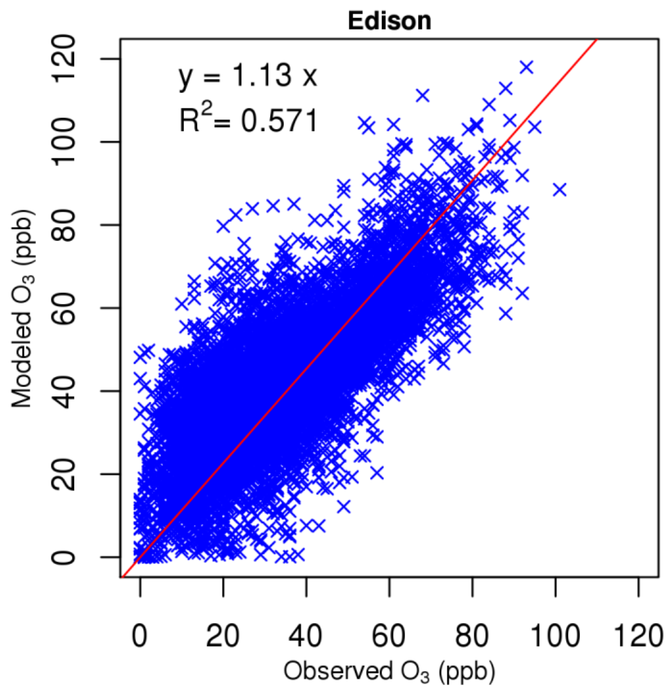

Figure S. 73 Scattering plot of observed and modeled 1-hour O_3 mixing ratio at Edison

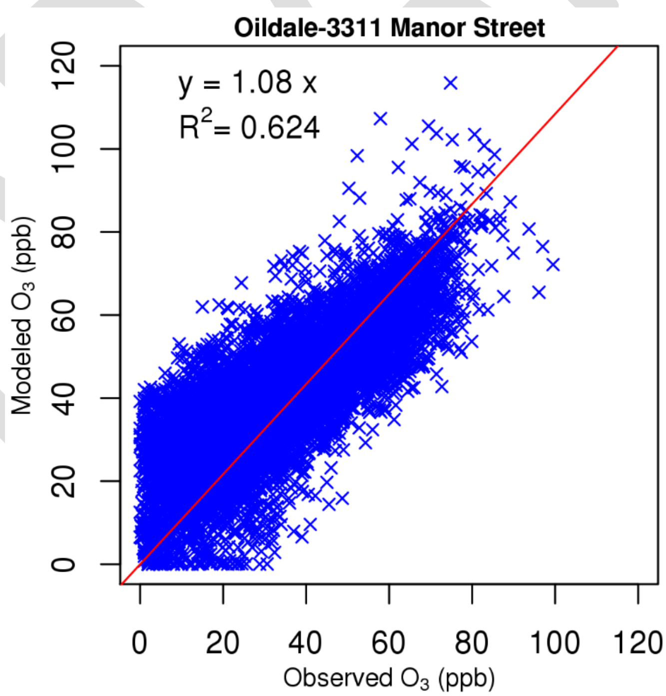

Figure S. 74 Scattering plot of observed and modeled 1-hour O_3 mixing ratio at Oildale

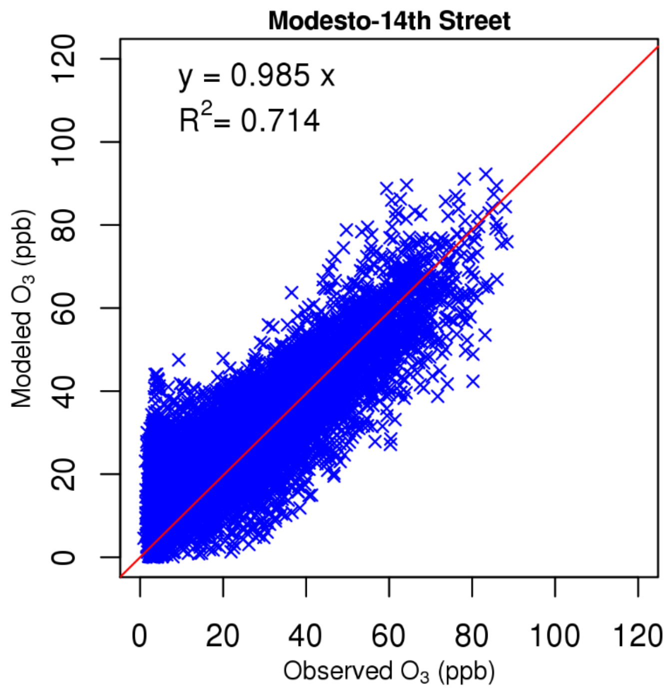

Figure S. 75 Scattering plot of observed and modeled 1-hour O_3 mixing ratio at Modesto -14th Street

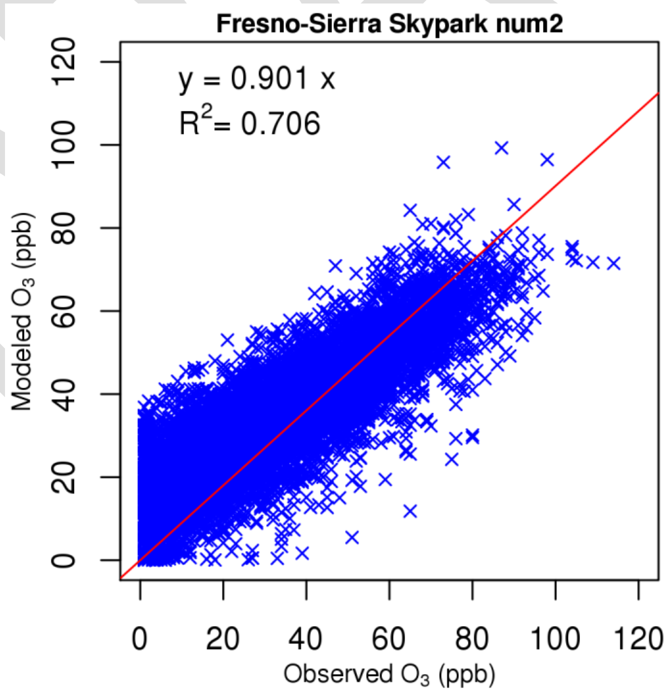

Figure S.76 Scattering plot of observed and modeled 1-hour O_3 mixing ratio at Fresno – Sierra Sky Park #2

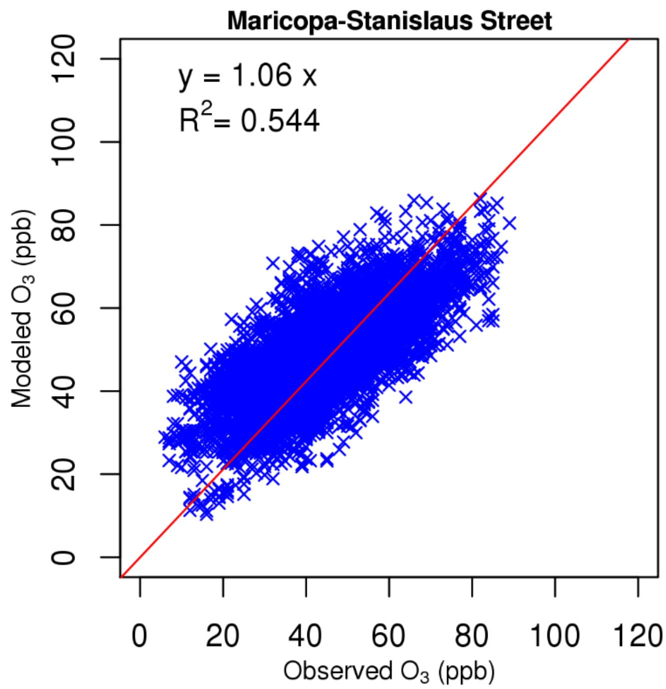

Figure S. 77 Scattering plot of observed and modeled 1-hour O_3 mixing ratio at Maricopa

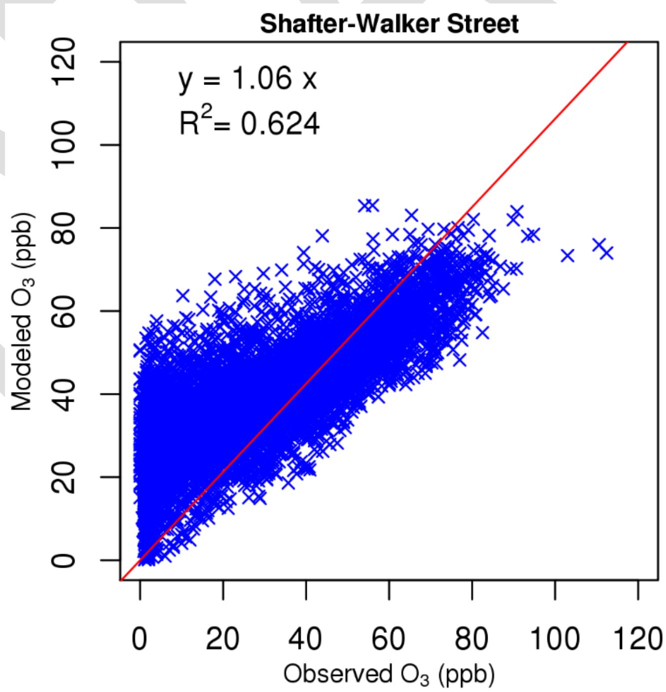

Figure S. 78 Scattering plot of observed and modeled 1-hour O_3 mixing ratio at Shafter

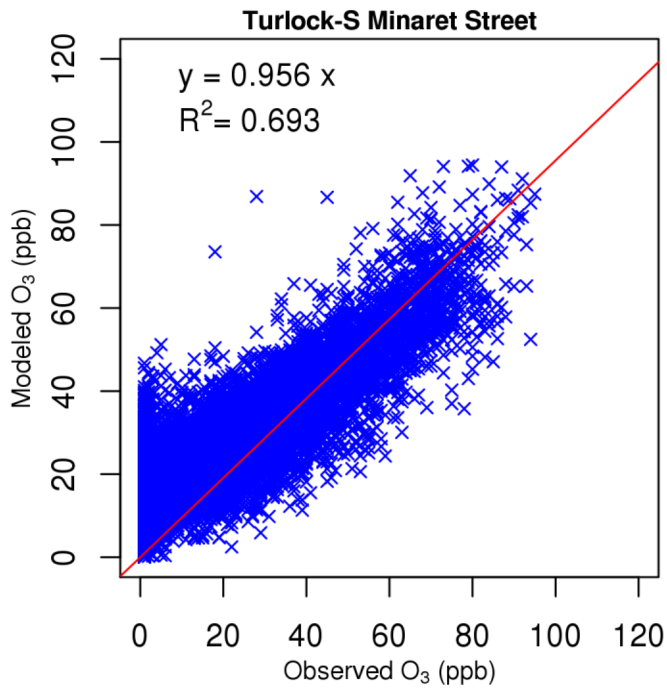

Figure S. 79 Scattering plot of observed and modeled 1-hour O_3 mixing ratio at Turlock

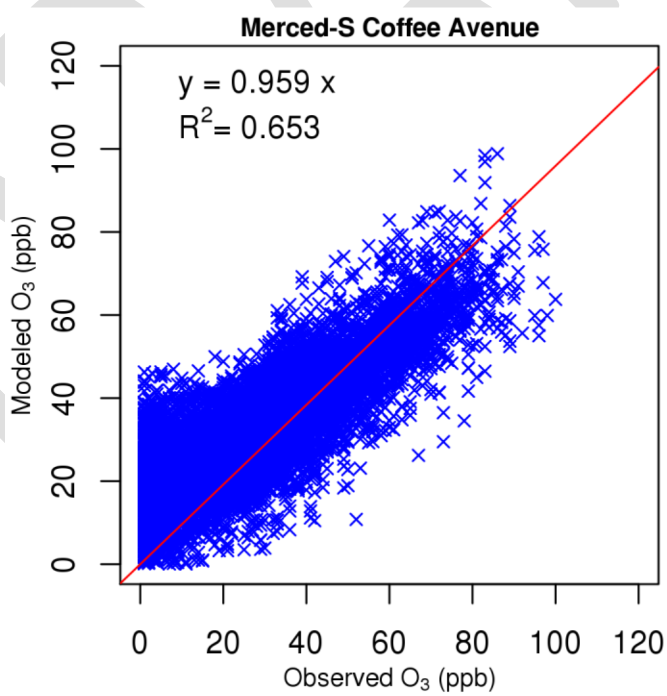

Figure S. 80 Scattering plot of observed and modeled 1-hour O_3 mixing ratio at Merced – S Coffee Avenue

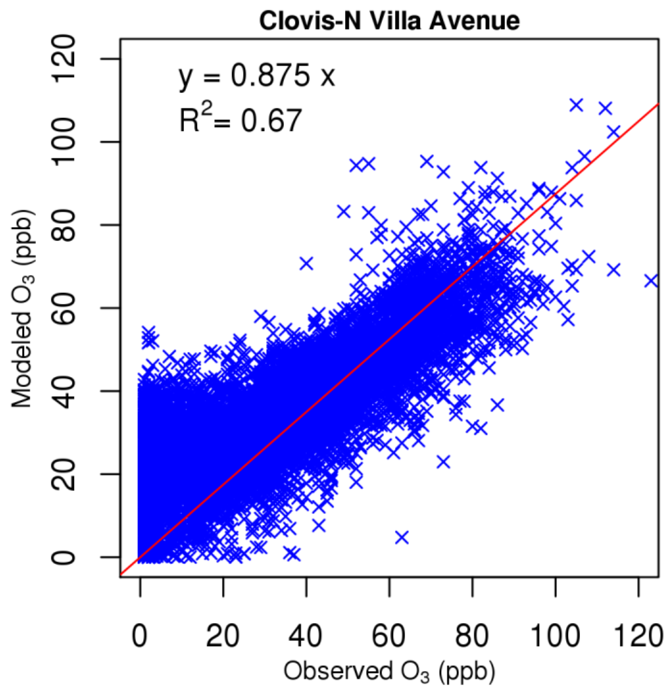

Figure S. 81 Scattering plot of observed and modeled 1-hour O_3 mixing ratio at Clovis

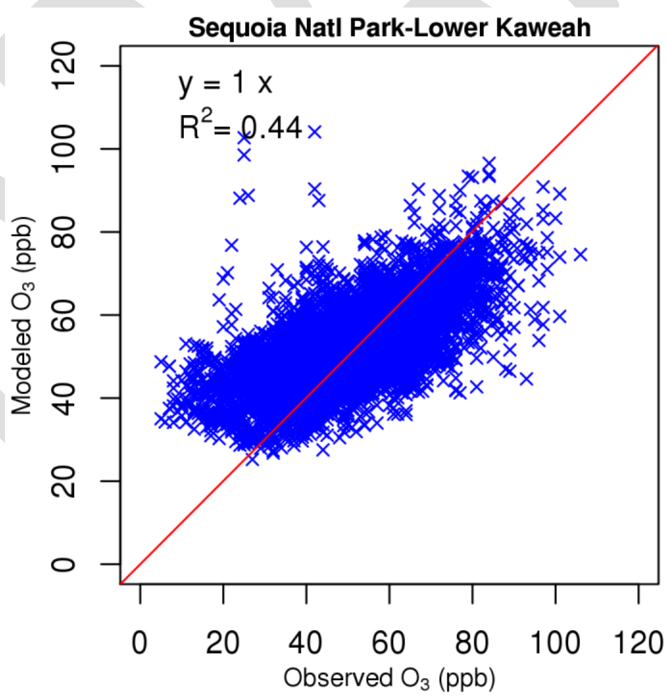

Figure S. 82 Scattering plot of observed and modeled 1-hour O_3 mixing ratio at Sequoia National Park

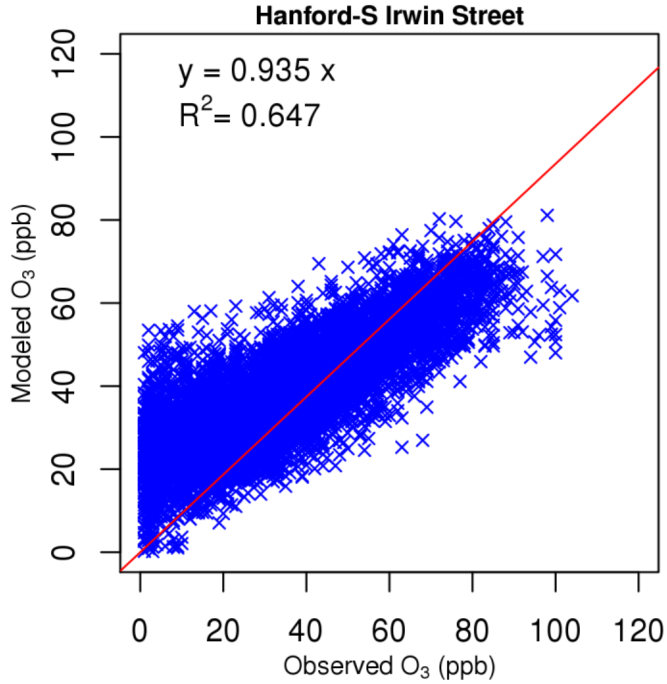

Figure S. 83 Scattering plot of observed and modeled 1-hour O_3 mixing ratio at Hanford

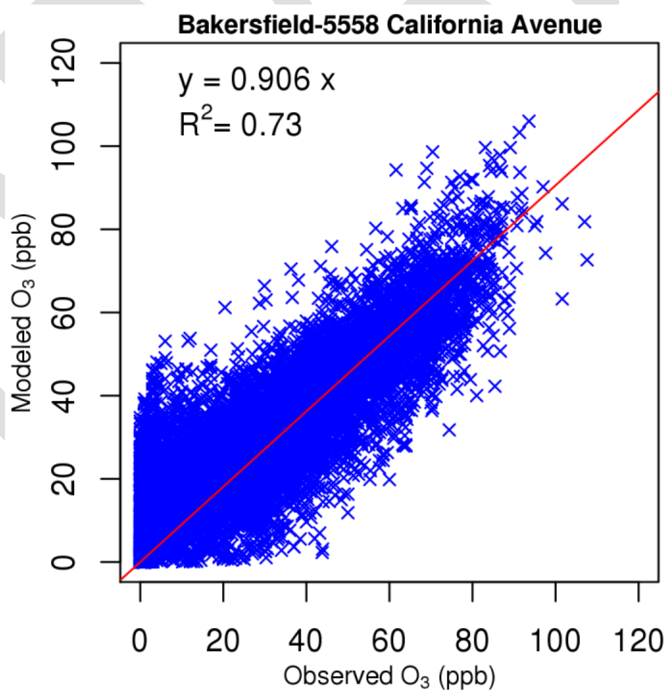

Figure S. 84 Scattering plot of observed and modeled 1-hour O_3 mixing ratio at Bakersfield – California Avenue

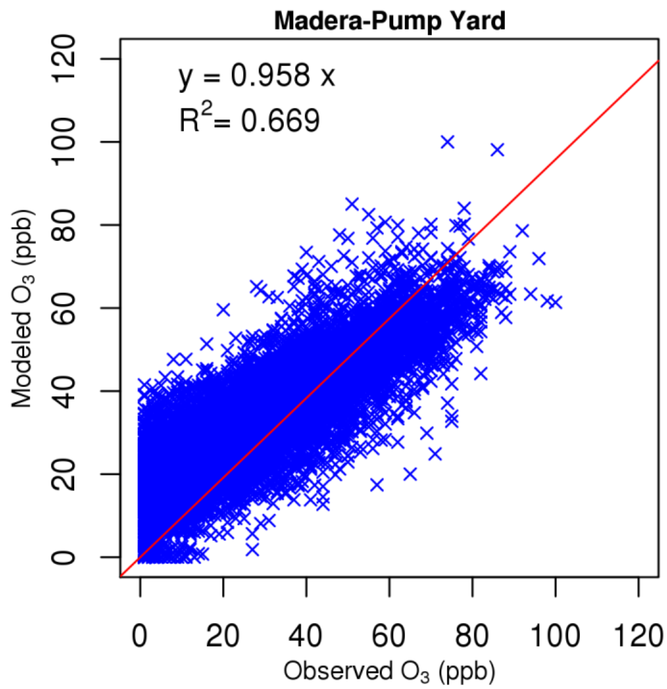

Figure S. 85 Scattering plot of observed and modeled 1-hour O_3 mixing ratio at Madera – Pump Yard

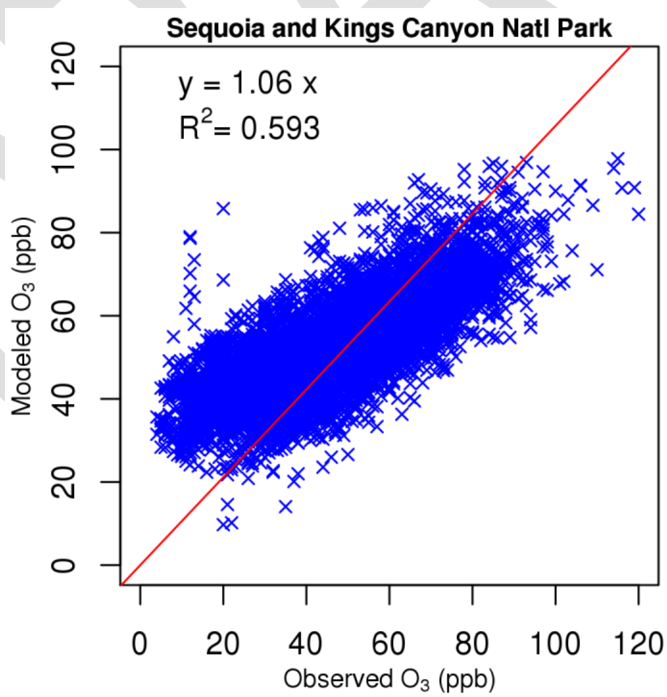

Figure S. 86 Scattering plot of observed and modeled 1-hour O_3 mixing ratio at Sequoia and Kings Canyon National Park

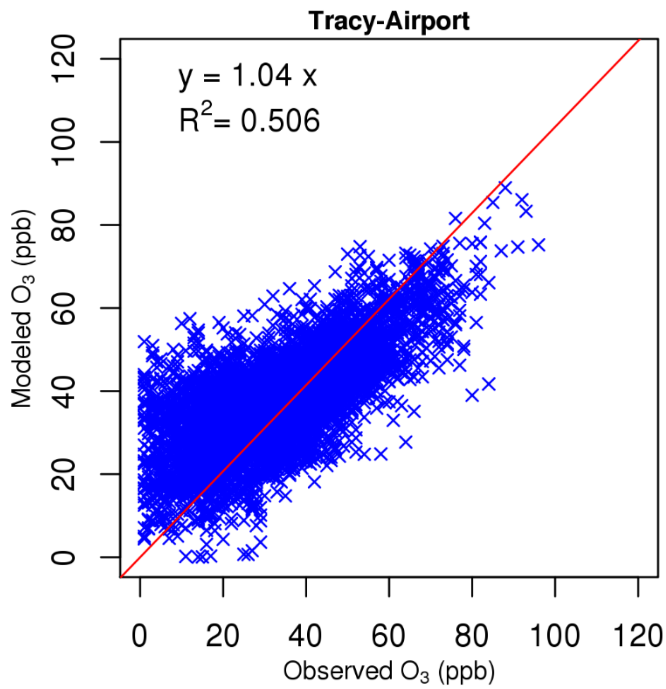

Figure S. 87 Scattering plot of observed and modeled 1-hour O_3 mixing ratio at Tracy

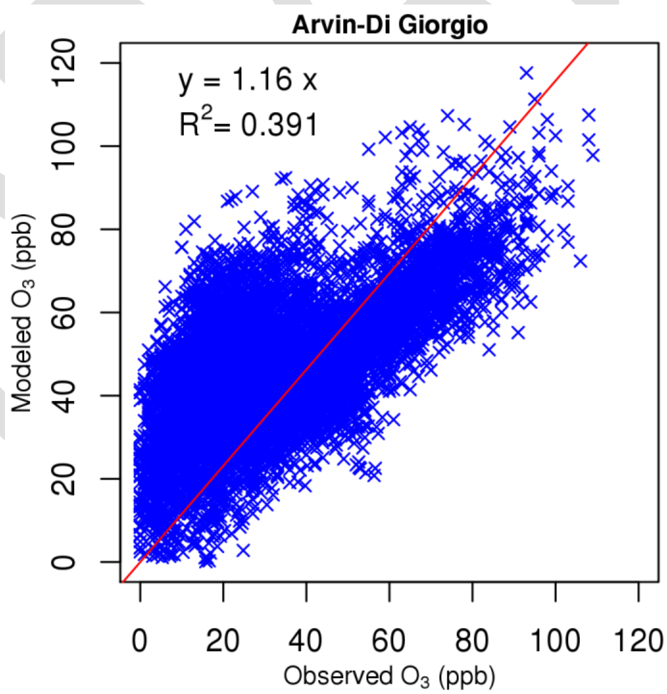

Figure S. 88 Scattering plot of observed and modeled 1-hour O_3 mixing ratio at Arvin

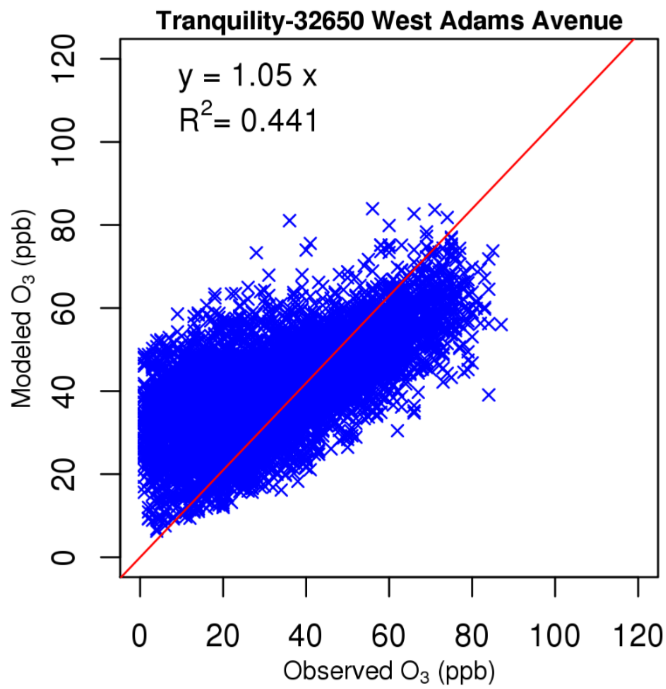

Figure S. 89 Scattering plot of observed and modeled 1-hour O_3 mixing ratio at Tranquility

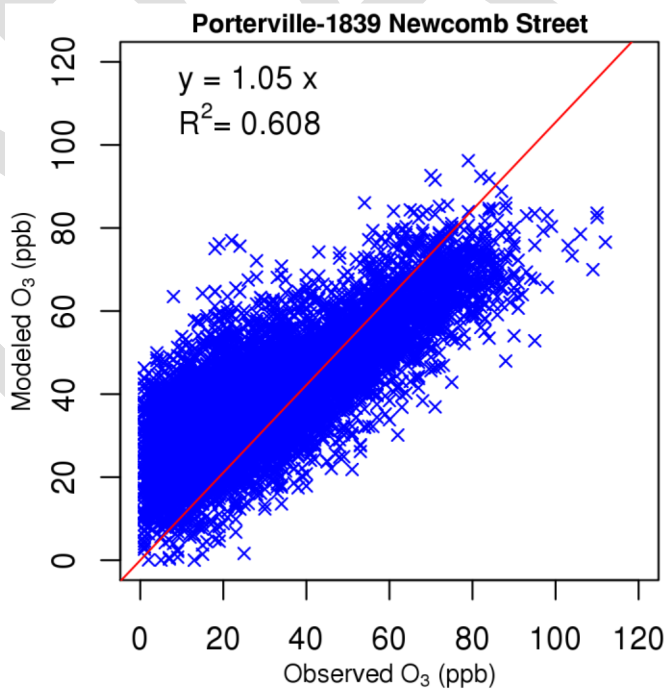

Figure S. 90 Scattering plot of observed and modeled 1-hour O_3 mixing ratio at Porterville

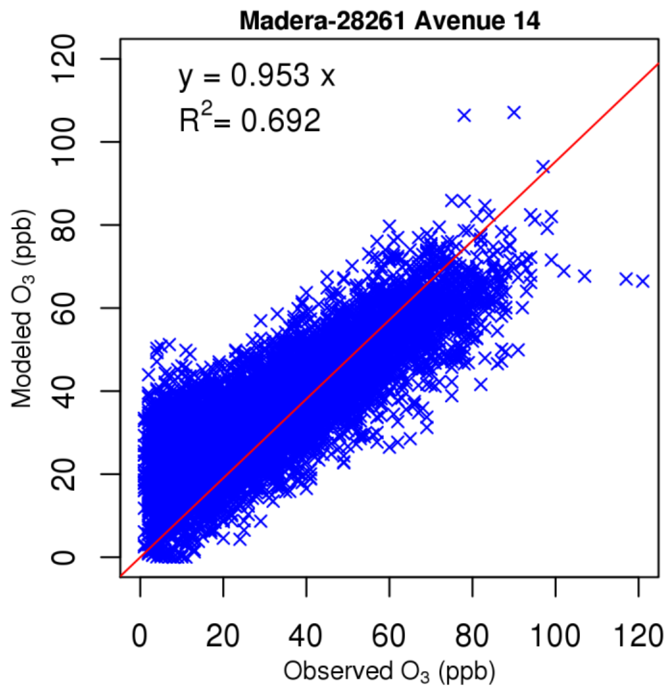

Figure S. 91 Scattering plot of observed and modeled 1-hour O_3 mixing ratio at Madera – 28261 Avenue 14

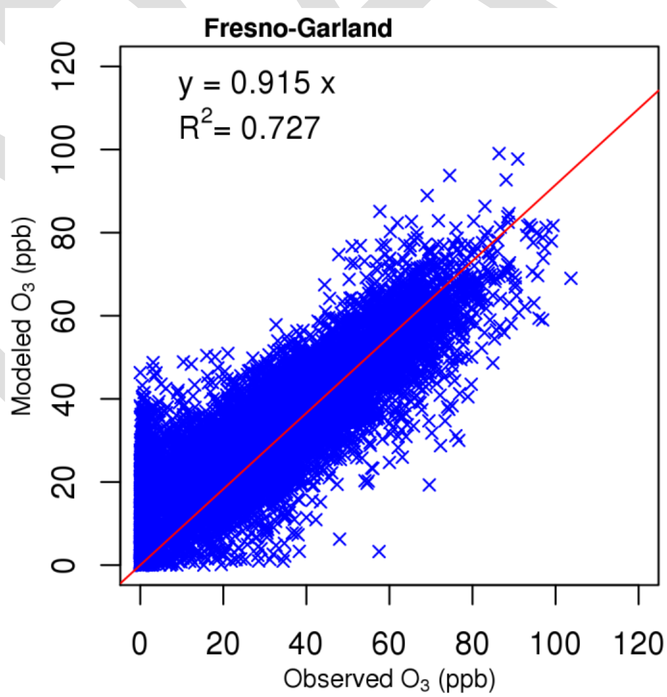

Figure S. 92 Scattering plot of observed and modeled 1-hour O_3 mixing ratio at Fresno-Garland

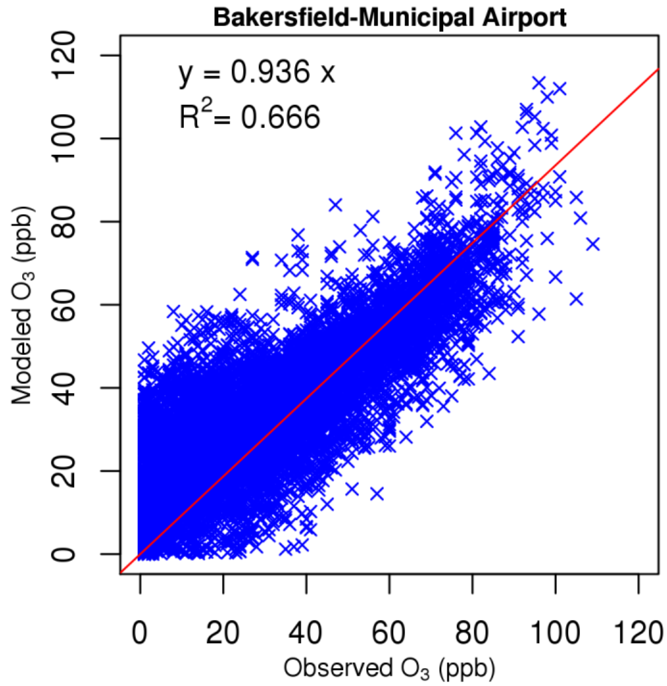

Figure S. 93 Scattering plot of observed and modeled 1-hour O_3 mixing ratio at Bakersfield – Municipal airport